

LB
2369.2
.B334
1995

IMPACT OF ALTERNATE REFRIGERANTS ON EVAPORATOR DESIGN

refrigerants on evaporator design AND types of compact heat exchangers. This

examined the **ANALYSIS OF COMPACT HEAT EXCHANGERS** in parallel

formulations of the geometries for the degree of Master of Science with a concentration
in Chemical engineering.

[Signature]
Dr. Prabhat, East Tennessee, Chattanooga

We have read this thesis
and recognized its acceptance

A Thesis

Presented for the

Master of Science Degree

[Signature]
Prof. Don S. Coats

The University of Tennessee at Chattanooga

[Signature]
Dr. Michael H. Jones

[Signature]
Dr. Susan M. [unclear]

Approved for the Graduate Division:

[Signature]
Dr. Edward E. Adair
Director of Graduate Studies

PARAG DADEECH

MAY 1995

I am submitting a thesis written by Parag Dadeech entitled "**Impact of alternate refrigerants on evaporator design and analysis of compact heat exchangers.**" I have examined the final copy of this thesis and recommend that it be accepted in partial fulfillment of the requirements for the degree of Master of Science with a concentration in Chemical engineering.

Mr. Parag Dadeech and Mr. Yash Dadeech

who have provided me with access to [REDACTED]

[REDACTED]
Dr. Prakash. Rao. Damshala, Chairperson

We have read this thesis
and recommend its acceptance :

[REDACTED]
Prof. Don S. Cassell

[REDACTED]
Dr. Michael. H. Jones

[REDACTED]
Dr. Shu-an-Hu

Accepted for the Graduate Division :

[REDACTED]
Dr. Deborah E. Arkfen

Director of Graduate Studies

ACKNOWLEDGMENTS

DEDICATION

I respectfully express my sincere appreciation and thanks to my research advisor,

Dr. Prakash Rao Ghantala for his excellent, guidance, support and being a friend throughout the course of this thesis, without which the successful completion would have been impossible. I also thank him for providing me the "CETA" research scholarship in Summer 1993.

Mr. Harish Chandra Dadeech and Mrs. Vibha Dadeech

who have provided me with inestimable educational opportunities.

Outgoing airplanes do heat and mass transfer on interrupted fin surfaces. These structures are primarily subject of my and research and are manufactured by leading companies like TRAME and MOENNE.

Brother,

Puneet Dadeech

Caseel for his valuable suggestions and guidance. I wish to thank him for the Engineering # 332 class which greatly improved my critical understanding of the Advanced

fluidodynamics concepts and made learning a wonderful experience. This was one of the best courses I have taken in my Engineering career. I also wish to thank Dr. Michael H.

Jones for his work as well as providing suggestions and comments. I would like to thank my

family, especially my father and mother for their patience, confidence in me and support and my brother for many light moments during the course of this work. Finally, I would

like to thank Dr. William O. Gurley for much guidance and encouragement and awarding me the Graduate assistantship during my stay at U. T. C.

ACKNOWLEDGMENTS

I respectfully express my sincere appreciation and thanks to my research advisor, Dr. Prakash Rao Damshala for his encouragement, guidance, support and being a friend throughout the course of this thesis, without which the successful completion would have been impossible. I also thank him for providing me the "CECA" research scholarship in Summer 1994, which considerably enhanced my knowledge of Compact heat exchangers, undergoing simultaneous heat and mass transfer on interrupted fin surfaces. These exchangers are presently subject of immense research and are manufactured by leading companies like TRANE and MODINE. I present my sincere thanks to Prof. Don. S. Cassel for his valuable suggestions and guidance. I wish to thank him for the Engineering # 532 class which greatly improved my critical understanding of the Advanced thermodynamics concepts and made learning a wonderful experience. This was one of the best courses I have taken in my Engineering career. I also wish to thank Dr. Michael H. Jones and Dr. Shu-an-Hu for taking time to be in this Thesis committee and for reviewing the work as well as providing suggestions and comments. I would like to thank my family, especially my father and mother for their patience, confidence in me and support and my brother for many light moments during the course of this work. Finally, I would like to thank Dr. William Q. Gurley for much guidance and encouragement and awarding me the Graduate assistantship during my stay at U.T.C.

ABSTRACT

This thesis deals with the evaluation of the impact of alternate refrigerants on the thermal design parameters of different heat exchangers, such as, plate fin and tube, shell and tube evaporator and compact heat exchangers. A computer code has been developed in Quick-Basic language to conduct this investigation.

Alternate refrigerants considered for this study are R-134a, R-152a, R-402a and R-404a and the performance of the heat exchanger employing these fluids is compared with that using the conventional refrigerants R-22 and R-12. Compact heat exchangers having Wavy and Offset strip fins are considered in this analysis. Parametric analysis is performed by varying the number of fins, air velocity and water velocity of plate fin tube heat exchanger.

The results of this study show that the thermal design parameters such as the heat transfer coefficients, pressure drop and heat exchanger area are greatly influenced by the refrigerant thermodynamic and transport properties. For an evaporator of fixed capacity, refrigerant R-152a resulted in highest overall heat transfer coefficient and lowest pressure drop followed by the refrigerants R-134a, R-22, R-12, R-404a and R-402a. The drop-in evaluation of refrigerants at evaporator temperature of 40F, show that the evaporator using refrigerant R-152a has the highest effectiveness followed by R-134a, R-22 and R-12. Drop-in evaluation is evaluated at four different evaporator temperatures and five different inlet refrigerant qualities and it is found that the highest values of evaporator effectiveness resulted when the evaporator temperature is lowest and the refrigerant inlet quality is highest. The results for plate fin tube heat exchanger indicate that increasing the number of fins increased the effectiveness, capacity and the air-side pressure drop, while increasing air velocity decreased the effectiveness of the exchanger. The results also show that variation of water velocity does not have any appreciable

impact on exchanger effectiveness and overall conductance at low fins per inch. Compact heat exchangers having plain, wavy or offset strip fins are compared on the basis of heat transfer area and results obtained from these analyses indicate that the offset strip fin heat exchanger has highest overall heat transfer coefficient and pressure drop followed by one with wavy and plain fins.

	SECTION	
	Shell and Tube heat exchanger	3
	Plate fin tube heat exchanger	4
	Alternative configurations	7
	Literature survey	8
	Aim of this thesis	10
1.	HEAT EXCHANGER ANALYSIS	13
	Plain fin tube evaporator design	23
	Drop-in evaluation	30
	Shell and tube evaporator design	35
	Parametric analysis of Plain fin tube heat exchanger	49
	Compact heat exchanger with interrupted surfaces	54
2.	RESULTS	63
	Evaluation for constant heat duty plain fin tube evaporator	63
	Drop-in evaluation	69
	Impact on shell and tube evaporator design	85
	Plate fin tube compact heat exchanger	90
	Compact heat exchanger with interrupted surfaces	102
3.	CONCLUSIONS	113
4.	RECOMMENDATIONS	118

TABLE OF CONTENTS

<u>CHAPTER</u>	<u>TITLE</u>	<u>PAGE No</u>
1.	INTRODUCTION.....	1
	Shell and Tube heat exchanger.....	3
	Plate Fin tube heat exchanger.....	5
	Alternate refrigerants.....	7
	Literature survey.....	8
	Aim of this thesis.....	10
2.	HEAT EXCHANGER ANALYSIS.....	12
	Plate fin tube evaporator design.....	13
	Drop-in evaluation.....	30
	Shell and tube evaporator design.....	35
	Parametric analysis of Plate fin tube heat exchanger.....	49
	Compact heat exchanger with interrupted surfaces.....	54
3.	RESULTS.....	63
	Evaluation for constant heat duty plate fin tube evaporator.....	63
	Drop-in evaluation.....	67
	Impact on shell and tube evaporator design.....	86
	Plate fin tube compact heat exchanger.....	90
	Compact heat exchanger with interrupted surfaces.....	109
4.	CONCLUSIONS.....	113
5.	RECOMMENDATIONS.....	.115

LIST OF REFERENCES116

APPENDICES

A-1. Figure 1.1, Interrupted surfaces types.....118

A-2 Computer code P1 (Impact on plate fin tube evaporator).....119

Computer code P2 (Drop-in evaluation).....124

Computer code P3 (Impact on shell and tube evaporator).....129

Computer code P4 (Analysis of plate fin tube HEX).....133

Computer code P5 (Analysis of interrupted surface HEX).....138

VITA.....148

NOMENCLATURE

<u>SYMBOL</u>	<u>DEFINITION</u>	<u>UNIT</u>
Ao	Heat transfer area	ft ²
Afr	Frontal area	ft ²
Ac	Minimum free flow area	ft ²
Aeffec	Effective heat transfer area	ft ²
ac	Shell side cross flow area	ft ²
aw	Window flow area	ft ²
Aref	Area for refrigerant flow	ft ²
APD	Air side pressure drop	inch. wg.
CL	Tube layout constant	----
CTP	Constant which accounts for incomplete coverage of shell inner diameter by tubes.	----
cp	Specific heat	Btu /lbm.F
cpa	Specific heat of air	0.24 Btu /lbm.F
cpl	Specific heat of liquid refrigerant	
Cr	Cmin/Cmax	----
cpw	Specific heat of water	Btu /lbm.F
Dto	Tube outer diameter	inch
Dti	Tube inner diameter	inch
Dh	Hydraulic diameter	inch
Ds	Shell inner diameter	inch
Dg	Gap between tubes	inch
EHX	Effectiveness of exchanger	----
f	Friction factor	---

<u>SYMBOL</u>	<u>DEFINITION</u>	<u>UNIT</u>
F	LMTD Correction factor	---
F _b	Correction factor for bundle bypass flow	---
F _l	Correction factor for baffle leakage	---
F _r	Correction factor for adverse temperature gradient	---
F _c	Correction factor for baffle cut and spacing	---
Fl _w	Water flow rate	Lbm / min
FP	Parameter to determine friction coefficients	----
G _c	Air mass flow based upon minimum free flow area	Lbm/sqft.hr
G _{fr}	Air mass flow over frontal surface	Lbm/sqft.hr
G _{ref}	Refrigerant flow rate per unit area	Lbm/sqft.hr
G _w	Shell side mass flow per unit area	Lbm/sqft.hr
g	Gravity acceleration	4.173E+08 ft/hrsq
h _i	Tube side heat transfer coefficient	Btu / hr-sqft-F
h _o	Air side heat transfer coefficient	Btu/hr-sqft-F
H	Enthalpy	Btu/lbm
H _{in}	Enthalpy entering the evaporator	Btu/lbm
H _{fg}	Enthalpy of vaporization	Btu/ lbm
h _{ideal}	Ideal heat transfer coefficient	Btu/hr-sqft-F
h _i	Tube side fluid ht.transfer coefficient	Btu/hr.sqft.F
h _o	Outside heat transfer coefficient	Btu/hr.sqft.F
h _l	Liquid heat transfer coefficient	Btu/hr.sqft.F
j	Colburn factor	----
JP	Parameter to determine heat transfer coefficient	----

<u>SYMBOL</u>	<u>DEFINITION</u>	<u>UNIT</u>
Ka	Thermal conductivity of air	Btu/hr.ft.F
Kal	Thermal conductivity of Aluminium	100 Btu/hr.ft.F
Kcu	Thermal conductivity of copper	227 Btu/hr.ft.F
Kw	Thermal conductivity of water	0.336 Btu/hr.ft.F
Kl	Thermal conductivity of satd liquid refrigerant	Btu/hr.ft.F
L	Tube length	ft
Ls	Shell length	ft
Lc	Baffle cut	inch
LMTD	Log mean temperature difference	deg F
NT	Number of tubes	---
Nb	Number of baffles	---
Nr	Number of vertical tube rows	---
Nr	Number of rows in air flow direction	---
Nw	Number of tube rows in window	---
NTU	NTU parameter	---
P	Tube pitch	inch
Pb	Baffle spacing	inch
PE	Evaporator pressure	psia
Pr	Prandtl number	---
PR	Pitch ratio	---
Q	Heat duty	BTU/hr
QA	Air volume flow rate	Scfm
R	Gas constant for air	53.32 ft-lbf / F.lbm
Re	Reynolds number	----

<u>SYMBOL</u>	<u>DEFINITION</u>	<u>UNIT</u>
Res	Shell side Reynolds number	----
S	Fins per inch	----
St	Stanton number	----
T	Fin thickness	inch
TE	Evaporator temperature	deg F
TAI	Air temperature in	deg F
TAO	Air temperature out	deg F
TWI	Water temperature in	deg F
TWO	Water temperature out	deg F
Uo	Overall heat transfer coefficient	Btu / hr.sqft.F
W	Depth of compact exchanger	ft
x	Exit refrigerant quality	
x1	Inlet refrigerant quality	
XA	Transverse spacing	inch
XB	Longitudinal spacing	inch
σ	Ratio of minimum free flow area to frontal area	----
α	Heat exchanger area to volume ratio	ft ⁻¹
η	Fin efficiency	----
η_{so}	Fin effectiveness	----
μ_a	Viscosity of air	lbm / ft.hr
μ_b	Viscosity at bulk fluid temperature	lbm / ft.hr
μ_w	Viscosity of water	lbm / ft.hr
μ	Viscosity	lbm / ft.hr
μ_L	Vicosity of satd liquid refrigerant	lbm / ft.hr

<u>SYMBOL</u>	<u>DEFINITION</u>	<u>UNIT</u>
ρ_{fr}	Density of fluid over the frontal surface	lbm / cuft
ρ	Density of shellside fluid	lbm / cuft
ρ_1	Density of air at entrance	lbm / cuft
ρ_2	Density of air at exit	lbm / cuft
ρ_w	Density of water	lbm / cuft
Δx	Change in quality of refrigerant	----
ΔP_f	Pressure drop in cross flow section of shell and tube heat exchanger	psi
ΔP_w	Pressure drop in the window section of shell and tube heat exchanger	psi
ΔP_{fi}	Pressure drop in the inlet/outlet section of shell and tube heat exchanger	psi

Subscripts

a	Air
l	Liquid
o	Outside, Offset
p	Plate or Plain
v	Vapor
w	Wavy

LIST OF FIGURES

<u>FIGURE</u>	<u>TITLE</u>	<u>PAGE No</u>
1.	Refrigeration cycle	2
2.	Shell and tube heat exchanger	4
3.	Plate fin tube heat exchanger	6
4.	Correlation of heat transfer data for smooth plate fin coils	19
5.	Variation in colburn factor with number of rows for smooth plate fin coils	20
6.	Correlation of friction data for smooth plate fin coils	29
7.	Diagram for shell side flow mechanism	38
8.	Internal cross flow section	45
9.	Window section	47
10.	Inlet and outlet section	48
11.	Wavy fins	56
12.	Offset strip fins	57
13.	Refrigerant side heat transfer coefficients, plate fin tube evaporator	65
14.	Overall heat transfer coefficients, plate fin tube evaporator	65
15.	Heat transfer area, plate fin tube evaporator	66
16.	Air pressure drop, plate fin tube evaporator	66
17.	Effect on evaporator effectiveness	83
18.	Effect on evaporator NTU	83
19-22	Effect of quality on Effectiveness	84-85

<u>FIGURE</u>	<u>TITLE</u>	<u>PAGE No</u>
23.	Refrigerant side heat transfer coefficients, shell and tube evaporator.	88
24.	Overall heat transfer coefficients, shell and tube evaporator	88
25.	Heat transfer area, shell and tube evaporator	89
26.	Shell side pressure drop, shell and tube evaporator	89
27.	Effect of fins per inch on exchanger effectiveness	92
28.	Effect of fins per inch on Colburn factor	93
29.	Effect of fins per inch on friction factor	93
30.	Effect of fins per inch on air side heat transfer coefficient	94
31.	Effect of fins per inch on overall heat transfer coefficient	94
32.	Effect of fins per inch on heat transfer area.	95
33.	Effect of fins per inch on overall conductance	95
34.	Effect of fins per inch on NTU	96
35.	Effect of fins per inch on air side pressure drop	96
36.	Effect of air velocity on exchanger effectiveness	99
37.	Effect of air velocity on Colburn factor	100
38.	Effect of air velocity on friction factor	100
39.	Effect of air velocity on air side heat transfer coefficient	101
40.	Effect of air velocity on overall heat transfer coefficient	101
41.	Effect of air velocity on overall conductance	102
42.	Effect of air velocity on NTU	102
43.	Effect of air velocity on air pressure drop	103
44.	Effect of fins per inch and air velocity on effectiveness	104
45.	Effect of fins per inch and air velocity on overall conductance	104

<u>FIGURE</u>	<u>TITLE</u>	<u>PAGE No</u>
46.	Effect of fins per inch and air velocity on NTU	106
47.	Effect of water velocity on overall conductance at various fins per inch.	107
48.	Effect of water velocity on effectiveness at various fins per inch.	108
49.	Air side ht transfer coefficients and overall heat transfer coefficients for different HEX	111
50.	j and f factors for different HEX	111
51.	Effectiveness values for different HEX	112
52.	Air side pressure drop for different HEX	112
1.1	Interrupted fin surfaces	118

LIST OF TABLES

<u>TABLE</u>	<u>TITLE</u>	<u>PAGE No</u>
1.	Plate fin tube exchanger data	14
2.	Refrigerant properties at 5 F	24
3.	Refrigerant properties at 25 F	24
4.	Refrigerant properties at 35 F	25
5.	Refrigerant properties at 40 F	25
6.	Constants for flow across ideal tube banks	40
7.	Values of F1 for various tube diameters and layout	43
8.	Values of F2 for various tube passes	44
9.	Values of F3 for various tube bundle construction	44
10.	Impact on plate fin tube evaporator design	63
11-30	Drop-in evaluation	67-80
31.	Impact on the shell and tube evaporator design	86
32.	Impact of fins per inch on exchanger design	90
33.	Impact of air velocity on exchanger design	97
34.	Analysis for interrupted surface HEX	109

CHAPTER 1

INTRODUCTION

A Heat exchanger is a device which provides for the transfer of internal thermal energy between two or more fluids at different temperatures. Heat transfer between the fluids takes place through a separating wall. Since the fluids are separated by a separating wall they do not mix. Common examples of such heat exchangers are the shell and tube exchangers, automobile radiators, condensers, evaporators, air preheaters and dry cooling towers. There are no internal energy sources in a heat exchanger, ruling out fired heaters, electric heaters, and nuclear fuel elements. If the fluids are immiscible, the separating wall may be eliminated, and the interface between the fluids serves as a heat transfer surface as in case of a direct contact heat exchanger.

A heat exchanger consists of the active heat exchanging elements such as a core or a matrix containing the heat transfer surface, and passive fluid distribution elements such as headers, manifolds, tanks, inlet-outlet nozzles and seals. Usually there are no moving parts in a heat exchanger, however, there are exceptions such as a rotary regenerative exchanger, in which the matrix is mechanically driven to rotate at some design speed. The heat transfer surface is the surface of the exchanger core which is in direct contact with fluids and through which heat is transferred by conduction. To increase heat transfer area, appendages known as fins may be intimately connected to the primary surface to provide extended, secondary or indirect surface. Fins may form flow passages for the individual fluids but do not separate the fluids. These secondary surfaces or fins may also be introduced primarily for structural strength purposes, or to provide thorough mixing of a highly viscous fluid. Heat exchangers are important in a wide range of industrial applications. They are used in process, power, automotive, air-conditioning, refrigeration, heat recovery, and manufacturing industries, as well as key components of many products available in the market place. Two main types of heat exchanger are :

- 1) Shell and tube heat exchanger . 2) Plate fin tube heat exchanger.

Both of these exchangers are widely used as evaporators and condensers in the refrigeration and air-conditioning industry. A typical refrigeration cycle is shown in Figure 1 which follows.

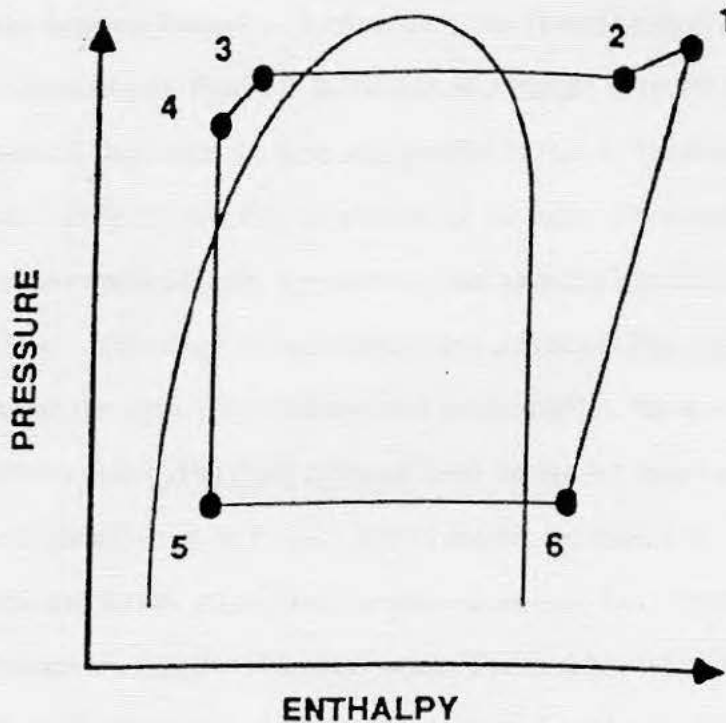


FIGURE 1: Refrigeration cycle

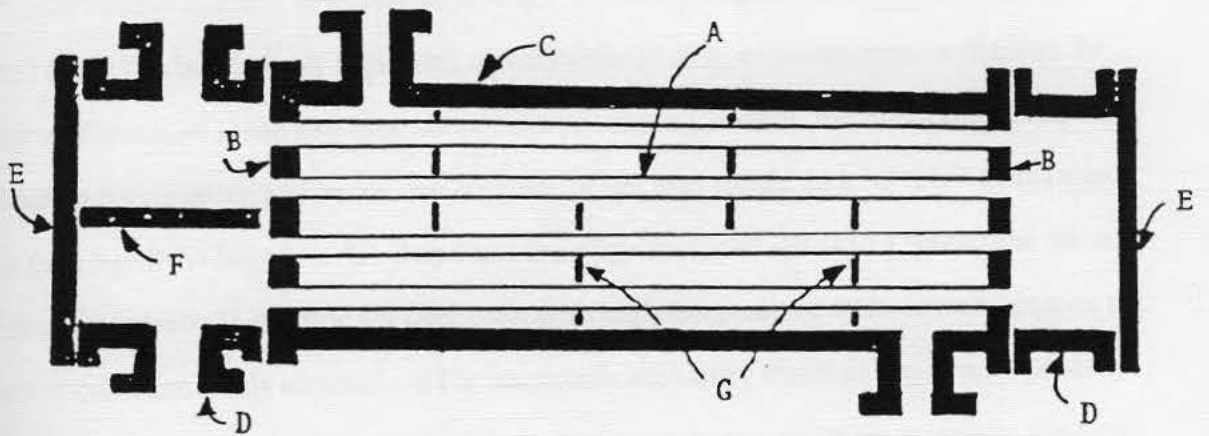
Mixture of refrigerant liquid and vapor is evaporated in the evaporator from state point 5 to state point 6. Saturated or superheated refrigerant vapor is compressed from state 6 to state 1. State 2 represents the refrigerant entrance into the condenser. Superheated vapor at a high temperature and pressure is condensed in condenser from state 2 to state 3.

State 4 represents the entrance into the evaporator expansion device and state 5 represents the refrigerant entrance into the evaporator. Heat is absorbed in the evaporator at a low temperature from the circulating chilled water or air and is rejected in the condenser at high temperature to the circulating water or air.

Shell and tube heat exchanger :- A cross-sectional sketch of shell and tube heat exchanger is illustrated in Figure 2. It consists of a bundle of round tubes packed together inside a cylindrical shell with the tube axis parallel to that of the shell. One fluid flows inside the tubes, while the other flows outside of the tubes. Shell and tube heat exchangers are normally used for transferring heat between liquids, either with or without phase change for a wide range of temperature and pressures. The major components of the exchanger are the shell, front and rear end heads, baffles, tubes, tubesheets, nozzles and pass partition plates. The most common shell design for single phase applications on the shell side is identified as an E shell. In this design, the shell side fluid enters at one end of the shell and leaves at the other. In some situations, it is desirable that the shell side fluid traverses the length of the shell twice. This is achieved by having inlet and outlet nozzles on the same side and by using a longitudinal baffle. This shell is identified as F shell. In some designs, the inlet and outlet nozzles are in the center and the shell side fluid then flows essentially at right angles to the tube side fluid. This shell is identified as an X shell. Shell inner diameter typically varies between 8 and 60 inches.

Baffles are used to increase the turbulence of the shell side fluid and to support the tubes. Baffles are supported by tie rods. Various types of baffles arrangements, such as longitudinal, segmental, rod baffles and disc & doughnut baffles are possible. Spacing between the baffles usually varies between 10% to 60% of the shell diameter. Tubes are generally 1/4 inches to 2 inches in outer diameter and are arranged in in-line or staggered patterns. Center line distance between 2 consecutive tubes (tube pitch) varies

FIGURE 2: Shell and Tube heat exchanger



A : Tubes , B: Tube sheets , C: Shell

D: Tube side channels and nozzles.

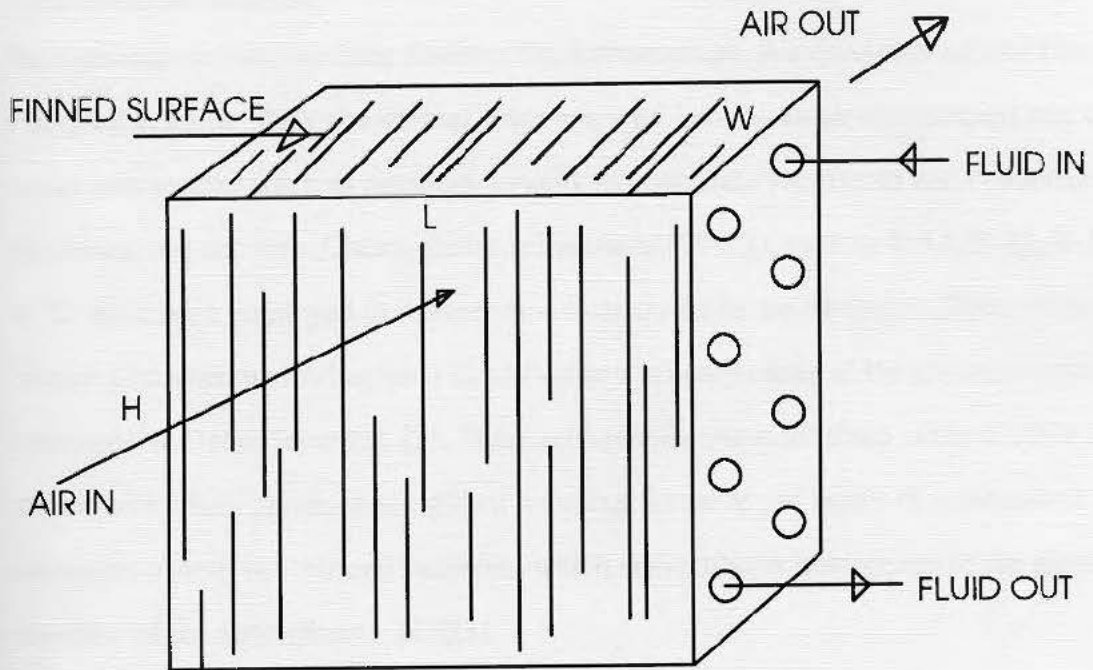
E: Channel Covers, F: Pass Divider , G: Baffles.

from (1.1 * tube diameter) to (2.5 * diameter) . The tube bundle is inserted into the various holes drilled in the tube sheet.

Shell and tube heat exchangers can also be described according to the way the tube bundles are attached to the shell for support. There are basically three types, namely, fixed tube sheet, floating head and U tube exchanger. The fixed tube sheet is the simplest and the most commonly used type. Both tube sheets are welded to the shell. The tube bundle is not accessible and therefore the exchanger is suited for clean fluids only. The floating head exchanger is widely used when the differential temperature between the shell and tubes is relatively high with a possibility of differential thermal expansion. In this configuration , with one tube sheet floating within the shell, the tube bundle can be removed for cleaning and hence can be used for unclean fluids. In a 'U tube' exchanger the tube bundle is bent to a 'U' shape and the other end is attached to a fixed tube sheet. The configuration is suitable for operation with high temperature differentials because the bent portion can freely expand and for operations with dirty fluids as the bundle is easily accessible for cleaning. Shell and tube heat exchanger is one of the most widely used and can be designed for almost any capacity.

Plate fin tube heat exchanger :- A typical core of plate fin tube fin heat exchanger consists of continuous plate fin sheets arranged on an array of tubes. This exchanger is illustrated in Figure 3. Fluids with low heat transfer coefficient, such as air flow over the finned surface and high heat transfer coefficient fluids flow through the tube side. Higher heat transfer area can be achieved in much smaller volume compared to shell and tube heat exchangers. Various kinds of interrupted fins have been employed on the outside tube surface. The interrupted fin surfaces make the heat exchanger much more compact. Substantial heat transfer enhancement is obtained in such heat exchanger as a result of periodic starting and development of boundary layers over interrupted surfaces [1],[15]. Each time an interrupted surface is encountered, the boundary layer is broken and formed

FIGURE 3 : Plate fin tube heat exchanger



H : Height of exchanger.

L: Length of exchanger.

W: Depth of exchanger.

again. The overall result is a thinning of the boundary layer that results in an increase in the local heat transfer coefficient. The different types of interrupted surfaces are illustrated in Figure 1.1 in appendix A1.

Alternate refrigerants :

Refrigerants are vital working fluids in the Refrigeration, Air-conditioning and Heat Pumping systems. They absorb heat from one area, such as an air-conditioned space, and reject into another, such as outdoors, usually through the evaporation and condensation processes, respectively. Chloro-flouro refrigerants (CFC s), such as R-11, R-12, R-13 & R-22 have been employed in refrigeration industry since the inception. These refrigerants contain Chlorine, which has been identified as a primary cause of the depletion of the stratospheric Ozone layer [2], [3]. These refrigerants also contribute to the CO₂ in the atmosphere which results in the global warming. In the lower layers of atmosphere, these molecules absorb the infrared radiation, which also partially contributes to the global warming of the atmosphere. [2],[3].

The destructive environmental implications resulted in the U.S. clean air act and the Montreal protocol. These regulations call for the complete production phase out of the CFC's in the United States by the end of the year 1995. A great deal of work has been done in the HVAC industry to identify and develop alternate refrigerants. R-32, R-123, R-124, R-125, R-134a, R-402a , R-404a, R-141b, R-500, R-152a and E-134 are few recently developed alternate refrigerants. Various binary and ternary blends of different refrigerants have also been produced. Binary blend consisting of R-32 / 134a (25 / 75 wt %), and ternary blend of R-32 / 125 / 134a (30 / 10 / 60 wt %) have been identified as possible replacements for R-22 and R-12 in refrigeration equipment. [4]. Various Azeotropic and Non-Azeotropic blends of different refrigerants have also been developed. An Azeotropic mixture of a refrigerant boils at a fixed temperature and exhibits the property of a single refrigerant. Refrigerant R-404a consisting of (R-125

44% , R-143a 52% and R-134a 4%) & R-402a consisting of (R-125 60% , R-290 2% and R-22 38%) are two examples of recently developed Azeotropic refrigerant blends. A Non-Azeotropic refrigerant mixture (NARM) exhibits non-isothermal phase change. Another characteristic of NARM's is that at a given bulk composition, the compositions of the individual liquid and vapor phases change during the phase change process. An example of a NARM is a refrigerant mixture consisting of (R-22, 45 wt % and R-114, 55 wt %).

In the alternate refrigerants, one or more chlorine atoms are substituted by hydrogen, carbon or fluorine atoms. Therefore the ozone depletion potential is reduced to zero. The global warming potential (GWP) of the refrigerant is also greatly reduced.

Literature survey :

Garza and Miller et al, [5] experimentally determined the thermodynamic properties of alternate refrigerants R-125 and R-141b. Wijaya and Spatz et al, [4] showed that the two-phase pressure drop and heat transfer characteristics of azeotropic blend of refrigerants (R-32 / R-125) (R-32, 50 wt % and R-125, 50 wt%) in a copper tube compact evaporator with 0.305 inches inner diameter tubes of 12 ft long subjected to constant mass flux are superior to those of R-22. At similar mass fluxes, the evaporation heat transfer coefficient of R-32 / R-125 blend was about 23% higher than refrigerant R-22. Poz and Conklin et al, [6] performed analysis of heat exchanger containing Non-azeotropic refrigerant mixtures (NARMs) of R-22 and R-114, (R-22 45 wt % and R-114 55 wt %) and calculated the heat and mass transfer between moist air and NARMs for Plain fin, Offset strip fin and counter flow heat exchangers. They indicated that the composition of the liquid and the vapor changes during the phase change process and divided the heat exchanger into three regions, namely, : Single phase liquid, Two-phase vapor-liquid and Single-phase vapor and developed a one dimensional model describing

the process of heat and mass transfer between the moist air and NARM's. The results of their work showed that an offset strip fin air-side evaporator increased the heat transfer compared with a plain-fin evaporator by a factor of 1.67 for 5 tube rows with a given face area at air velocity of 5 m/s. Kattan and Favrat et al, [7] analyzed the two phase flow pattern for conventional refrigerant R-502 and new refrigerants, R-402a and R-404a in a direct expansion evaporator. They also performed in-tube flow boiling experiments and showed that heat transfer coefficients for refrigerant R-404a was slightly larger than those for R-502 under the same test conditions, while those for R-402a was slightly smaller. Sami and Tulej et al., [8] experimentally analyzed the heat transfer and the pressure drop characteristics of ternary refrigerant mixtures inside enhanced-surface compact heat exchangers. They determined evaporative heat transfer coefficient and pressure drops for refrigerant blends R23 / R22 / R152a and R23 / R22/ R134a at various refrigerant mass fluxes. Their results showed that the refrigerant blend consisting of R23 / R22 / R152 had superior boiling and condensation heat transfer coefficients compared to the blend consisting R23 / R22 / R134a. Darabi and Salehi et al., [9] presented various correlations for flow boiling regime for alternate refrigerants. Earlier, correlations were presented by Chen, Pierre, Zuber et al [2]. Equations developed by Gungor and Winterton, Liu, Kandlikar, Shah et al, [2] are among the widely used correlations for estimating the two-phase heat transfer coefficients for alternate refrigerants.

Serious research and development efforts in field of compact heat exchangers started after World War-I and accelerated with the introduction of Aluminium brazing after World-War II. Since the energy crisis of the early 1970's, increasing use has been made of the compact heat exchangers in many energy conversion, conservation and recovery systems. Most of the research done in this field is proprietary. Weiting et al., [10], developed empirical correlations for heat transfer and flow friction characteristics for the Offset strip fin heat exchangers. Beecher and Fagan et al., [11] studied the effects

of fin patterns and depth on the air-side heat transfer and pressure drop for Wavy fins and experimentally obtained correlations for heat transfer and friction factor. McQuiston et al., [12] developed the correlations for the plain fins and performed extensive work in the area of Plain fin tube heat exchangers. He developed experimentally correlations for the air-side friction factor and the Colburn factor for Plate-fin tube heat exchangers in terms of parameters which he referred as JP and FP factors. He also showed experimentally that moisture condensation increases the heat transfer. A. Sahnoun and R.L Webb, [18] predicted the air-side heat transfer and friction factor for the louver-fin geometry.

Aim of this Thesis :

The first part of this thesis deals with evaluation of the impact of alternate refrigerants on the thermal-hydraulic design of plate fin tube and shell and tube evaporator performance using four alternate refrigerants namely, R-134a, R-152a, R-404a and R-402a and compare the performance of these units with the conventional refrigerants R-12 and R-22. The equation developed by Liu and Winterton is employed for calculating the heat transfer coefficient for the refrigerant side two-phase flow.

The first part of the thesis deals with the design for the following two cases :

1) Design of constant heat duty evaporator.

In this case the heat duty of the evaporator is constant. The impact of the alternate refrigerants on the heat transfer coefficients, heat transfer area and pressure drops is evaluated for plate fin tube and shell and tube evaporator.

2) Evaporator design of constant volume.

In this case the impact of the alternate refrigerants is evaluated in an evaporator of fixed volume (i.e., drop-in evaluation in an existing machine).

The second part of this thesis deals with comprehensive analysis of compact heat exchangers. Parametric analysis of plate fin tube heat exchanger is done by varying the

design parameters such as fins per inch, air velocity and water velocity. Analysis of compact heat exchanger with interrupted fin surfaces is performed and the results are compared with plate fin tube heat exchanger.

Chapter 2 deals with analysis of different heat exchangers. Chapter 3 presents the results of design and analysis. Conclusions and recommendations are presented in Chapter 4 and Chapter 5 respectively.

CHAPTER 2

HEAT EXCHANGER ANALYSIS

Heat exchanger area of the hot and cold fluid streams is typically estimated in heat exchanger design problems, when the fluid flow rates, inlet fluid temperatures and required exit fluid temperatures are specified. The rate of heat transfer to be accomplished in a heat exchanger is defined as heat duty of a heat exchanger. Rating problems of heat exchanger, on the other hand, deal with prediction of exit fluid temperatures and heat duty for a given size heat exchanger. In this chapter, first the design of a plate fin tube evaporator is done for the case of constant heat duty, namely estimating the overall size of the unit consisting of standard size tubes. As the pressure drop of the refrigerant is typically negligible in case of evaporating fluid, its estimate is not made, however the air pressure drop outside the tubes is calculated as a part of this design process. For comparison purposes the design process is done for potential four refrigerant substitutes, as well as for the conventional refrigerants.

In the second part of this chapter, performance evaluation of a given size evaporator with specified overall dimensions is done. This process is presented for two alternate refrigerants, as well as for two conventional fluids for comparison. The results of this analysis provide the estimate of heat duty and evaporator effectiveness for four different evaporating temperatures, and at refrigerant qualities varying from zero to thirty-nine percent.

The third part of this chapter deals with shell and tube evaporator design consisting of single shell and two tube passes. In this design process, estimates of length of tube, number of baffles and shell side pressure drop are presented for a given diameter of the shell and number of tubes of known diameter. This process is again repeated for two conventional refrigerants for comparison purposes.

In the fourth stage, the plate fin tube heat exchanger has been critically examined through parametric analysis by varying the fins per inch, air velocity and water velocity passing through the tubes. Finally, the influence of wavy or offset strip fins in place of plate fins is evaluated.

Plate fin tube evaporator design

Plate fin tube evaporator is designed to meet a specific heat duty requirement.

Air flows in cross flow over the frontal surface of the heat exchanger (finned surface) and alternate refrigerants flow through the tube side. Four alternate refrigerants, namely, R-152a, R-134a, R-404a and R-402a are considered individually. The performance of heat exchanger employing these fluids, is compared with that employing the conventional CFC refrigerants, R-12 and R-22. The composition of the refrigerants considered in this analysis is as follows :

<u>Refrigerant</u>	<u>Composition.</u>
R-134a	1,1,1,2- Tetra-Flouro-Ethane
R-152a	1,1 Di-flouro-Ethane
R-404a	Azeotropic blend consisting of R-125 60%, R-290 2% and R-22 38%
R-402a	Azeotropic blend consisting of R-125 44%, R-143a 52% and R-134a 4%
R-12	Dichloro-diflouro-Methane
R-22	Chloro-diflouro-Methane

Some of the geometrical parameters typically employed, are fixed as follows :

Tube outer diameter, D_{to} = .525 inches.

Tube inner diameter, D_{ti} = .483 inches.

The above values of tube diameters were frequently observed in the literature survey of plate fin tube heat exchangers. The tube diameter generally ranges from 0.25 inches to 1.0 inch.

Transverse spacing, $X_A = 1.25$ inches

Longitudinal spacing, $X_B = 1.083$ inches

Tube spacing in heat exchangers generally varies from 1 to 2 inches.

Tube arrangement is staggered.

Fins per inch, $S = 8$

Fin thickness, $T = .006$ inches

Fins per inch, generally varies from 2 to 14 per inch, fin thickness varies from .006 to 0.01 inch; above values are typical of a plate fin tube heat exchanger.

Fin material employed is aluminium, due to its light weight and good thermal conductivity while tube material is copper.

Plate fin tube exchanger data :

Design and analysis of compact heat exchanger involves several parameters related to exchanger geometry such as, number of fins per inch S , hydraulic diameter D_h , ratio of minimum free flow area to frontal area A_{min}/A_{fr} , ratio of exchanger area to volume α , and ratio of fin area to heat transfer area, A_f/A . A typical range of these parameters are shown in Table 1.

TABLE 1 : COMPACT HEAT EXCHANGER DATA

<u>S, number of fins per inch.</u>	<u>D_h, hydraulic diameter, inch.</u>	<u>A_{min}/A_{fr}</u>	<u>exchanger area to vol ratio, α, per ft.</u>	<u>fin area to heat transfer area, A_f/A</u>
2.92	.3792	.58	73	.81
6.67	.1824	.56	147	.91
9.17	.1322	.55	198	.93
11.7	.1092	.54	238	.94
14.5	.084	.53	306	.96

Data presented in table 1 were obtained from Mcquiston et al., [12] for plate fin tube heat exchangers. These data are valid for the following range of exchanger geometry :

Tube outer diameter between .375 to .625 inches.

Tube spacing between 1 to 2 inches.

Fin pitch 4 to 14 fins per inch.

Fin thickness .006 to .01 inches.

Air face velocity = 200 to 800 feet per minute.

Since most of the analysis of heat exchanger is to be performed on a computer, curve fitted relations for hydraulic diameter D_h , ratio of minimum free flow area to frontal area σ , ratio of heat exchanger area to volume ratio α , and ratio of fin area to heat transfer area (A_f / A), were obtained as a function of fins per inch from data presented in Table 1, using the software [13]. The statistical variance of these equations is approximately 99.9%. The relations obtained from curve fits of the data are as follows :

$$D_h = -.02569963 + .9617315 \cdot S^{-.80734} \quad (1)$$

$$\sigma = \left[1.6891125 + .019386 S^{0.5} \ln(S) \right]^{-1} \quad (2)$$

$$\alpha = 14.65963 + 19.76648 (S) \quad (3)$$

$$\frac{A_f}{A} = \left[.92185 + \frac{.336112}{\ln(S)} \right]^{-1} \quad (4)$$

In addition to fixing the geometrical parameters, flow conditions are also fixed as follows.

Flow conditions:

Air pressure, PA = 14.7 psi. abs

Entering Air temperature, TAI	= 85 F
Leaving Air temperature, TAO	= 50 F
Air vol flow rate, QA	= 6300 scfm
Air velocity, VA	= 750 fpm

Desired values for the air velocity should be less than 900 fpm, to avoid possible sound and vibration problems.

Refrigerant velocity, VR = 1 fps

Refrigerant velocity is generally less than 5 fps.

Evaporator temperature, TE = 40 F

Quality of refrigerant entering evaporator = 0, satd liquid

Quality of refrigerant leaving evaporator = 100 %

Evaporator Pressure corresponds to the pressure of saturated liquid refrigerant at evaporator temperature.

EVAPORATOR DESIGN CALCULATIONS

The correlations for coefficient of heat transfer and friction factor are expressed in terms of JP and FP parameters respectively as follows :

Calculations for JP Parameter and j factor for the air side :

Based on the experimental data, the JP parameter and the j factor for the air-side are found to depend on the air flow rates, fin spacing, fin thickness and evaporator geometry characterized by tube inner and outer diameters, tube transverse and longitudinal spacing and tube arrangement (inline, staggered, rotated square, etc). The steps in calculation of the j factor are as follows :

$$m_a = G_{fr} \cdot A_{fr} = G_c \cdot A_c \quad (5)$$

$$G_c = \frac{G_{fr}}{\sigma} \quad (6)$$

ma is the air mass flow rate, Afr is the air flow frontal area , Ac is the minimum free flow area.

$$A_{fr} = Q_A / V_A$$

$$G_{fr} = \rho_{fr} \cdot V_A \quad (7)$$

$$\rho_{fr} = \frac{[P.A.144]}{R} \frac{1}{[T.A.I + 460]} \quad (8)$$

Gc is the air side mass flow rate based on minimum free flow area, pfr is the air density entering the heat exchanger.

$$JP = Re_D^{-.4} \cdot \left(\frac{A}{A_t} \right)^{-.15} \quad (9) \quad [12]$$

Re_D is air-side Reynolds number based on Gc.

$\left(\frac{A}{A_t} \right)$ is the ratio of total heat transfer area (sum of bare tube and fin side heat transfer areas) to the bare tube heat transfer area.

$$\frac{A}{A_t} = \frac{4 \cdot X_A \cdot X_B}{3.1415 \cdot D_h \cdot D_{to}} \cdot \sigma \quad (10)$$

$$Re_D = \frac{G_c \cdot D_{to}}{\mu} \quad (11)$$

$$J_4 = .0014 + .2618 JP \quad (12) \quad [12]$$

j₄ is colburn factor when number of rows in the air flow direction are less than or equal to four.

For rows greater than four, the j factor is greatly dependent on the Reynolds number based on the longitudinal spacing. The row effect is greatest at low Reynolds number and gradually disappears at Reynold number greater than 15,000 [14].

$$\frac{j_n}{j_4} = \frac{1 - 1280 \cdot N_r \cdot Re_{xb}^{-1.2}}{1 - 5120 \cdot Re_{xb}^{-1.2}} \quad (13)$$

$$Re_{xb} = \frac{Re \cdot X_B}{D_{to}} \quad (14)$$

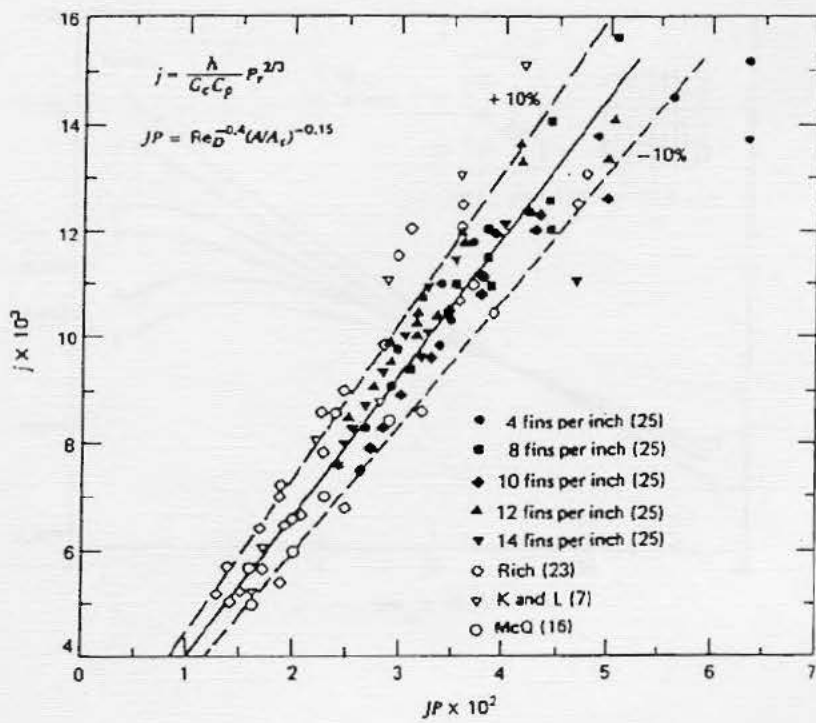
Re_{xb} = Reynolds number based on longitudinal spacing, X_B .

j_n = colburn factor for n number of rows which is greater than four.

N_r = number of tube rows in the air-flow direction.

The relationship between the JP parameter and the j factor is illustrated in Fig 4. This data was obtained experimentally by McQuiston et al, for plate fin coils at various air flow rates, fin spacing and tube rows. The variation of j factor with the number of rows is illustrated in Figure 5 .

FIG 4 Correlation of heat transfer data for smooth plate-fin-coils. [12]



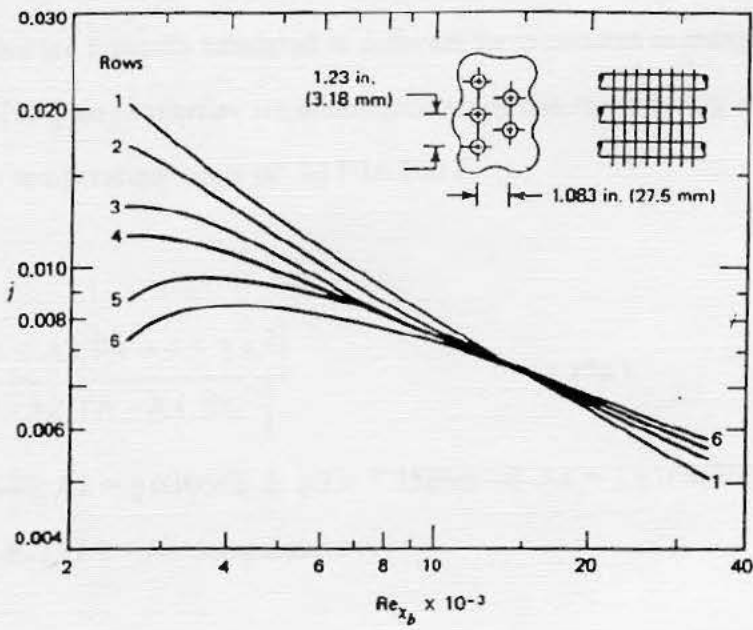


FIG 5: Variation in j factor with number of rows for smooth-plate-fin coils. [14]

Calculation of air side heat transfer coefficient :-

Colburn factor, j is related to Stanton St , and Prandtl Pr , numbers as :

$$J = St \cdot Pr^{.666} = \left(\frac{h_o}{G_c \cdot c_{pa}} \right) \left(\frac{\mu_a \cdot c_{pa}}{k_a} \right)^{.666} \quad (15)$$

$$h_o = \frac{J \cdot G_c \cdot c_p}{(Pr^{.6666})} \quad (16)$$

h_o is the air side heat transfer coefficient.

Fluid properties are typically tabulated at different temperatures in many texts. Based on these values, [19] air properties are determined using the curve fitting software, [13], and are valid over temperature range of 32 F to 200 F.

Air viscosity :

$$\mu_a = \frac{[A1 + A3 \cdot TA + A5 \cdot TA^2]}{[1 + A2 \cdot TA + A4 \cdot TA^2]} \quad (17a)$$

$A1 = .1980649$, $A2 = 3.03064E-3$, $A3 = 7.75636E-4$, $A4 = 1.61686E-6$

$A5 = 7.0747 E-7$, $TA =$ Air temperature

Air specific heat :

$c_{pa} = .24$ Btu/hr-lbm-F

Air thermal conductivity :

$$k_a = A6 + A7 \cdot TA + A8 \cdot TA^2 + \frac{A9}{TA} + \frac{A10}{TA^2} \quad (17b)$$

$A6 = .013071906$, $A7 = 2.59434E-5$, $A8 = -5.0315E-9$, $A9 = 3.736332E-3$

$A10 = .041698788$

The influence of fins on heat transfer from the finned surface, is typically expressed in terms of fin efficiency.

Calculations for fin efficiency and effectiveness :

To account for the variation in heat flux between the root of the fin and the fin tip, fin efficiency is calculated. The fin shape is hexagonal due to the staggered configuration. Calculations for fin efficiency and surface effectiveness taken from reference [2] are as follows :

$$\text{Dim1} = \frac{XA}{2} = 0.625 \text{ inch}$$

$$\text{Dim2} = \left[XB^2 + \left[\frac{XA}{2} \right]^2 \right]^{.5} = .625 \text{ inch}$$

Since Dim1 = Dim2, or $\beta = \text{Dim1} / \text{Dim2} = 1$, we have

$$\psi = (\text{Dim2} \cdot 2) / D_{to}$$

$$\frac{Re}{r} = 1.27(\Psi)(\beta - .3)^5; \text{ Re is the fin equivalent radius}$$

$$\phi = \left[\frac{Re}{r} - 1 \right] \left[1 + 35 \text{Ln} \frac{Re}{r} \right]; \phi \text{ is fin resistance number (constant)}$$

$$m = \left[\frac{2 \cdot ho}{\text{Kal} \cdot (T / 12)} \right]^{0.5}$$

$\eta = \tanh(m \cdot r \cdot \Phi) / (m \cdot r \cdot \phi)$; where η is the fin efficiency.

$$\eta_{so} = 1 - ((Af/A) \cdot (1 - \eta)); \text{ where } \eta_{so} \text{ is fin surface effectiveness.} \quad (17c)$$

Calculations for Refrigerant side heat transfer coefficient :

The refrigerant on tube side is undergoing evaporation.

Liu and Winterton equation, [9] is used for calculating the refrigerant side two-phase heat transfer coefficient.

$$h_i = \left[(E \cdot h_l)^2 + (S \cdot h_{\text{pool}})^2 \right]^{0.5} \quad (18)$$

h_i = two-phase refrigerant side heat transfer coefficient.

E = enhancement factor for the forced convection heat transfer.

S = suppression factor, takes into account suppression of nucleate boiling due to increase in forced convection.

h_l = liquid-only heat transfer coefficient, calculated using the Dittus-Boelter equation.

$$h_l = 0.023 \cdot \frac{k_l}{D_{ti}} \cdot Re_l^{0.8} \cdot Pr_l^{0.4} \quad (18 b)$$

$$h_{\text{pool}} = 0.00122 \cdot \left[\frac{k_l^{.79} \cdot c_{pl}^{.45} \cdot \rho_L^{.49}}{SIG^{.5} \cdot \mu_l^{.29} \cdot h_{fg}^{.24} \cdot \rho_v^{.24}} \right]$$

h_{pool} = pool boiling heat transfer coefficient.

$$E = \left[1 + x \cdot Pr_l \cdot \left(\frac{\rho_l}{\rho_v} - 1 \right) \right]^{0.35}$$

x is the quality of the refrigerant exiting the evaporator.

$$S = \frac{1}{1 + 0.055(E^{.1}) \cdot (Re_l)^{.16}}$$

Refrigerant properties:

The properties of the refrigerants R-152a, R-134a, R-402 a, R-404a, R-11 and R-12 are tabulated in Tables 2 through 5. [2], [3], [4]

TABLE 2 : Properties of refrigerants at 5 F

<u>Properties</u>	<u>Refrigerant</u>			
	<u>R-134a</u>	<u>R-152a</u>	<u>R-12</u>	<u>R-22</u>
Pressure, psia	23.76	21.57	26.46	42.96
Density, liq, lbm/cuft	83.72	61.92	90.05	83.09
Density, vap	.517	.302	.680	.806
Enthalpy, liq, Btu/lbm	13.63	17.47	9.54	11.92
Enthalpy, vap	103.74	155.65	78.11	105.00
Enthalpy of vaporization	90.11	138.18	68.57	93.08
Sp. ht, liq, Btu/lbm-F	.309	.396	.215	.271
Viscosity, liq, lbm/ft-hr	.843	.617	.735	.597
Th. conductivity, liq, Btu/hr-ft-F	.058	.0718	.0478	.0593
Surface tension, lbm/sqhr	396629.92	427754.95	405196.44	450884.55

TABLE 3 : Properties of refrigerants at 25 F

<u>Properties</u>	<u>Refrigerant</u>			
	<u>R-134a</u>	<u>R-152a</u>	<u>R-12</u>	<u>R-22</u>
Pressure , psia	36.78	33.23	39.26	63.52
Density , liq, lbm/cuft	81.55	60.41	87.90	80.84
Density , vap	.784	.456	.986	1.172
Enthalpy, liq, Btu/lbm	19.89	25.49	13.91	17.47
Enthalpy, vap	106.61	159.03	80.30	106.89
Enthalpy of vaporization	86.72	133.53	66.39	89.41
Sp. ht , liq, Btu/lbm-F	.316	.404	.219	.277
Viscosity, liq, lbm/ft-hr	.730	.542	.650	.530
Th. conductivity, liq, Btu/hr.ft.F	.0550	.0681	.0454	.0566
Surface tension, lbm/sq.hr	350370.71	393203.31	405196.44	450884.55

TABLE 4 : Properties of refrigerants at 35 F

<u>Properties</u>	<u>Refrigerant</u>			
	<u>R-134a</u>	<u>R-152a</u>	<u>R-12</u>	<u>R-22</u>
Pressure, psia	45.07	40.65	47.20	76.24
Density, liq, lbm/cuft	80.42	59.62	86.79	79.67
Density, vap	.953	.553	1.175	1.39
Enthalpy, liq, Btu/lbm	23.08	29.57	16.127	20.27
Enthalpy, vap	108.01	160.66	81.36	107.76
Enthalpy of vaporization	84.93	131.09	65.24	87.49
Sp.ht, liq, Btu/lbm-F	.320	.409	.222	.28
Viscosity, liq, lbm/ft-hr	.681	.509	.612	.499
Th. conductivity, liq, Btu/hr.ft.F	.0536	.0662	.0442	.0552
Surface tension, lbm/sq.hr	327812.2	370644.8	405196.44	450884.55

TABLE 5 : Properties of refrigerants at 40 F

<u>Properties</u>	<u>Refrigerant</u>					
	<u>R-134a</u>	<u>R-152a</u>	<u>R-12</u>	<u>R-402a</u>	<u>R-404a</u>	<u>R-22</u>
Pressure (psia)	49.72	44.81	51.60	102.2	95.8	83.28
Density, liq(lbm/cuft)	79.85	59.23	86.23	78.5	72.7	79.07
Density, vap(lbm/cuft)	1.048	.608	1.27	2.32	2.05	1.52
Enthalpy, liq (Btu/lbm)	24.69	31.62	17.24	----	-----	21.68
Enthalpy, vap (Btu/lbm)	108.70	161.47	81.89	----	-----	108.19
Enthalpy of vap, Hfg	84.01	129.84	64.64	68.7	71.7	86.50
Sp ht, liq (Btu/lbm-F)	.322	.411	.223	.289	.321	.282
Viscosity, liq (lbm/ft-hr)	.658	.494	.595	.495	.437	.484
Th. conductivity, liq	.0528	.653	.0436	.0423	.0423	.0545
Surface tension	316410.42	359531.3	405222.3	249872.85	213034.45	450913.0

The overall heat transfer coefficient can be obtained from :-

$$\frac{1}{U_o} = \frac{1}{h_o \eta_{so}} + \frac{1}{h_i \left(\frac{A_i}{A_o} \right)} + R_w A_o \quad (19)$$

$\frac{A_i}{A_o}$ = refrigerant side to the air-side heat transfer area ratio.

$$\frac{A_i}{A_o} = \frac{3.1415 \cdot D_{ti}}{X_A \cdot X_B \cdot \alpha}$$

R_w = tube wall resistance.

$$R_w \cdot A_o = \frac{D_{ti} \cdot \ln \left(\frac{D_{ti}}{D_{to}} \right)}{2 \cdot K_{cu} \cdot \frac{A_i}{A_o}} \quad (19b)$$

K_{cu} = thermal conductivity of copper.

Calculation for the Height and Length of Heat Exchanger :

$$A_{fr} = \frac{Q_A}{V_A} \quad (20)$$

$$m_{ref} = \rho_{ref} \cdot V_{ref} \cdot A_{ref} \quad (21)$$

$$A_{ref} = \frac{\Pi}{4} \cdot [D_{ti}^2] \cdot N_{tr} \quad (22)$$

A_{fr} = evaporator frontal area.

m_{ref} and A_{ref} = refrigerant mass flow rates, flow areas respectively.

N_{tr} = number of rows in the transverse direction.

$$H = N_{tr} \cdot [X_A/2] \quad (23a)$$

$$L = A_{fr} / H \quad (23b)$$

H and L are the exchanger height and length respectively.

Computation of heat transfer area and number of rows :

$$Q = m_a \cdot C_{pa} \cdot [T_{AI} - T_{AO}]$$

$$A_o = \frac{Q}{U_o \cdot F \cdot \text{LMTD}}$$

$$W = \frac{A_o}{\alpha}$$

$$N_r = \frac{W \cdot 12}{XB} \quad (23c)$$

The overall dimensions of the plate fin heat exchanger is thus determined from the equations (23a), (23b) and (23c)

Q = rate of heat transfer, W = exchanger depth

Nr = number of tube rows in the air flow direction.

Computation of FP parameter and friction factor :

Generalized correlation for the friction factor is more involved than heat transfer data and depends on evaporator, fin geometry and the air side flow rate.

The FP parameter and friction factor are calculated as follows. [12]

$$FP = Re_D^{-.25} \left[\frac{D_{to}}{D^*} \right]^{.25} \left[\frac{XA - D_{to}}{4(S1 - T)} \right]^{-.4} \left[\frac{XA}{D^*} - 1 \right]^{-.5} \quad (24)$$

where, D^* is hydraulic diameter for the air side flow over the finned surface, defined by

$$D^* = \frac{D_{to} \left(\frac{A}{At} \right)}{1 + \left(\frac{XA - D_{to}}{S1} \right)}$$

and S1 is fin pitch given by $S1 = 1/S$.

$$f = .004904 + 1.382 (FP^2) \quad (25)$$

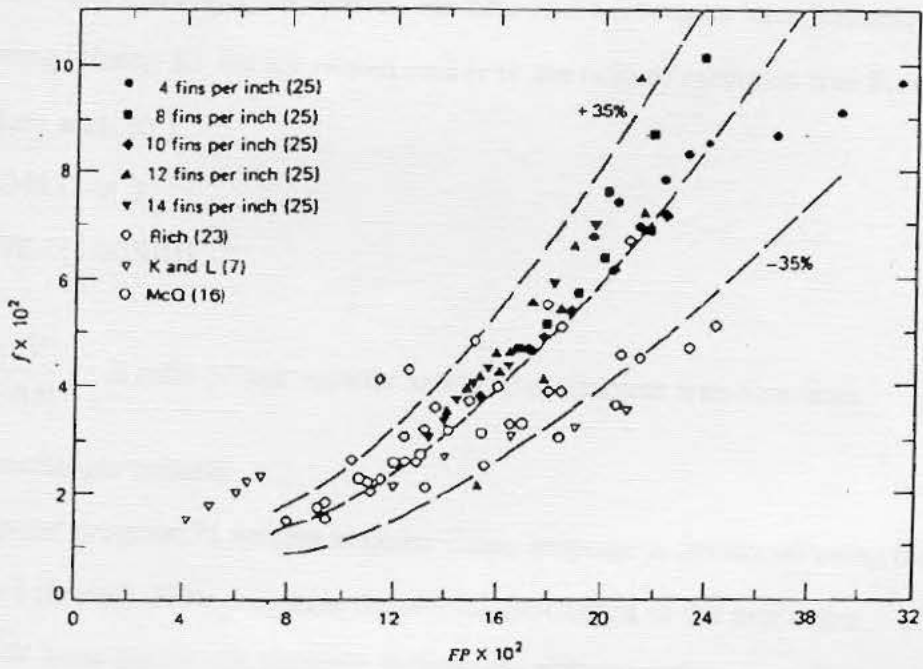
f is the air side flow friction factor .

Relationship between FP parameter and the friction factor is illustrated in Figure 6.



FIG 6

Correlation of friction data for smooth plate-fin-coils. [12]



Air Pressure Drop: [12]

Air pressure drop due to the air flow rate depends on air density at inlet and outlet, entrance and exit loss coefficients, friction factor, heat transfer area, evaporator, fin geometry and is given by:

$$APD = \frac{G_c^2}{2 \cdot g_c \cdot \rho_1} \left[(K_i + 1 - \rho^2) + 2 \left(\frac{\rho_1}{\rho_2} - 1 \right) + f \frac{A}{A_c \rho_m} - (1 - \sigma^2 - K_e) \frac{\rho_1}{\rho_2} \right] \dots (26)$$

APD = air side pressure drop.

K_i , K_e are entrance and exit loss coefficients and depend on the type of surface, contraction ratio and Reynolds number. Fin tube heat exchangers have Reynolds number approaching infinity. K_i , K_e are related mainly to the ratio of minimum free flow area to frontal flow area, (σ).

$$K_i = .4048 (1 - \sigma)$$

$$K_e = [.998 - (1.005 \cdot \sigma)]$$

$\frac{A}{A_c} = \frac{\alpha \cdot V}{\sigma \cdot A_{fr}}$, is ratio of heat transfer area to the minimum free-flow area.

V is the exchanger volume.

The computer program P1 written in Quick Basic language is developed using the above equations 1 through 26 to determine the overall dimensions of the exchanger, ($L \times H \times W$) and the air side pressure drop for six different refrigerants. The results obtained from this program are presented in next chapter.

“Drop in” evaluation of alternate refrigerants for plate fin tube evaporator :

Performance of the evaporator, such as the one designed above employing an alternate refrigerant, is evaluated using the developed computer program P2, to compare with that using the conventional refrigerant. The volume of the evaporator is specified. The mass flow rate of the refrigerant, air-side velocity, inlet refrigerant quality/enthalpy and the

inlet air temperature are fixed. The impact on the effectiveness, capacity and pressure drop of the evaporator for the alternate refrigerant refrigerant is determined. The effect of the evaporator temperature and the refrigerant quality at the inlet on the evaporator performance is also evaluated.

In order to perform this evaluation, the following data is fixed :

Data related to the evaporator geometry :

Height of the evaporator, $H = .8$ ft.

Length of the evaporator, $L = 10$ ft.

Depth of the evaporator, $W = 0.8$ ft.

Fins per inch, $S = 8$.

Fin thickness, $T = 0.006$ inches.

Tube outer diameter, $D_{to} = 1.25$ inches.

Tube inner diameter, $D_{ti} = 1.083$ inches.

Transverse spacing, $X_A = 1.25$ inches.

Longitudinal spacing, $X_B = 1.083$ inches.

Data related to Flow conditions :

Refrigerant mass flow rate, $R_{mass} = 2700$ lbm / hr.

Air frontal velocity, $V_A = 750$ fpm

Evaporator temperature, $T_E = 40$ F, 35 F, 25 F and 5 F (varied)

Quality of refrigerant in = 0%, 10%, 20%, 30% and 39% (varied)

Air temperature inlet, $T_{AI} = 85$ F.

APPROACH :

The steps involved in performing this evaluation are as follows :

1) Calculate the heat transfer area.

$$AO = V \cdot \alpha$$

α is the heat exchanger area to volume ratio.

Recall equation 3 : $\alpha = 14.659 + 19.766(S)$

2) Properties of air at the inlet temperature are calculated employing equations 17a and 17b.

3) Calculate air side heat transfer coefficient based on inlet air temperature.

Recall equation 16: $h_o(1) = j \cdot G_c \cdot c_{pa} / (Pr_a)^{0.666}$

$h_o(1)$ = Initial estimate (first iterated value) of h_o .

4) Compute the Refrigerant side heat transfer coefficient, h_i , using equation 18. The initial value, $h_i(1)$ of h_i is calculated using the first guess of exit quality, as 1, i.e

$$x(1) = 1.$$

5) Calculate the overall heat transfer coefficient, U_o .

Recall eqn 19: $1/U_o(1) = 1/(h_o(1) \cdot \eta_{so}) + 1/(h_i(1) \cdot A_i/A_o) + R_w \cdot A_o$

6) Calculate the exchanger NTU.

$$NTU(1) = U_o(1) \cdot AO / C_{min}$$

C_{min} is the product of mass flow rate and specific heat of air. C_{min} is C_{air} here, because C_{ref} is infinity (refrigerant undergoes phase change).

Calculate the effectiveness of the evaporator. Equation for counter-flow is used. Cross-flow heat exchanger with multiple tube passes approaches counterflow [17].

$$EHX(1) = 1 - (e^{-NTU(1)}).$$

7) Initial guess values for the outlet temperatures of the air and the refrigerant enthalpy are calculated from :

$TAO(1) = TAI - EHX(1) \cdot (TAI - TE)$ Air exit temperature, initial

$HRO(1) = EHX(1) \cdot (C_{min} / m_{ref}) \cdot (TAI - TE) + H_{in}$ Refrigerant exit enthalpy, initial

$Q(1) = C_{air} \cdot (TAO(1) - TE)$ or $m_{ref} \cdot (HRO(1) - H_L)$

$X(2) = Q(1) / (m_{ref} \cdot h_{fg}) + X_1$

X(2) is the value of the exit quality of the refrigerant (from second iteration).

X1 is the inlet quality of the refrigerant

8) The steps from 2 through 7 are repeated. Air side heat transfer coefficient, h_o (new) is calculated at the bulk air temperature. Refrigerant side heat transfer coefficient, h_i (new) is calculated using the exit quality x , as calculated in step 7.

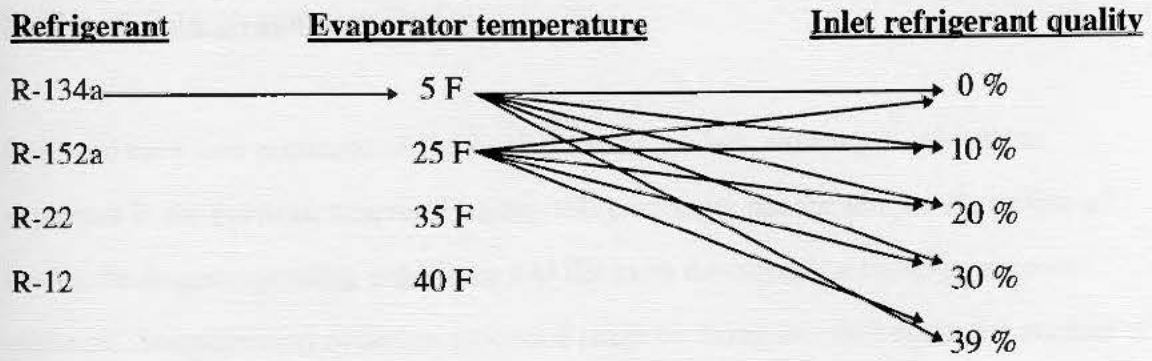
9) Calculations are repeated until,

Absolute value of $\{EHX(new) - EHX(old)\}$ is less than the specified tolerance.

10) Finally, the pressure drop on the air side is calculated using equation 26.

A computer program P2, written in QuickBasic language is developed following the above ten steps to determine the heat duty, exit fluid temperature, heat exchanger effectiveness and the air side pressure drop.

The evaporator performance-data points were obtained by running the computer program eighty times i.e. (twenty times for each refrigerant) to encompass the range of cases shown below :



For R-134a, at a given evaporator temperature, the program was run at five values of the inlet refrigerant qualities, i.e, twenty times in all. The results obtained from this program are presented in the next chapter.

Shell and Tube Evaporator Design :

Shell and tube heat exchanger is the work horse of the heat exchanger industry as explained in the previous chapter. Besides, this exchanger has the unique distinction of having the largest operating experience and the most developed technology since its existence. Simplification of design process is made by fixing the shell diameter, number of tubes and baffle spacing. The required length of tube, number of baffles, shell side pressure drop are estimated from the procedure outlined below.

Shell side fluid is chilled water while refrigerant is flowing through tubes. Exchanger is designed for specified heat duty.

Data fixed for geometrical parameters :

Tube outer diameter, D_{to} = .75 inch

Tube inner diameter, D_{ti} = .606 inch

Tube pitch, P = 1 inch

The tube pitch is the center-line distance between two consecutive tubes in the heat exchanger. The tube pitch is generally between 0.5 to 1.25 inches.

Layout angle, θ = 30 degree

Tube layout angle is usually 30, 45, 60 or 90 degrees

Layout pattern is triangular.

Different types of layout pattern are possible, i.e, square, triangular or rotated square.

Transverse spacing, X_A = $P \cdot \sin\theta$ = .5

Longitudinal spacing, X_B = $P \cdot \cos\theta$ = .866

Tube metal thermal conductivity, K_{cu} = 227 Btu / hr-sqft-F, tube material is copper.

Shell inner diameter, D_s = 20 inch

Baffle spacing, P_b = 40 % of D_s = 8 inch

Baffle spacing between 10% to 60% of the shell diameter was most frequently observed during the literature survey.

Baffle cut, $L_c = 20\%$ of $D_s = 4$ inch

number of shell passes = 1

number of tube passes = 2

Data fixed for Flow conditions

The refrigerant and water flow conditions are as follows :

Water flow rate, $Fl_w = 3260$ lbm / min

Entering water temperature, $T_{WI} = 45.2$ F

Leaving water temperature, $T_{WO} = 44.6$ F

Water temperatures, typical of cooling tower.

Evaporator temperature, $T_E = 40$ F

Quality of refrigerant entering evaporator = 0%, saturated liquid state.

Quality of refrigerant leaving evaporator = 100 %

Calculation of shell side geometrical parameters

Number of tubes :

Number of tubes in the exchanger is a function of shell inner diameter, tube pitch, layout pattern, number of tube side passes and the tube outer diameter.

Number of tubes are determined from the following equation. [16].

$$NT = \frac{.78539 \left[\frac{CTP}{CL} \right] \cdot [D_s^2]}{PR^2 \cdot [D_{to}^2]} \quad (27)$$

NT = number of tubes

The constant CTP accounts for incomplete coverage of shell inner diameter by tubes.

CTP = .9 for one tube pass, 0.8 for two tube pass, 0.7 for four tube passes.

CL is tube layout constant.

CL = .87 for triangular and square arrangement, 1 for rotated square square arrangement.

PR = pitch ratio = P / D_{to} .

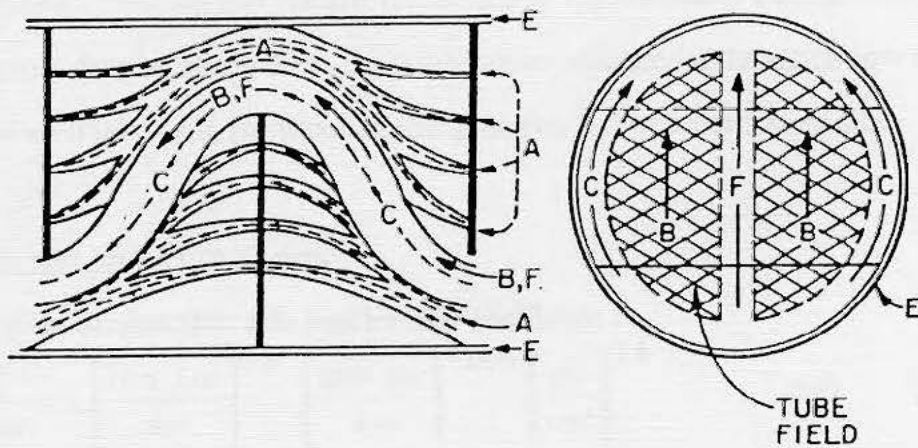
Literature search revealed several methods for the shell side design. The methods as outlined by Taborek et al, Palen et al, Delaware et al., [17] are popular methods.

Delaware method is followed for shell side thermal-hydraulic design. Description of this method follows.

Delaware method :-

Shell side flow mechanism is explained in Fig 7. Five different streams have been identified on the shell side. Stream B is the main cross flow stream flowing through one window across the cross flow section and out through the opposite window. This is the stream that is desired on the shell side of the exchanger. However, because of the mechanical clearance required in a shell and tube exchanger, there are four other streams which compete with the B stream. Stream A is the leakage stream passing through the clearances between the tubes and the baffle, from one baffle compartment to the next. C stream is bundle bypass stream flowing around the tube bundle between the outermost tubes in the bundle and the inside of the shell. The E stream is the shell-to-baffle leakage stream flowing through the clearance between the baffles and the inside diameter of the shell. The last of the identified major stream is the F stream, which flows through any channels within the tube bundle caused by the provision of pass dividers in the exchanger header, i.e. only in multiple tube pass configurations. For the two tube pass configuration, as in this analysis, the pass divider is oriented perpendicular to the direction of the main cross flow stream and does not provide an internal bypass stream.

Figure 7 : Diagram for shell side flow mechanism (Delaware method)



In the Delaware method, the B stream is regarded as the essential stream in the exchanger with the other streams exerting various modifying effects upon the performance as predicted from the B stream alone. The various leakage and bypass streams effect the heat transfer in two ways: 1) They reduce the B stream and therefore the local heat transfer coefficient, and 2) they alter the shell side temperature profile. The Delaware method in effect lumps these two effects together into various correction factors for the shell side flow. This decreases the heat transfer coefficient by approximately 60% and increases shell side pressure drop by nearly 20 % from the values calculated if the entire flow took place across an ideal tube bank corresponding in geometry to one crossflow section.

Shell side heat transfer coefficient

Computation of ideal shell side heat transfer coefficient :

$$\frac{h_{ideal}}{c_{pw} \cdot G_w} = a \cdot \left[\frac{D_{to} \cdot G_w}{\mu_w} \right]^{-m} \cdot \left[\frac{c_{pw} \cdot \mu_w}{k_w} \right]^{-.666} \cdot \left[\frac{\mu_w}{\mu_{wl}} \right]^{1.4} \quad (28) \quad [18]$$

h_{ideal} = heat transfer coefficient for pure cross flow in an ideal tube bank.

μ_{wl} = viscosity at the wall temperature.

G_w = mass flow of water in lbm / sqft-hr.

a and m are constants, tabulated in Table 6, and depend upon the shellside Reynolds number and tube layout pattern.

Table 6: Constants for flow across ideal tube banks [18]

$D_{to} \cdot G_w / \mu_w$	Tube-pitch	m	a
Above 200,000	Staggered	.3	.166
Above 200,000	In - Line	.3	.124
300 to 200,000	Staggered	.365	.273
300 to 200,000	In-Line	.349	.211
Below 300	Staggered	.640	1.309
Below 300	In - line	.569	.742

G_w = shell side mass velocity.

$$G_w = (F_{lw} \cdot 60) / a_c$$

Shell side cross flow area, a_c depends upon tube pitch, baffle spacing, tube outer diameter and the shell inner diameter.

For triangular and square tube patterns,

$$a_c = \frac{D_s \cdot P_b \cdot [P - D_{to}]}{P} \quad (29) \quad [18]$$

For rotated triangular tube patterns,

$$a_c = \frac{1.155 \cdot D_s \cdot P_b \cdot [P - D_{to}]}{P}, \text{ when } XA \text{ is less than } 3.73 D_{to}.$$

$$a_c = D_s \cdot P_b \cdot \left[1 - .577 \left[\frac{D_{to}}{P} \right] \right], \text{ when } XA \text{ is greater than } 3.73 D_{to}. \quad [18]$$

Computation of actual shell side coefficient

From Delaware method,

$$h_o = h_{ideal} \cdot F_1 \cdot F_r \cdot F_c \cdot F_b \quad (30) \quad [1]$$

F_1 , is the correction factor for baffle leakage effects, including both shell to baffle and tube to baffle leakage. The correlation for F_1 penalizes the design if the baffles are put too close together, leading to an excessive fraction of flow being in the leakage streams compared to the crossflow. [18]

$$F_1 = 0.8 \left[\frac{P_b}{D_s} \right]^{\frac{1}{6}} \text{ for fouled bundles.}$$

$$F_1 = 0.8 \left[\frac{P_b}{D_s} \right]^{\frac{1}{4}} \text{ for clean bundles.}$$

F_r , is the correction factor for adverse temperature gradient build-up. It applies only in deep laminar flow when the shell side Reynolds number is less than 100. In laminar flow the heat transfer coefficient decreases with increasing distance from the start of heating because of the development of an adverse temperature gradient from the conduction process. This temperature gradient decreases the heat transfer coefficient.

$$F_r = 1 \quad \text{when } Re_s \text{ is greater than } 100.$$

$$F_r = 0.2 [Re_s]^{.333} \quad \text{when } Re_s \text{ is less than } 100.$$

F_c , is correction factor for baffle cut and spacing [18]. This correction factor is essentially a function of the fraction of the total tubes in the heat exchanger that are in crossflow (i.e ., located between the baffle tips of adjacent baffles). This value is equal to 1.0 for a heat exchanger in which there are no tubes in the window, increases to a value as high as 1.15 for a design in which windows are relatively small, and decreases to a value of about .52 for very large baffle cuts. A typical value for a well- designed heat exchanger is about 1.0 . F_c value of 1.1 is assumed. F_b is the correction factor for the bundle bypass

flow i.e, C stream in Figure 7. For relatively small difference between the outermost tubes and the shell, as in a fixed tube sheet construction, F_b is nearly 0.9, whereas for much larger clearances required by pull through floating head construction, F_b is about 0.7 [18] Proper use of sealing strips can increase F_b from 0.7 to 0.9 in pull through floating head heat exchangers. F_b value of 0.9 is assumed in this analysis.

Computation of Refrigerant side heat transfer coefficient :

Two phase flow heat transfer coefficient on the refrigerant side is computed using equation 18.

Overall heat transfer coefficient and heat transfer area :

Overall heat transfer coefficient is computed using:

$$1 / U_o = 1 / h_o + 1 / h_i + (D_{to} - D_{ti}) \cdot (D_{to} / D_{ti}) / (12 \cdot K_{cu})$$

$$A_o = Q / (U_o \cdot F \cdot LMTD.)$$

$$A_{effec} = A_o \cdot F_1 \cdot F_2 \cdot F_3$$

A_{effec} is the effective heat transfer area. [1].

F_1 is tube layout correction factor. It depends upon tube pitch, layout pattern and tube outside diameter.

F_2 is correction factor for the number of tube passes.

F_3 is correction factor for shell construction / tube bundle layout.

These correction factors are tabulated in Tables 7 through 9.

Tube length and number of baffles

$$L = \frac{A_{effec}}{\pi \cdot D_{to} \cdot N_t} \quad ; \quad L \text{ is the tube length.} \quad (30a)$$

$$N_b = \frac{L_s}{P_b} - 1 \quad ; \quad N_b \text{ is number of baffles.} \quad (30b)$$

$$L_s \text{ is the shell length ; } L_s = \frac{L}{\text{number of tube passes}} \quad (30c)$$

TABLE 7 : values of F1 for various tube diameters and layouts [1].

Tube outside diameter, in.	Tube Pitch, in	Layout	F1
5/8	13/16	triangular	0.9
5/8	13/16	square , rotated square	1.04
3/4	15/16	triangular	1.00
3/4	15/16	square , rotated square	1.16
3/4	1	triangular	1.14
3/4	1	square , rotated square	1.31
1	1 1/4	triangular	1.34
1	1 1/4	square , rotated square	1.54

$$F1 = \frac{[\text{Heat transfer area / cross-sectional area of unit cell}]_{\text{reference}}}{[\text{Heat transfer area / cross-sectional area of unit cell}]_{\text{new case}}}$$

Shell Inside diameter, in	F2			
	number of tube side passes.			
	2	4	6	8
up to 12	1.2	1.40	1.80	--
13-1/4 to 17- 1/4	1.06	0.18	1.25	1.50
19-1/4 to 23-1/4	1.04	1.14	1.19	1.35
25 to 33	1.03	1.12	1.16	1.20
35 to 45	1.02	1.08	1.12	1.16
48 to 60	1.02	1.05	1.08	1.12
above 60	1.01	1.03	1.04	1.06

TABLE 8 values of F2 for various tube passes [1].

Type of tube bundle construction.	F3				
	inside shell diameter				
	up to 12	13 1/4 - 21 1/4	23 1/4 - 35	35-48	48+
Fixed tube sheet	1	1	1	1	1
split backing ring	1.30	1.15	1.09	1.06	1.04
outside packed floating head	1.30	1.15	1.09	1.06	1.04
U tube	1.12	1.08	1.03	1.01	1.01
Pull through floating head	----	1.40	1.25	1.18	1.15

TABLE 9 : values of F3 for various tube bundle construction [1].

Shell side pressure drop:-

The pressure drop consists of

- 1) internal crossflow section
- 2) window section
- 3) inlet and outlet section

Internal crossflow section pressure drop : Internal crossflow section of evaporator is shown in Figure 8.

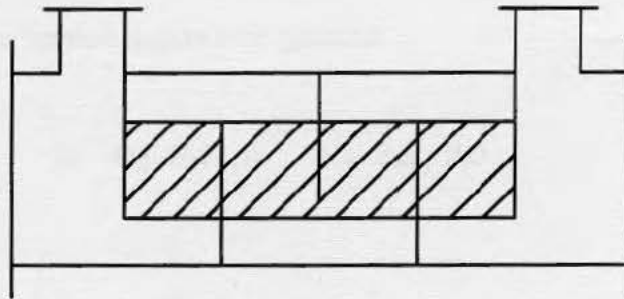


FIG 8 Internal cross flow section

The pressure drop is calculated as follows. [18] :

$$\Delta P_f = \frac{4 f G_w^2 N_r [N_b - 1] R_l . R_b . \phi}{2 . (144) g . \rho_w} \quad (31)$$

ΔP_f = pressure drop for cross flow across tube bundle.

N_r is the number of vertical rows.

$N_r = b D_s / X_A$, where $b = 0.7$ for triangular tube patterns

$b = .6$ for square tube patterns

$b = 0.85$ for rotated square tube patterns

$$\phi = \left[\frac{\mu w l}{\mu w} \right]^n, \quad \text{where } n = .14 \text{ for } Re_s \text{ greater than } 300$$

where $n = .25$ for Re_s less than 300

The friction factor, f , is calculated as follows:

$$f = \frac{z}{\left[\frac{D_g G_w}{\mu w} \right]^{.25}} \quad \text{for } D_g G_w / \mu w \text{ greater than } 100.$$

where, $z = 1.0$ for square and triangular tube patterns.

$z = 0.75$ for rotated square tube patterns

$$f = \frac{r}{\left[\frac{D_g G_w}{\mu w} \right]^{.725}} \quad \text{for } D_g G_w / \mu w \text{ less than } 100.$$

where, $r = 10$ for triangular patterns

$r = 5.7$ for square and rotated tube patterns

D_g is defined as the gap between the tubes:

$$D_g = P - D_t$$

Correction factors:

R_l is the correction factor for effect of baffle leakage on the pressure drop.

$$R_l = 0.6 \left[\frac{P_b}{D_s} \right]^{.5} \quad \text{for clean bundles}$$

$$R_l = 0.75 \left[\frac{P_b}{D_s} \right]^{\frac{1}{3}} \quad \text{for bundles with assumed fouling.}$$

R_b is the correction factor for effect of bundle bypass on the pressure drop.

R_b can be approximated from the following equations :

$$R_b = 0.8 [D_s]^{0.08} \text{ for clean bundles}$$

$$R_b = 0.85 [D_s]^{0.08} \text{ for bundle with assumed fouling.}$$

Window section pressure drop:

Window section of the evaporator is shown in Fig 9.

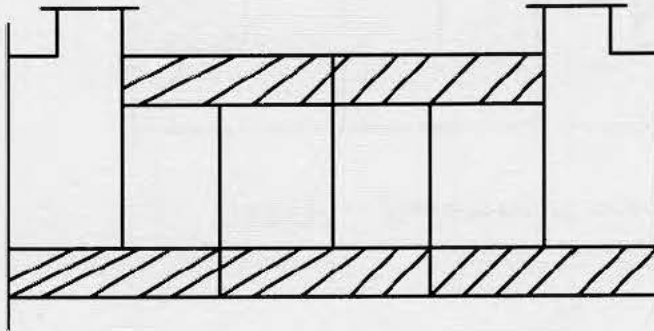


Fig 9 : Window section of the evaporator

$$\Delta P_w = \left[\frac{G_w^2 \phi_{ac} \cdot N_b \cdot R_l \cdot [2 + N_w]}{2 \cdot (144) \cdot \rho \cdot g \cdot a_w} \right] \quad (33) \quad [18]$$

ΔP_w is window section pressure drop.

a_w is window section flow area approximated by following equations.

$$a_w = 0.055 D_s^2 \quad \text{for triangular tube patterns.}$$

$$a_w = .66 D_s^2 \quad \text{for square and rotated square patterns.}$$

N_w is the number of tube rows in the baffle window.

$(2 + N_w)$ can be approximated with the following term:

$$2 + N_w = m [D_s]^{.625}$$

where $m = 3.5$ for triangular tube patterns

$m = 3.2$ for square tube patterns

$m = 3.9$ for rotated square tube patterns.

Inlet and outlet section pressure drop : Inlet and outlet section of the evaporator is shown in Figure10.

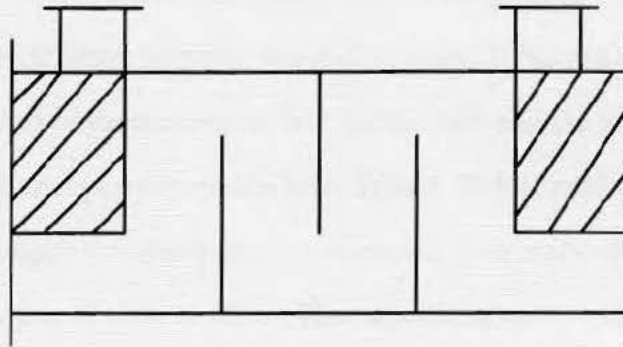


Figure 10 : Inlet and outlet sections.

$$\Delta P_{fi} = \frac{4(2.66)f \cdot Gw^2 \cdot Nr \cdot Rb \cdot \phi}{2(144)g\rho} \quad (34) \quad [18]$$

ΔP_{fi} is pressure drop for the inlet and outlet sections.

The total pressure drop on the shell side is then given by :

$$\Delta P_s = \Delta P_f + \Delta P_{fi} \dots\dots\dots(35)$$

The design of shell and tube heat exchanger is now complete. The Equations 30a, 30b and 30c provide the length of the tube, number of baffles and the length of the shell respectively, while the equation 35 gives the total shell side pressure drop. A computer program P3 written in Quick Basic language is developed using Equations 27 through 35 to determine these design parameters. This design procedure is repeated for six different refrigerants.

Plate fin tube compact heat exchanger :

The number of fins on the exchanger surface, air velocity, water/ refrigerant velocity are important design parameters affecting the performance of the plate fin tube compact heat exchanger. The effect of the number of fins, air velocity and the water velocity on the plate fin tube exchanger performance is investigated. Before performance analysis of plate fin tube exchanger is undertaken, it is necessary to specify exchanger geometry. The height, length , number of rows in the air flow direction, outer and inner tube diameter, transverse and longitudinal spacing, fin thickness, fluid inlet temperatures are fixed. The number of fins per inch, air velocity and water velocity are variables. The impact on Colburn, friction factors, effectiveness, air-side pressure drop, air-side heat transfer coefficients and overall heat transfer coefficient is analyzed.

Fixed geometrical parameters :

Height of exchanger, H	= 3 ft
Length of exchanger, L	= 4 ft
Number of rows	= 4
Tube outer diameter, D _{to}	= .525 inch
Tube inner diameter, D _{ti}	= .483 inch
Transverse spacing, X _A	= 1.25 inch
Longitudinal spacing, X _B	= 1.083 inch
Fin thickness, T	= .006 inch
Fins per inch, S varied from 4 to 14.	

Fixed Flow conditions :

Entering air temperature, T _{AI}	= 70 F
Entering water temperature, T _{WI}	= 50 F

Air face velocity, V_A, varied from 200 to 800 feet per minute.

Water velocity, VW, varied from 1 to 6 feet per second.

Effect of fins per inch :

Air velocity was fixed at 500 fpm, water velocity fixed at 2 fps. Number of fins per inch were increased from 4 to 14.

Effect of air velocity :

Water velocity fixed at 2 fps. Number of fins fixed at 4 per inch. Air velocity was varied from 200 to 800 fpm.

Effect of water velocity :

Air velocity fixed at 500 fpm. Number of fins fixed at 4 per inch. Water velocity, varied from 1 to 6 fps.

To investigate the impact of the air velocity and the number of fins simultaneously on the exchanger performance, the program was run sixteen times. At a fixed value for the number of fins, the program was run for four air velocities (200 , 400, 600 and 800 fpm). Four different values of fins per inch were selected, (4 fpi, 6fpi, 8 fpi and 10 fpi).

Methodology

1) Calculate the heat transfer area.

$$A_0 = \alpha \cdot V$$

$$\alpha = 14.65963 + 19.76648 (S)$$

2) Determine the initial value of the water side heat transfer coefficient hi (1) based on inlet temperature of water using equation 18b.

$$\frac{hi(1) \cdot D_{ti}}{k_w} = 0.023 Re_w^{.8} \cdot Pr_w^{.3}$$

Properties of water [13].

Water density :

$$p_w = A_{11} + (A_{12} \cdot T_W) + (A_{13} \cdot T_W^2) + (A_{14} \cdot T_W^3).$$

$$A_{11} = 62.13798536$$

$$A_{12} = 7.133019 \text{ E-}03$$

$$A_{13} = -1.1418\text{E-}04$$

$$A_{14} = 1.15173\text{E-}07.$$

Water thermal conductivity :

$$k_w = A_{15} + (A_{16} \cdot T_W) + (A_{17} \cdot T_W^2) + (A_{18} \cdot T_W^3).$$

$$A_{15} = 0.291975$$

$$A_{16} = 9.59507\text{E-}04$$

$$A_{17} = -2.821\text{E-}06$$

$$A_{18} = 2.58806\text{E-}09$$

Water viscosity :

$$\mu_w = A_{19} + (A_{20} \cdot T_W) + (A_{21} \cdot T_W^{2.5}) + (A_{22} \cdot T_W^3) + (A_{23} \cdot \text{LOG} (T_W^2))$$

$$A_{19} = 9.949940748$$

$$A_{20} = 0.045519659$$

$$A_{21} = -6.2578\text{E-}06$$

$$A_{22} = 2.09856\text{E-}07$$

$$A_{23} = -.58617528$$

The properties are valid over a temperature range of 40 F to 150 F.

3) Determine air-side heat transfer coefficient based on inlet air temperature using equation 16.

4) Calculate Overall heat transfer coefficient using equation 19.

$$\frac{1}{U_o(1)} = \frac{1}{h_o(1) \cdot \eta_{so}} + \frac{1}{h_i(1) \cdot \frac{A_i}{A_o}} + R_w A_o$$

5) Determine exchanger NTU and effectiveness.

$$NTU(1) = \frac{U_o(1) \cdot A_o}{C_{min}} ; \text{ where } C_{min} \text{ is the minimum of the product of mass flow rate and}$$

specific heat for the two fluids considered.

$$EHX(1) = \frac{1 - \exp[-NTU(1)(1 - Cr)]}{1 - Cr \exp[-NTU(1)(1 - Cr)]}$$

$$Cr = C_{min} / C_{max},$$

6) Estimate the initial guess for the air and water outlet temperatures as follows :

If $C_{air} < C_{water}$, then:

$$TAO(1) = TAI - EHX(1) \cdot (TAI - TWI)$$

$$TWO(1) = TWI + Cr(TAI - TAO(1))$$

If $C_{water} < C_{air}$, then

$$TAO(1) = TAI - (C_{wat} / C_{air}) \cdot (TWO(1) - TWI)$$

$$TWO(1) = TWI + (EHX(1)) \cdot (TAI - TWI).$$

$$Q(1) = m_a \cdot c_{pa} \cdot [TAI - TAO(1)]$$

7) Steps 2 through 6 are repeated using new estimated average temperatures.

Continue the process until the absolute value of $EHX_{new} - EHX_{old}$ is less than the specified tolerance.

8) The air side pressure drop is then computed as before. A program written in Quick Basic language is developed using equations presented in the above eight steps to

determine heat duty, effectiveness and air side pressure drop. These calculations are repeated for different ranges of fins per inch, air velocities and water velocity. The results, of this analysis are presented in Chapter 3.

Interrupted surfaces are widely employed in present HVAC systems. The interrupted surfaces increase the heat transfer performance, however, additional manufacturing effort is required to either deform and shape the surface or, in the case of stamping, to cut slots on the surface. The plate-fin designs periodically are modified slightly by metal stamping processes to form wavy fin patterns. Offset-strip fins are made by cutting, and then offsetting the strips from the plate fin tube heat exchanger. The resulting surfaces differ in the size, shape, and location of the strip, including the distance the strip is lifted above the plate and whether all strips are lifted uniformly or not. It should also be noted that even though the heat transfer performance increases, the pressure drop on the air-side, and hence, required fan power, also increases. Wavy and Offset-strip fins on the heat exchanger surfaces are considered and the performance compared with the plate fins.

It was found that very scarce literature on interrupted surface heat exchangers is available because of the proprietary nature of this field and because the fin geometries vary slightly from manufacturer to manufacturer. Generalized correlations for heat transfer and friction factor data for the interrupted surface heat exchangers are virtually nonexistent because of large number of parameters are required to define these surfaces. The following correlations for heat transfer and friction factor were obtained after an extensive literature survey :

Compact heat exchanger with interrupted fins :

Wavy corrugated, louvered, Offset strip, Diamond ripple surfaces are widely employed in current HVAC systems. The interrupted surfaces increase the heat transfer performance, however, additional manufacturing effort is required to either deform and shape the surface or, in the case of louvering, to cut slits on the surface. The plate-fins discussed previously are modified slightly by metal stamping processes to form wavy fin patterns. Offset-strip fins are made by cutting, and then offsetting the strips from the plate fin tube heat exchanger. The resulting surfaces differ in the size, shape, and location of the strip, including the distance the strip is lifted above the plate and whether all strips are lifted uniformly or not. It should also be noted that even though the heat transfer performance increases, the pressure drop on the air-side, and, hence, required fan power, also increases. Wavy and Offset strip fins on the heat exchanger surface are considered and the performance compared with the plate fins.

It was found that very scarce literature on interrupted surface heat exchangers is available because of the proprietary nature of this field and because the fin geometries vary slightly from manufacturer to manufacturer. Generalized correlations for heat transfer and friction factor data for the interrupted surface heat exchangers are virtually nonexistent because of large number of parameters are required to define these surfaces. The following correlations for heat transfer and friction factor were obtained after an extensive literature survey :

Wavy Fins:

Beecher and Fagan et al., [11] correlations.

$$j = 0.14 \times \text{Re}D^{-0.328} \times \left(\frac{XA}{XB}\right)^{-0.502} \times \left(\frac{1}{S \times D_{to}}\right)^{0.0312}$$

$$f = .508 \times \text{Re}D^{-0.521} \times \left(\frac{XA}{D_{to}}\right)^{1.318}$$

$$f_{tb} = (0.118 / \left(\frac{XA - D_{to}}{D_{to}}\right)^{1.08} + 0.25) \times \text{Re}D^{-0.16}$$

$$f_w = f + f_{tb}$$

j = Colburn factor

f = friction factor for air flow over the finned surface.

f_{tb} = friction factor for flow over the tubes.

f_w = friction factor for the wavy fins.

$\text{Re}D$ = Air side Reynolds number based on tube outer diameter.

Two main types of wavy fins are being used in the HVAC industry [11], Sine-Wave type wavy fin and Triangular-type wavy fin. Wavy fins are illustrated in Figure 11.

Other type Fin surfaces:

CGF is shown in Figure 12. Fins are offset a half the fin spacing. The correlations for the heat transfer and the friction factor were developed by Wirtz et al., [10] are employed.

A literature search revealed that this is the only correlation available for the performance of rectangular offset strip fins.

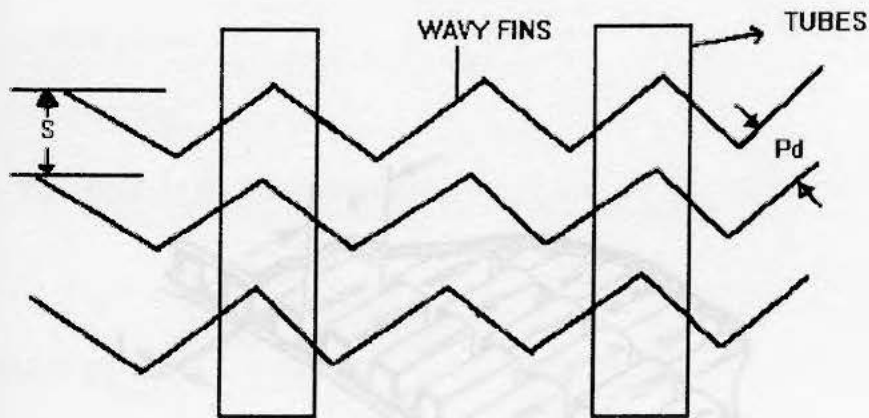


Figure 11 : Wavy Fins

Pd = Pattern depth for wavy fins.

S = Fin pitch for wavy fins.

The correlations are valid for fin pattern depths from 0.018 to 0.125 inches, fin density of 4 to 16 per inch and up to 4 patterns per longitudinal tube row.

Offset strip Fin surfaces :

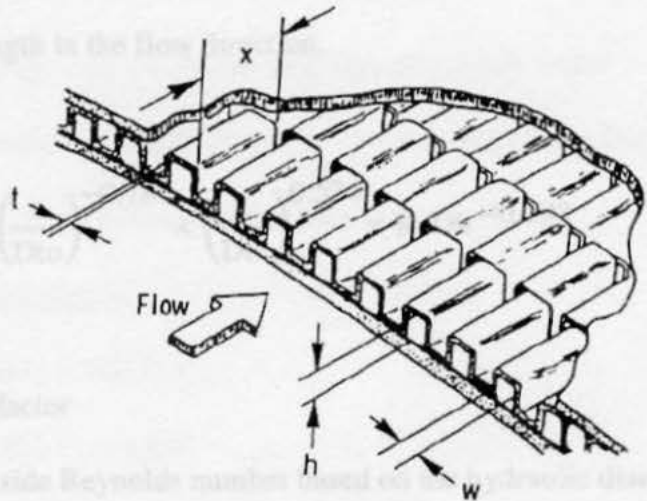
OSF is shown in Figure 12. Fins are offset at half the fin spacing. The correlations for the heat transfer and the friction factor data developed by Wieting et al., [10] are employed. A literature search revealed that this is the only correlation available for the performance of rectangular-offset strip fins.

$$j = 0.243 \times \left(\frac{x}{D_{ho}}\right)^{-0.322} \times \left(\frac{T}{D_{ho}}\right)^{0.289} \times Re_D^{-0.386}$$

j = Colburn factor

T = Fin thickness

x = Fin length to the flow



f = friction factor

Re_D = air side Reynolds number based on the hydraulic diameter of the offset strip fin surface.

Figure 12 : Offset Strip Fins [10]

The hydraulic diameter for the offset strip fin is given by :

$$D_h = 2wh / (w + h)$$

D_h = hydraulic diameter.

w = flow passage width.

h = height of the offset strip fin.

Fixed geometrical parameters

- 1) Tube outer diameter, D_{ho} = 0.525 inches
- 2) Tube inner diameter, D_{hi} = 0.403 inches
- 3) Fin thickness, T = 0.005 inches
- 4) No of fins per inch = 6

$$j = 0.242 \times \left(\frac{x}{D_{to}}\right)^{-0.322} \times \left(\frac{T}{D_{to}}\right)^{0.089} \times Re_D^{-0.368}$$

j = Colburn factor

T = Fin thickness

x = Fin length in the flow direction.

$$f = 1.136 \times \left(\frac{x}{D_{to}}\right)^{-0.781} \times \left(\frac{t}{D_{to}}\right)^{0.534} \times Re_{Dh}^{-0.198}$$

f = friction factor

Re_{Dh} = air side Reynolds number based on the hydraulic diameter of the offset strip fin surface.

The hydraulic diameter for the offset strip fin is given by :

$$D_h = 2wh / (w + h)$$

D_h = hydraulic diameter.

w = flow passage width.

h = height of the offset strip fin.

Fixed geometrical parameters :

- 1) Tube outer diameter, $D_{to} = 0.525$ inches.
- 2) Tube inner diameter, $D_{ti} = 0.483$ inches.
- 3) Fin thickness, $T = 0.006$ inches.
- 4) No of fins per inch = 6.

- 5) Height of exchanger = 3 ft.
- 6) Length of exchanger = 4 ft.
- 7) Height of Offset strip fin, $h = .67$ inches.
- 8) Length of Offset strip fin, $x = .0938$ inches.
- 9) Flow passage width of Offset strip fins, $w = 0.108$ inches.

The above values of the fin height, length and width were frequently observed during the literature survey of offset strip fins heat exchanger.

Fixed flow conditions :

- 10) Air velocity = 500 fpm
- 11) Water velocity = 2 fps
- 12) Air temperature entering, $TAI = 70$ F
- 13) Water temperature entering, $TWI = 50$ F

BASIS OF COMPARISON :

Heat transfer area is 580 square ft, assumed to be common for these three geometries.

ASSUMPTIONS :

(A_{min} / A_{fr}) and (A_f / A) for OSF and wavy fin is same as that of Plate fins at fixed number of fins per inch.

Methodology:

- 1) Determine the water side heat transfer coefficient, h_i based on inlet temperature of water.

$$h_i(1) D_{ti} / k_w(1) = 0.023 * Re_w(1)^{0.8} * Pr_w(1)^{0.3}$$

- 2) Calculate the air side heat transfer coefficient $h_o(1)$ based on the inlet air temperature.

$$hop(1) = j_p \cdot G_c \cdot c_{pa} / (Pra(1)^{.666})$$

$$how(1) = j_w \cdot G_c \cdot c_{pa} / (Pra(1)^{.666})$$

$$hoo(1) = j_o \cdot G_c \cdot c_{pa} / (Pra(1)^{.666})$$

hop(1), how(1) and hoo(1) are the first estimate (iterated values) for the air side heat transfer coefficient of plate fin, wavy fin and OSF, respectively.

3) Calculate the overall heat transfer coefficient, Uo(1) based on the inlet air temperature.

$$1/[Uop(1)] = 1 / (hop(1) \cdot \eta_{sop}(1)) + 1 / (hip(1) \cdot Ai / Ao) + R_w \cdot Ao$$

$$1/[Uow(1)] = 1 / (how(1) \cdot \eta_{sow}(1)) + 1 / (hiw(1) \cdot Ai / Ao) + R_w \cdot Ao$$

$$1/[Uoo(1)] = 1 / (hoo(1) \cdot \eta_{soo}(1)) + 1 / (hio(1) \cdot Ai / Ao) + R_w \cdot Ao$$

Uop, Uow and Uoo are the overall heat transfer coefficients for plate fin, wavy fin and OSF respectively.

$\eta_{sop}(1)$, $\eta_{sow}(1)$ and $\eta_{soo}(1)$ are the initial estimates for fin effectiveness.

(Ai / Ao) is ratio of the tube flow area to the heat transfer area and is given by :

$$Ai / Ao = (D_{to} / D_{ti}) \cdot (1 - (A_f / A))$$

4) Next, the NTU and the effectiveness for the plate, wavy and the offset strip fins heat exchanger are calculated.

$$NTUp = Uop \cdot Ao / C_{min}$$

$$NTUw = Uow \cdot Ao / C_{min}$$

$$NTUo = Uoo \cdot Ao / C_{min}$$

$$EHX_p = \{1 - \exp[-NTUp(1 - Cr)]\} / \{1 - Cr \cdot \exp[-NTUp(1 - Cr)]\}$$

$$EHX_w = \{ 1 - \text{EXP} [-NTU_w (1 - Cr)] \} / \{ 1 - Cr \cdot \text{exp} [-NTU_w(1-Cr)] \}.$$

$$EHX_o = \{ 1 - \text{EXP} [-NTU_o (1 - Cr)] \} / \{ 1 - Cr \cdot \text{exp} [-NTU_o(1-Cr)] \}.$$

5) Initial values of the outlet temperatures for the air and water are calculated.

If C_{air} is C_{min} ;

$$TAOp(1) = TAI - EHXp(1) \cdot (TAI - TWI)$$

$$TWOp(1) = TWI + Cr (TAI - TAOp(1))$$

$$TAOw(1) = TAI - EHXw(1) \cdot (TAI - TWI)$$

$$TWOw(1) = TWI + Cr (TAI - TAOw(1))$$

$$TAOo(1) = TAI - EHXo(1) \cdot (TAI - TWI)$$

$$TWOo(1) = TWI + Cr (TAI - TAOo(1))$$

If C_{water} is C_{min} ;

$$TAOp(1) = TAI - [(Cr) * (TWOp(1) - TWI)]$$

$$TWOp(1) = TWI + [EHXp(1) * (TAI - TWI)]$$

$$TAOw(1) = TAI - [(Cr) * (TWOw(1) - TWI)]$$

$$TWOw(1) = TWI + [EHXw(1) * (TAI - TWI)]$$

$$TAOo(1) = TAI - [(Cr) * (TWOo(1) - TWI)]$$

$$TWOo(1) = TWI + [EHXo(1) * (TAI - TWI)]$$

6) The calculations involving steps 1 through 5 are repeated at new bulk temperature. The iterations are continued until:

Absolute value of $(EHX_{new\ Plate} - EHX_{old\ Plate})$ is less than the specified tolerance.

Absolute value of $(EHX_{new\ offset} - EHX_{old\ offset})$ is less than the specified tolerance.

CHAPTER 5

Absolute value of (EHX new wavy - EHX old wavy) is less than the specified tolerance.

7) Air side pressure drop is then calculated using equation 26.

A computer program P5 written in Quick Basic language is developed using equations presented in the above seven steps to determine the heat duty, effectiveness and the air side pressure drop. These calculations are repeated for plate, wavy and offset strip fin tube heat exchangers. The results of this analysis are presented in next chapter.

Table 10: Impact of refrigerants on Plate fin tube evaporator design.

Heat duty (Refr.) = 231155.2 Btu/hr

Refr type	Evaporator area, m ²	Refr flow rate kg/hr	h _i (Refr side) Btu/hr-sq.F	h _o (air side) Btu/hr-sq.F	U _o Btu/hr-sq.F
R-132a	44.61	1760.24	1067.54	12.60	8.61
R-134a	49.72	2031.48	967.41		8.71
R-22	63.24	2673.22	779.28		8.81
R-12	81.00	3173.34	713.63		8.91
R-404a	98.80	3723.92	658.95		9.01
R-497a	142.2	5564.70	532.92		9.11

CHAPTER 3

RESULTS

The results obtained from the computer programs P1 through P5 are presented in tabulated form first and then are shown as respective plots in this chapter. The trends exhibited by the results are discussed in the next chapter.

Evaluation for constant heat duty plate fin tube heat exchanger :

Results obtained from computer code P1 are presented in Table 10.

Table 10 : Impact of refrigerants on Plate fin tube evaporator design.

$$\text{Heat duty (fixed)} = 231155.2 \text{ Btu / hr}$$

Ref type	Evaporator press, psia	Ref.flow rate lbm/hr	hi (Ref side) Btu/hr.sqft.F	ho (air side) Btu/hr.sqft.F	Uo Btu/hr.sqft.F
R-152a	44.81	1780.24	1067.94	12.63	8.81
R-134a	49.72	2751.48	967.41	↓	8.71
R-22	83.28	2672.22	779.28		8.48
R-12	51.60	3575.54	718.03		8.38
R-404a	95.80	3223.92	658.93		8.29
R-402a	102.2	3364.70	632.88		8.21

Table 10 : Continued

Ref type	Ao sqft.	H ft.	L ft.	W ft.	VOL. cu. ft.	APD in. water gauge
R-152a	1127.12	.72	11.52	.77	6.52	.86
R-134a	1139.54	.83	10.08	.78	6.59	.87
R-22	1171.38	.83	10.08	.80	6.77	.89
R-12	1185.35	1.04	8.06	.81	6.86	.90
R-404a	1201.26	1.04	8.06	.82	6.95	.91
R-402a	1209.26	1.04	8.06	.83	6.99	.92

The thermal design parameters i.e, heat transfer area, overall heat transfer coefficients, air pressure drop are influenced greatly by the refrigerant thermodynamic and transport properties. Among the six refrigerants compared, R-152a resulted in the highest value of refrigerant-side heat transfer coefficient, (1067.94 Btu / hr.sqft.F) and overall heat transfer coefficient, (8.81 Btu/hr.sqft-F) followed by R-134a, R-22 , R-12, R-404a and R-402a. Lowest overall heat transfer coefficient, (8.21 Btu/hr.sqft-F) was generated by R-402a design. Air-side heat transfer coefficient, was constant for all the six cases at 12.63 Btu/hr.sqft-F. Heat transfer area increased from 1127.12 sqft (for R-152a) to 1209.26 sq ft (for R-402a). Air-side pressure drop was lowest for R-152a, (0.862 in.wg.) and highest for R-402a, (.922 in. wg). The heat exchanger volume increases from 6.785 cu ft (for R-152a) to 6.99 cuft (for R-402a). These results are illustrated in Figures 13 through 16.

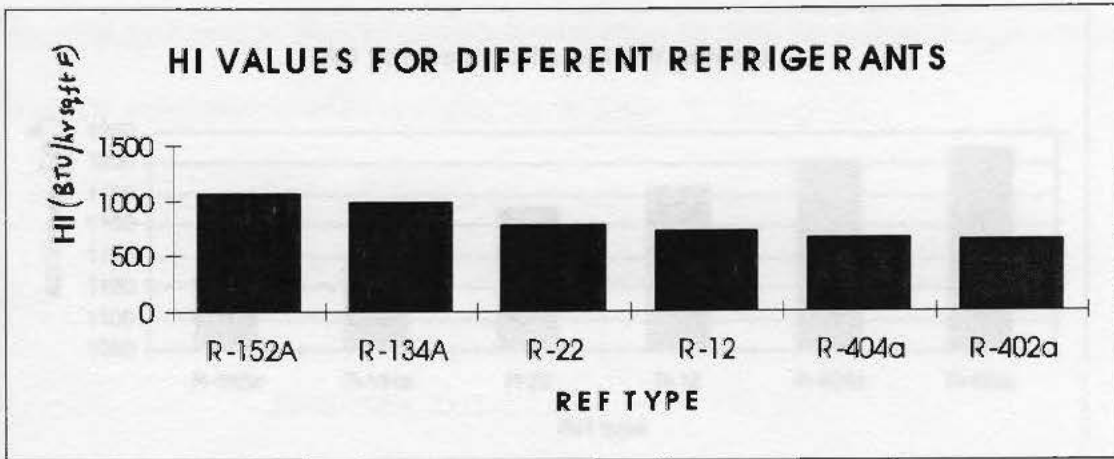


FIGURE 13 : HI values for plate fin tube evaporator

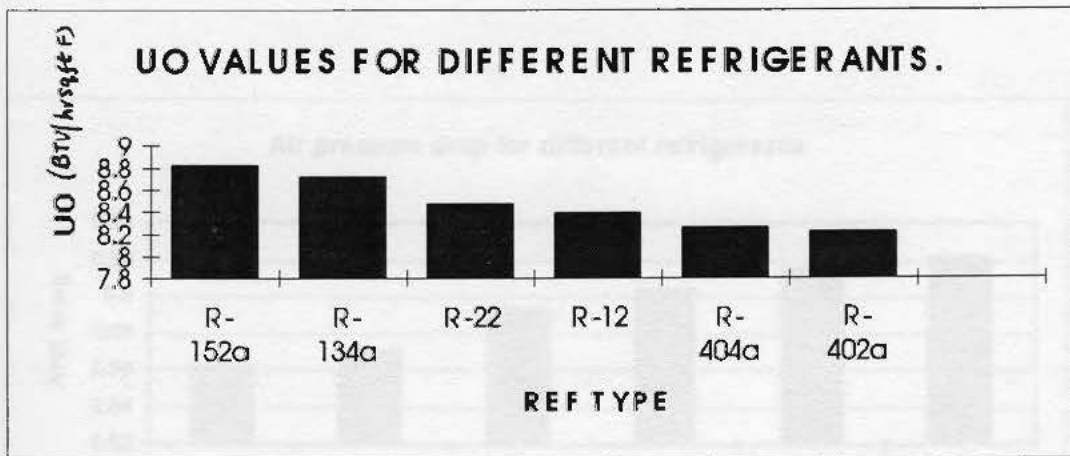


FIGURE 14 : UO Values for plate fin tube evaporator

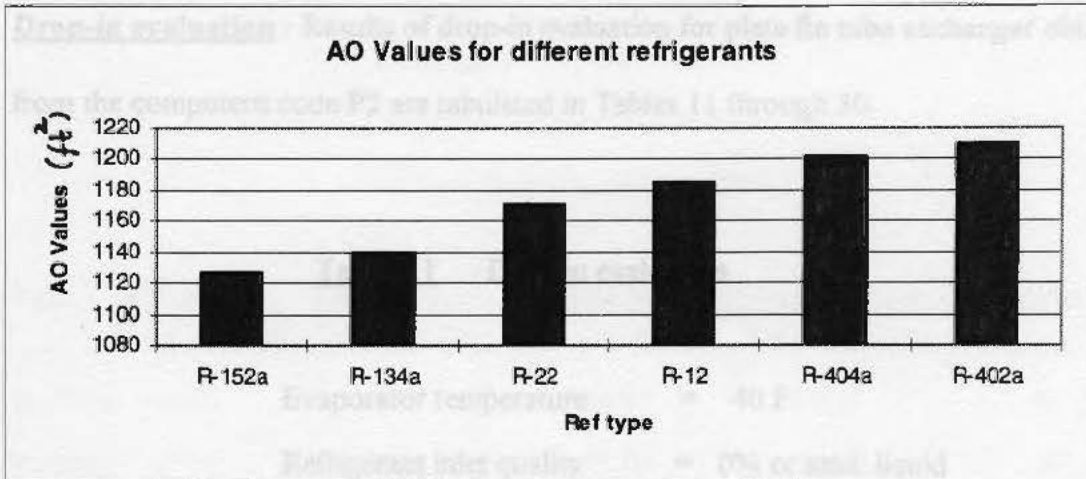


FIGURE 15 : Heat transfer areas for plate fin tube evaporator

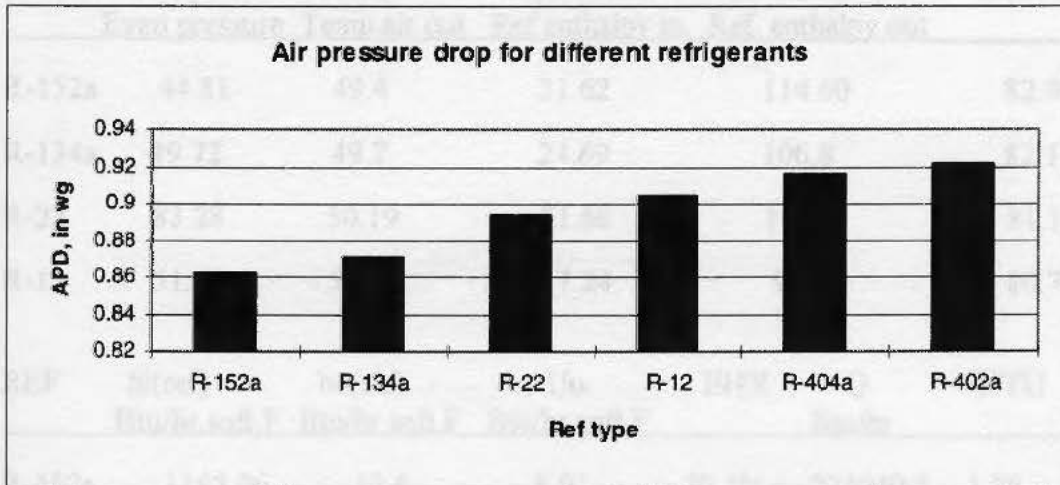


FIGURE 16 : Air pressure drop for plate fin tube evaporator

Drop-in evaluation : Results of drop-in evaluation for plate fin tube exchanger obtained from the computer code P2 are tabulated in Tables 11 through 30.

Table 11 Drop-in evaluation

Evaporator temperature	=	40 F
Refrigerant inlet quality	=	0% or satd. liquid
Refrigerant flow rate, fixed	=	2700 lbm/hr
Air velocity, fixed	=	750 fpm
Evaporator volume, fixed	=	6.4 cuft
Temperature air in, fixed	=	85 F

Ref	PE, psia Evap pressure	TAO, F Temp air out	Hin, Btu/lbm Ref enthalpy in.	Hout, Btu/lbm Ref. enthalpy out	Hout-Hin
R-152a	44.81	49.4	31.62	114.60	82.98
R-134a	49.72	49.7	24.69	106.8	82.11
R-22	83.28	50.19	21.68	102.8	81.12
R-12	51.60	50.36	17.24	97.99	80.75

REF	hi(ref) Btu/hr.sqft.F	ho(air) Btu/hr.sqft.F	Uo Btu/hr.sqft.F	EHX	Q Btu/hr	NTU	APD in.wg
R-152a	1165.96	12.6	8.91	79.1%	224049.5	1.56	.88
R-134a	931.61	12.6	8.69	78.3%	221775.5	1.52	.88
R-22	747.5	12.6	8.44	77.3%	219025.7	1.48	.88
R-12	696.3	12.6	8.35	76.97%	218012.1	1.46	.88

Table 12 Drop-in evaluation

Evaporator temperature = 40 F

Refrigerant inlet quality = 10%

Ref	PE, psia Evap pressure	TAO, F Temp air out	Hin, Btu/lbm Ref enthalpy in.	Hout, Btu/lbm Ref. enthalpy out	Hout-Hin
R-152a	44.81	49.37	44.60	127.7	83.1
R-134a	49.72	49.7	33.09	115.3	82.21
R-22	83.28	50.1	30.33	111.6	81.27
R-12	51.60	50.3	23.70	104.5	80.8

REF	hi(ref) Btu/hr.sqft.F	ho(air) Btu/hr.sqft.F	Uo Btu/hr.sqft.F	EHX	Q Btu/hr	NTU	APD in.wg
R-152a	1210.8	12.6	8.94	79.22%	224386.3	1.57	.88
R-134a	956.8	12.6	8.72	78.41%	222072.9	1.53	.88
R-22	769.2	12.6	8.48	77.4%	219414.5	1.49	.88
R-12	712.3	12.6	8.38	77.09%	218343.3	1.47	.88

Table :13 Drop-in evaluation

Evaporator temperature = 40 F

Refrigerant inlet quality = 20%

Ref Hin	PE, psia Evap pressure	TAO, F Temp air out	Hin, Btu/lbm Ref enthalpy in.	Hout, Btu/lbm Ref. enthalpy out	Hout- Hin
R-152a	44.81	49.3	57.59	140.8	83.21
R-134a	49.72	49.67	41.49	123.8	82.31
R-22	83.28	50.08	38.98	120.3	81.32
R-12	51.60	50.25	30.17	111.1	80.93

REF	hi(ref) Btu/hr.sqft.F	ho(air) Btu/hr.sqft.F	Uo Btu/hr.sqft.F	EHX	Q Btu/hr	NTU	APD in.wg
R-152a	1252.7	12.6	8.97	79.33%	224679.7	1.576	.88
R-134a	980.9	12.6	8.74	78.5%	222341.9	1.537	.88
R-22	789.7	12.6	8.51	77.5%	219764.4	1.495	.88
R-12	727.6	12.6	8.41	77.2%	218647.7	1.478	.88

Table :14 Drop-in evaluation

Evaporator temperature = 40 F

Refrigerant inlet quality = 30%

Ref	PE, psia Evap pressure	TAO, F Temp air out	Hin, Btu/lbm Ref enthalpy in.	Hout, Btu/lbm Ref. enthalpy out	Hout-Hin
R-152a	44.81	49.259	70.58	153.89	83.31
R-134a	49.72	49.63	49.89	132.33	82.44
R-22	83.28	50.03	47.63	129.15	81.52
R-12	51.60	50.21	36.63	117.72	81.09

REF	hi(ref) Btu/hr.sqft.F	ho(air) Btu/hr.sqft.F	Uo Btu/hr.sqft.F	EHX	Q Btu/hr	NTU	APD in.wg
R-152a	1292.12	12.6	8.99	79.42%	224938.7	1.58	.88
R-134a	1003.9	12.6	8.77	78.59%	222587.3	1.541	.88
R-22	809.25	12.6	8.54	77.7%	220081.8	1.500	.88
R-12	742.38	12.6	8.43	77.3%	218928.8	1.482	.88

Table 15: Drop-in evaluation

Evaporator temperature = 40 F

Refrigerant inlet quality = 39%

Ref	PE, psia Evap pressure	TAO, F Temp air out	Hin, Btu/lbm Ref enthalpy in.	Hout, Btu/lbm Ref. enthalpy out	Hout-Hin
R-152a	44.81	49.22	82.26	165.65	83.39
R-134a	49.72	49.6	57.45	139.97	82.52
R-22	83.28	49.98	55.42	137.03	81.61
R-12	51.60	50.17	42.45	123.63	81.18

REF	HI(ref) Btu/hr.sqft.F	HO(air) Btu/hr.sqft.F	UO Btu/hr.sqft.F	EHX	Q Btu/hr	NTU	APD in.wg
R-152a	1325.7	12.6	9.01	79.49%	225147.7	1.584	.88
R-134a	1023.7	12.6	8.79	78.66%	222790.6	1.544	.88
R-22	826.1	12.6	8.56	77.8%	220343.8	1.505	.88
R-12	755.1	12.6	8.46	77.3%	219164.4	1.483	.88

Table 16:

Evaporator temperature = 35 F

Refrigerant inlet quality = 0%

Ref	PE, psia Evap pressure	TAO, F Temp air out	Hin, Btu/lbm Ref enthalpy in.	Hout, Btu/lbm Ref. enthalpy out	Hout-Hin
R-152a	40.65	45.36	29.67	121.9	92.33
R-134a	45.07	45.73	23.08	114.6	91.52
R-22	76.24	46.19	20.27	110.7	90.43
R-12	47.20	46.36	16.12	106.1	89.98

REF	hi(ref) Btu/hr.sqft.F	ho(air) Btu/hr.sqft.F	Uo Btu/hr.sqft.F	EHX	Q Btu/hr	NTU	APD in.wg
R-152a	1234.1	12.6	8.95	79.27%	249479.5	1.57	.87
R-134a	989.4	12.6	8.75	78.53%	247127	1.53	.87
R-22	792.0	12.6	8.51	77.60%	2442034	1.49	.87
R-12	739.5	12.6	8.41	77.20%	243173.7	1.48	.87

Table :17 Drop-in evaluation

Evaporator temperature = 35 F

Refrigerant inlet quality = 10%

Ref	PE, psia Evap pressure	TAO, F Temp air out	Hin, Btu/lbm Ref enthalpy in.	Hout, Btu/lbm Ref. enthalpy out	Hout-Hin
R-152a	40.65	45.3	42.68	135.2	92.52
R-134a	45.07	45.6	31.57	123.2	91.62
R-22	76.24	46.1	29.01	119.6	90.58
R-12	47.20	46.3	22.64	112.8	90.16

REF	hi(ref) Btu/hr.sqft.F	ho(air) Btu/hr.sqft.F	Uo Btu/hr.sqft.F	EHX	Q Btu/hr	NTU	APD in.wg
R-152a	1279.2	12.6	8.98	79.38%	249817.1	1.579	.87
R-134a	1014.7	12.6	8.78	78.62%	247421.7	1.542	.87
R-22	813.5	12.6	8.54	77.72%	244584.4	1.50	.87
R-12	755.3	12.6	8.45	77.37%	243498.7	1.486	.87

Table :18 Drop-in evaluation

Evaporator temperature = 35 F

Refrigerant inlet quality = 20%

Ref	PE, psia Evap pressure	TAO, F Temp air out	Hin, Btu/lbm Ref enthalpy in	Hout, Btu/lbm Ref. enthalpy out	Hout-Hin
R-152a	40.65	45.25	55.79	148.4	92.6
R-134a	45.07	45.64	40.07	131.8	91.72
R-22	76.24	46.08	37.77	128.4	90.63
R-12	47.20	46.26	29.17	119.4	90.22

REF	hi(ref) Btu/hr.sqft.F	ho(air) Btu/hr.sqft.F	Uo Btu/hr.sqft.F	EHX	Q Btu/hr	NTU	APD in.wg
R-152a	1321.5	12.6	9.01	79.48%	250113	1.58	.87
R-134a	1038.9	12.6	8.80	78.71%	247689.9	1.54	.87
R-22	834.11	12.6	8.57	77.83%	244938.9	1.506	.87
R-12	770.60	12.6	8.48	77.47%	243799.1	1.49	.87

Table :19 Drop-in evaluation

Evaporator temperature = 35 F

Refrigerant inlet quality = 30%

Ref	PE, psia Evap pressure	TAO, F Temp air out	Hin, Btu/lbm Ref enthalpy in	Hout, Btu/lbm Ref. enthalpy out	Hout-Hin
R-152a	40.65	45.2	68.90	161.63	92.72
R-134a	45.07	45.6	48.56	140.39	91.83
R-22	76.24	46.0	46.52	137.35	90.83
R-12	47.20	46.2	35.69	126.09	90.4

REF	HI(ref) Btu/hr.sqft.F	HO(air) Btu/hr.sqft.F	UO Btu/hr.sqft.F	EHX	Q Btu/hr	NTU	APD in.wg
R-152a	1361.49	12.6	9.03	79.56%	250375.5	1.587	.87
R-134a	1062.1	12.6	8.82	78.7%	247935.7	1.550	.87
R-22	853.71	12.6	8.60	77.93%	245257.4	1.511	.87
R-12	785.26	12.6	8.50	77.56%	2440779	1.494	.87

Table :20 Drop-in evaluation

Evaporator temperature = 35F

Refrigerant inlet quality = 39%

Ref	PE, psia Evap pressure	TAO, F Temp air out	Hin, Btu/lbm Ref enthalpy in.	Hout, Btu/lbm Ref. enthalpy out	Hout-Hin
R-152a	40.65	45.18	80.69	173.51	92.82
R-134a	45.07	45.5	56.20	148.11	91.91
R-22	76.24	45.9	54.39	145.33	90.94
R-12	47.20	46.1	41.57	132.05	90.48

REF	hi(ref) Btu/hr.sqft.F	ho(air) Btu/hr.sqft.F	Uo Btu/hr.sqft.F	EHX	Q Btu/hr	NTU	APD in.wg
R-152a	1395.6	12.6	9.05	79.6%	250588.3	1.591	.87
R-134a	1082.1	12.6	8.84	78.85%	248140.2	1.553	.87
R-22	870.6	12.6	8.62	78.02%	245521.5	1.515	.87
R-12	798.0	12.6	8.52	77.63%	244312.5	1.497	.87

Table:21 Drop-in evaluation

Evaporator temperature = 25 F

Refrigerant inlet quality = 0%

Ref	PE, psia Evap pressure	TAO, F Temp air out	Hin, Btu/lbm Ref enthalpy in.	Hout, Btu/lbm Ref. enthalpy out	Hout-Hin
R-152a	33.23	37.2	25.49	136.8	111.31
R-134a	36.78	37.6	19.89	130.2	110.4
R-22	63.52	38.1	17.47	126.6	109.18
R-12	39.26	38.3	13.91	122.7	108.82

REF	hi(ref) Btu/hr.sqft.F	ho(air) Btu/hr.sqft.F	Uo Btu/hr.sqft.F	EHX	Q Btu/hr	NTU	APD in.wg
R-152a	1379.0	12.6	9.04	79.58%	300530	1.58	.86
R-134a	1111.9	12.6	8.86	78.9%	298063.9	1.55	.86
R-22	1039.7	12.6	8.63	78.06%	294796.6	1.51	.86
R-12	882.9	12.6	8.56	77.20%	293821.7	1.50	.86

Table :22 Drop-in evaluation

Evaporator temperature = 25 F

Refrigerant inlet quality = 10 %

Ref	PE, psia Evap pressure	TAO, F Temp air out	Hin, Btu/lbm Ref enthalpy in	Hout, Btu/lbm Ref enthalpy out	Hout-Hin
R-152a	33.23	37.19	38.84	150.28	111.44
R-134a	36.78	37.59	28.56	139.0	110.43
R-22	63.52	38.10	26.41	135.7	109.28
R-12	39.26	38.27	20.54	129.4	108.85

REF	HI(ref) Btu/hr.sqft.F	HO(air) Btu/hr.sqft.F	UO Btu/hr.sqft.F	EHX	Q Btu/hr	NTU	APD in.wg
R-152a	1424.5	12.6	9.06	79.67%	300859	1.593	.86
R-134a	1137.5	12.6	8.88	79%	298349.5	1.56	.86
R-22	904.5	12.6	8.66	78.16%	295172.7	1.521	.86
R-12	847.1	12.6	8.58	7.87%	294131.1	1.509	.86

Table :23 Drop-in evaluation

Evaporator temperature = 25 F

Refrigerant inlet quality = 20%

Ref	PE, psia Evap pressure	TAO, F Temp air out	Hin, Btu/lbm Ref enthalpy in.	Hout, Btu/lbm Ref. enthalpy out	Hout-Hin
R-152a	33.23	37.15	52.20	163.7	111.5
R-134a	36.78	37.55	37.24	147.8	110.55
R-22	63.52	38.04	35.35	144.8	109.44
R-12	39.26	38.22	27.18	136.2	109.01

REF	hi(ref) Btu/hr.sqft.F	ho(air) Btu/hr.sqft.F	Uo Btu/hr.sqft.F	EHX	Q Btu/hr	NTU	APD in.wg
R-152a	1467.8	12.6	9.08	79.7%	301154	1.59	.86
R-134a	1162.1	12.6	8.90	79.07%	298611.8	1.564	.86
R-22	925.12	12.6	8.68	78.25%	295516.5	1.525	.86
R-12	862.31	12.6	8.60	77.96%	294419.4	1.512	.86

TABLE 24 Drop-in evaluation
Evaporator temperature = 25 F

Refrigerant inlet quality = 30 %

Ref	PE, psia Evap pressure	TAO, F Temp air out	Hin, Btu/lbm Ref enthalpy in.	Hout, Btu/lbm Ref. enthalpy out	Hout-Hin		
R-152a	33.23	37.10	65.55	177.19	111.64		
R-134a	36.78	37.51	45.91	156.59	110.68		
R-22	63.52	37.99	44.3	153.86	109.56		
R-12	39.26	38.17	33.82	142.97	109.15		

REF	hi(ref) Btu/hr.sqft.F	ho(air) Btu/hr.sqft.F	Uo Btu/hr.sqft.F	EHX	Q Btu/hr	NTU	APD in.wg
R-152a	1508.8	12.6	9.10	79.8%	301418	1.600	.86
R-134a	1185.7	12.6	8.92	79.14%	298853.8	1.567	.86
R-22	944.9	12.6	8.70	78.34%	295832.6	1.529	.86
R-12	876.9	12.6	8.62	78.03%	294689.3	1.515	.86

Table 25 Drop-in evaluation

Evaporator temperature = 25 F

Refrigerant inlet quality = 39%

Ref	PE, psia Evap pressure	TAO, F Temp air out	Hin, Btu/lbm Ref enthalpy in.	Hout, Btu/lbm Ref. enthalpy out	Hout-Hin	
R-152a	33.23	37.07	77.57	189.29	111.72	
R-134a	36.78	37.48	53.7	164.47	110.77	
R-22	63.52	37.95	52.34	162.07	109.73	
R-12	39.26	38.14	39.80	149.03	109.23	

REF	HI(ref) Btu/hr.sqft.F	HO(air) Btu/hr.sqft.F	UO Btu/hr.sqft.F	EHX	Q Btu/hr	NTU	APD in.wg
R-152a	1544.68	12.6	9.12	79.87%	301633.6	1.603	.86
R-134a	1206.2	12.6	8.93	79.19%	299056.7	1.569	.86
R-22	962.04	12.6	8.72	78.41%	296096.3	1.532	.86
R-12	889.79	12.6	8.64	78.09%	294917.8	1.518	.86

Table:26 Drop-in evaluation

Evaporator temperature = 5 F

Refrigerant inlet quality = 0%

Ref	PE, psia Evap pressure	TAO, F Temp air out	Hin, Btu/lbm Ref enthalpy in.	Hout, Btu/lbm Ref. enthalpy out	Hout-Hin
R-152a	21.57	20.91	17.47	166.8	149.33
R-134a	23.76	21.32	13.63	162.0	148.37
R-22	42.96	21.92	11.92	158.7	146.78
R-12	26.46	22.06	9.54	156.2	146.66

REF	hi(ref) Btu/hr.sqft.F	ho(air) Btu/hr.sqft.F	Uo Btu/hr.sqft.F	EHX	Q Btu/hr	NTU	APD in.wg
R-152a	1720.3	12.6	9.18	80.10%	403308.6	1.61	.85
R-134a	1400.5	12.6	9.04	79.6%	400785	1.58	.85
R-22	1095.5	12.6	8.84	78.85%	397035.3	1.55	.85
R-12	1041.9	12.6	8.79	78.68%	396155.8	1.54	.85

Table 27 Drop-in evaluation

Evaporator temperature = 5 F

Refrigerant inlet quality = 10%

Ref	PE, psia Evap pressure	TAO, F Temp air out	Hin, Btu/lbm Ref enthalpy in.	Hout, Btu/lbm Ref. enthalpy out	Hout-Hin	
R-152a	21.57	20.87	31.29	180.2	148.91	
R-134a	23.76	21.27	22.64	171.1	148.46	
R-22	42.96	21.86	21.23	168.4	147.17	
R-12	26.46	22.01	16.40	163.2	146.8	

REF	hi(ref) Btu/hr.sqft.F	ho(air) Btu/hr.sqft.F	Uo Btu/hr.sqft.F	EHX	Q Btu/hr	NTU	APD in.wg
R-152a	1769.2	12.6	9.20	80.16%	403615.1	1.617	.85
R-134a	1427.5	12.6	9.06	79.65%	401041.3	1.592	.85
R-22	1117.8	12.6	8.86	78.92%	397377	1.557	.85
R-12	1057.9	12.6	8.81	78.73%	396427.5	1.548	.85

Table 28: Drop-in evaluation

Evaporator temperature = 5 F

Refrigerant inlet quality = 20%

Ref	PE, psia Evap pressure	TAO, F Temp air out	Hin, Btu/lbm Ref enthalpy in.	Hout, Btu/lbm Ref. enthalpy out	Hout-Hin
R-152a	21.57	20.82	45.10	194.7	149.6
R-134a	23.76	21.2	31.65	180.2	148.55
R-22	42.96	21.86	30.54	177.8	147.26
R-12	26.46	22.01	23.25	170.1	146.85

REF	hi(ref) Btu/hr.sqft.F	ho(air) Btu/hr.sqft.F	Uo Btu/hr.sqft.F	EHX	Q Btu/hr	NTU	APD in.wg
R-152a	1815.7	12.6	9.22	80.2%	403891.3	1.62	.85
R-134a	1453.6	12.6	9.07	79.69%	401279.8	1.59	.85
R-22	1139.2	12.6	8.87	78.96%	397693.7	1.559	.85
R-12	1073.5	12.6	8.82	78.7%	396683.9	1.55	.85

Table 29 Drop-in evaluation

Evaporator temperature = 5 F

Refrigerant inlet quality = 30%

Ref	PE, psia Evap pressure	TAO, F Temp air out	Hin, Btu/lbm Ref enthalpy in.	Hout, Btu/lbm Ref. enthalpy out	Hout-Hin
R-152a	21.57	20.28	58.93	208.6	149.67
R-134a	23.76	21.20	40.66	189.3	148.64
R-22	42.96	21.76	39.85	187.2	147.35
R-12	26.46	21.93	30.11	177.1	146.98

REF	hi(ref) Btu/hr.sqft.F	ho(air) Btu/hr.sqft.F	Uo Btu/hr.sqft.F	EHX	Q Btu/hr	NTU	APD in.wg
R-152a	1860.1	12.6	9.23	80.26%	404142.1	1.622	.85
R-134a	1478.9	12.6	9.08	79.7%	401502.7	1.596	.85
R-22	1159.9	12.6	8.89	79.04%	397988.6	1.562	.85
R-12	1088.6	12.6	8.83	78.8%	396926.7	1.55	.85

Table 30: Drop-in evaluation

Evaporator temperature = 5 F

Refrigerant inlet quality = 39%

Ref	PE, psia Evap pressure	TAO, F Temp air out	Hin, Btu/lbm Ref enthalpy in.	Hout, Btu/lbm Ref. enthalpy out	Hout-Hin
R-152a	21.57	20.75	71.36	221.1	149.74
R-134a	23.76	21.17	48.77	197.5	148.73
R-22	42.96	21.72	48.22	195.7	147.48
R-12	26.46	21.91	36.28	183.3	147.02

REF	hi(ref) Btu/hr.sqft.F	hoair) Btu/hr.sqft.F	Uo Btu/hr.sqft.F	EHX	Q Btu/hr	NTU	APD in.wg
R-152a	1898.88	12.6	9.24	80.3%	404349.3	1.624	.85
R-134a	1500.9	12.6	9.09	79.78%	401691.2	1.598	.85
R-22	1178.0	12.6	8.90	79.09%	398237.4	1.565	.85
R-12	1101.9	12.6	8.84	78.87%	397134.4	1.55	.85

The results for the drop-in evaluation show that the effectiveness of the R-152a evaporator is maximum at fixed evaporator temperature and refrigerant inlet quality compared to all other refrigerants. At 40 F, and zero inlet refrigerant quality, the effectiveness of R-152a evaporator was found to be 79.10%, followed by R-134a, 78.3%, R-22, 77.3% and R-12, 76.97%. Maximum refrigerant-side heat transfer coefficient was obtained for the R-152a evaporator, 1165.96 Btu/hr-sqft-F, followed by R-134a, R-22 and R-12 respectively. The evaporator NTU increased from 1.46, (R-12) to 1.56, (R-152a). The air side heat transfer coefficient was constant at 12.6 Btu/hr-sqft.F. At 40 F, and 10% inlet refrigerant quality, the effectiveness of the R-152a evaporator was found to be 79.22% followed by R-134a, (78.41)%, R-22 (77.4%) and R-12 (77.09%).

Effect of the evaporator temperature :

Decrease in the evaporator temperature is found to increase the effectiveness and capacity for all the refrigerants. At 40 F and zero inlet refrigerant quality, the effectiveness of R-152a evaporator was found to be 79.10%. However, at the evaporator temperatures of 35 F, 25 F and 5 F the effectiveness increased to 79.27%, 79.58% and 80.10%, respectively. The effectiveness of R-134a evaporator also increased from 78.3% to 79.6% on decreasing the evaporator temperature from, 40 F to 35F. It was also observed during this investigation that the effectiveness of R-12, which is the least favorable refrigerant at the lowest evaporator temperature of 5 F and zero inlet refrigerant quality, (78.68%) is

greater than R-152a, which is the best refrigerant at higher evaporator temperatures of 35 F (78.53%) and 40 F (78.3%) respectively. The effectiveness of R-134a, (second best) at 5 F, (79.6%) was found to be greater than R-152a at 40 F, (79.10 %). The effect of the evaporator temperatures on the effectiveness of the different refrigerants with zero inlet refrigerant quality are illustrated in Figures 17 and 18.

Effect of refrigerant inlet quality :

Increase in the refrigerant inlet quality increased the effectiveness and capacity for all the refrigerants. At evaporator temperature of 40 F, increasing the refrigerant inlet quality from 0% to 39% for R-152a, increased the evaporator effectiveness from 79.10% to 79.49%. The refrigerant side heat transfer coefficient increased from 1165.9 to 1325.7 Btu/hr.sqft.F. It was observed that at fixed evaporator temperature, the effectiveness of R-134a did not exceed or equal the effectiveness of R-152a, even at the highest quality tested. However the effectiveness of R-12 was nearly equal to R-22 at the highest quality. Figures 19 through 22 show the effect of quality on evaporator performance.

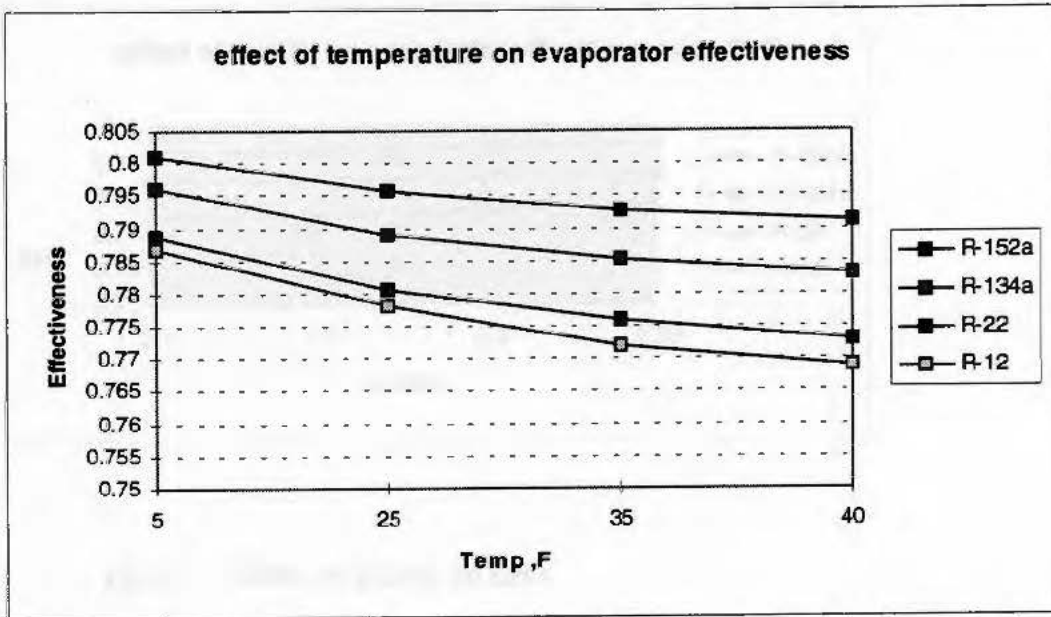


FIGURE 17 : Drop-in evaluation of alternate refrigerants at various evaporator temperatures.

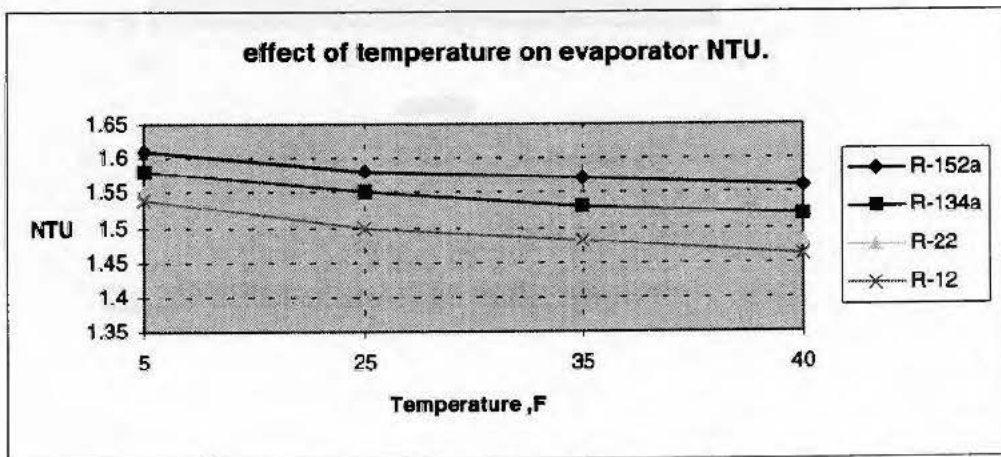


FIGURE 18 : Drop-in evaluation of alternate refrigerants at various evaporator temperatures.

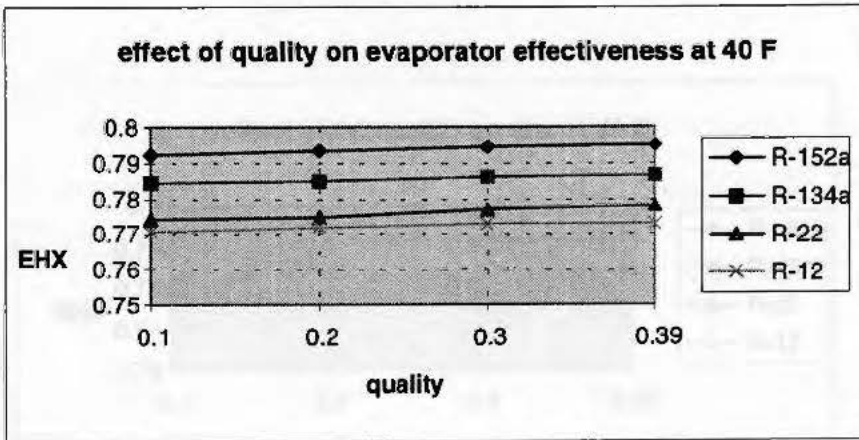


Fig 19 : Effect of quality on EHX

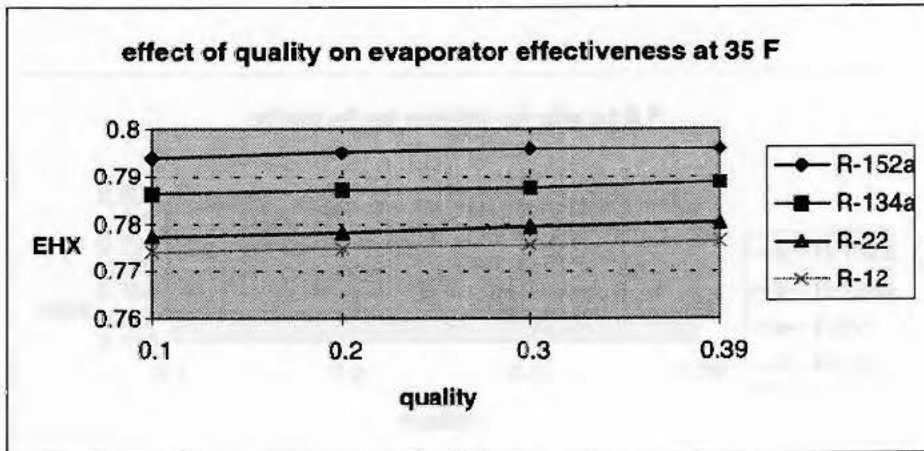


Fig 20 : Effect of quality on EHX.

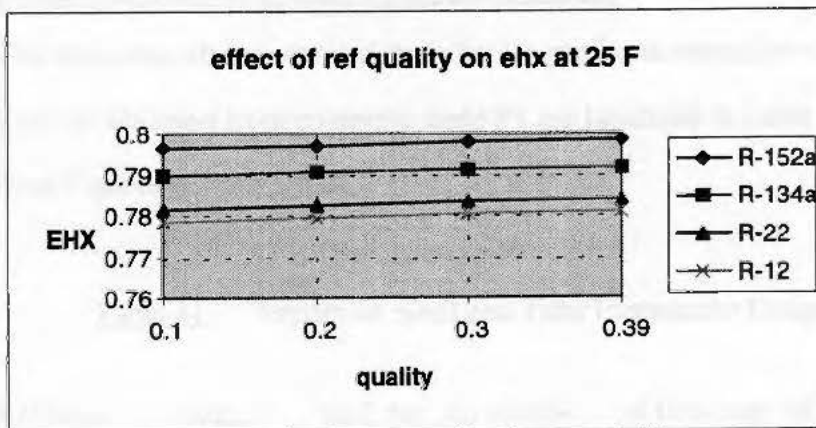


Fig 21 : Effect of quality on EHX at 25 F.

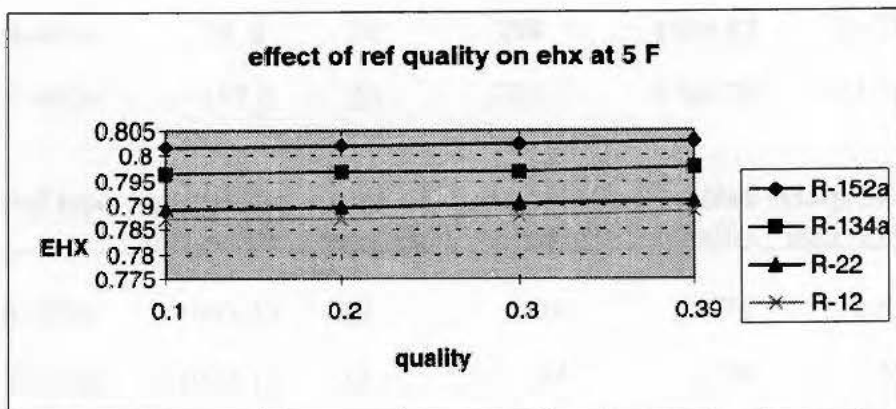


Fig 22 : Effect of quality on EHX at 5F.

Impact on Shell and Tube Evaporator Design :

The alternate refrigerants appear to have a profound impact on the design parameters. Results obtained from computer code P3 are tabulated in Table 31 and shown in plots from Figures 23 through 26.

Table 31: Impact on Shell and Tube Evaporator Design

Ref type	evap press,psia	shell dia Ds, inch	no of tubes NT	ref flow rate lbm/hr	hi(ref side) Btu/hr.sqft.F	ho(shell side) Btu/hr.sqft.F
R-152a	44.81	20	289	903.85	35.15	815.10
R-134a	49.72	20	289	1396.96	34.78	815.10
R-12	51.60	20	289	1815.34	30.25	815.10
R-404a	95.8	20	289	1636.82	29.29	815.10
R-402a	102.2	20	289	1708.30	27.38	815.10

Ref type	heat transfer area,A,sqft	tube length,L,ft	no of baffles NB	shell side-pressure drop,psi baffle inlet /outlet window total
R-152a	1045.53	19	14	3.76 2.03 3.07 8.87
R-134a	1056.11	19	14	3.76 2.03 3.07 8.87
R-12	1207.59	22	16	4.34 2.03 3.51 9.89
R-404a	1245.61	22	16	4.34 2.03 3.51 9.89
R-402a	1329.53	24	17	4.94 2.03 3.95 10.91

Heat Duty = 117360.4 Btu/hr

The results indicate that R-152a is the best refrigerant for this type of heat exchanger followed by R-134a, R-12, R-404a and R-402a. The refrigerant side heat transfer coefficient was highest for the evaporator working with R-152a, 35.15 Btu/hr.sqft.F and least for the R-402a evaporator, 27.38 Btu/hr.sqft.F. Shell side heat transfer coefficient was maintained constant in all the cases at 815.10 Btu/hr.sqft.F.

The number of baffles in the evaporator increased from 14 for R-152a, to 17 for R-402a. Minimum heat transfer area of 1046 sqft was obtained for the R-152a evaporator, compared to a maximum of 1330 sqft for R-402a. The shell side pressure drop ranged from a minimum of 8.87 psi for R-152a to a maximum of 10.9 psi for R-402a.

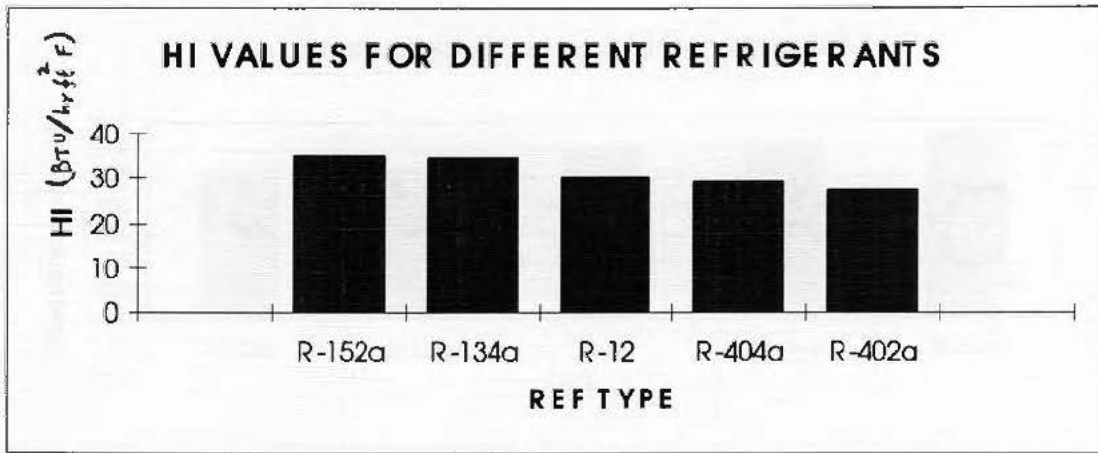


Figure 23: HI values for shell and tube evaporator

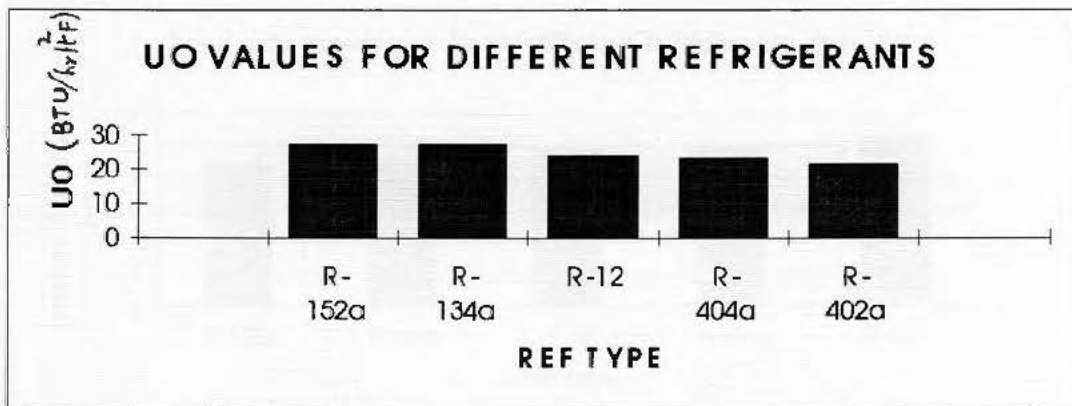


Figure 24: UO values for shell and tube evaporator.

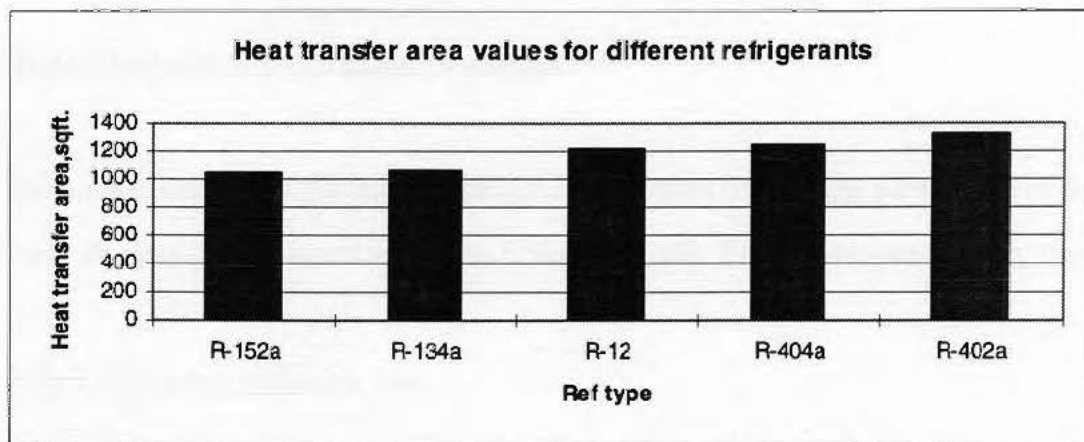


Figure 25 : Heat transfer area for shell and tube evaporator.

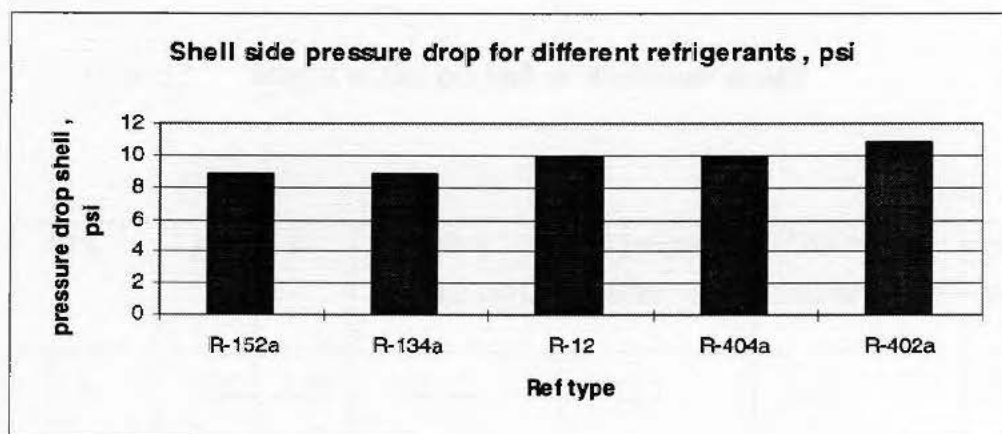


Figure 26: Shell pressure drop.

Plate-Fin Tube Compact Heat Exchanger

Parametric analysis of this heat exchanger is performed for varying parameters of fins per inch, air velocity and water velocities. Computer code P4 is developed to carry this study.

Effect of number of fins per inch:

Program P4, was run at various fins per inch in order to investigate the impact on heat exchanger performance. Fins per inch were increased from 4 to 14. Air velocity and water velocity were constant at 500 fpm and 2 fps. Results of this analysis are shown in Table 32.

Table 32 Impact of fins per inch on exchanger design

FPI	j	f	HO(air) Btu /hr.sqft.F	HI (water) Btu/hr.sqft.F	UO Btu/hr.sqft.F	AO sqft.
4	.0086	.056	10.26	383.3	7.33	406.0
6	.0081	.044	9.94	↓	6.74	577.2
8	.0078	.036	9.75		6.30	748.5
10	.0076	.031	9.61		5.94	919.7
12	.0074	.027	9.50		5.64	1091.0
14	.0073	.025	9.42		5.38	1262.3

Table 32 (continued)

FPI	UOAO Btu/ hr-F	NTU	EHX	APD inch .wg.
4	2978.46	.46	.34	.17
6	3892.55	.60	.42	.20
8	4719.63	.72	.47	.22
10	5472.39	.84	.52	.25
12	6161.34	.95	.56	.27
14	6794.87	1.049	.59	.29

Increase in fins per inch decreased the Colburn and friction factor. Colburn factor decreased from .0086 to .00731. Friction factor decreased from .056 to .0251. R.K Shah et al, [17] explains that increase in fins increases boundary layer thickness resulting in fully developed flow, which decrease f and j factors. Air side heat transfer coefficient decreased from 10.26 Btu / hr- sqft -F to 9.428 Btu /hr-sqft-F. Overall heat transfer coefficient (U_o) decreased from 7.33 to 5.38 Btu /hr-sqft-F, however the overall conductance ($U_o A_o$), increased from 2978.46 to 6794.82 Btu /hr -F, because heat transfer area increased from 406.0 to 1262.3 sqft, due to increase in fins per inch. NTU is the main parameter controlling the effectiveness of the heat exchanger. NTU increased from .46 to 1.049. Heat exchanger effectiveness increased from 34.6 % to 59.4 % .

Although, the air side friction factor decreased, air side pressure drop increased from .175 to .297 inches water gauge, due to increase in heat transfer area, (nearly 311%). The results are illustrated graphically in Figures 27 through 35.

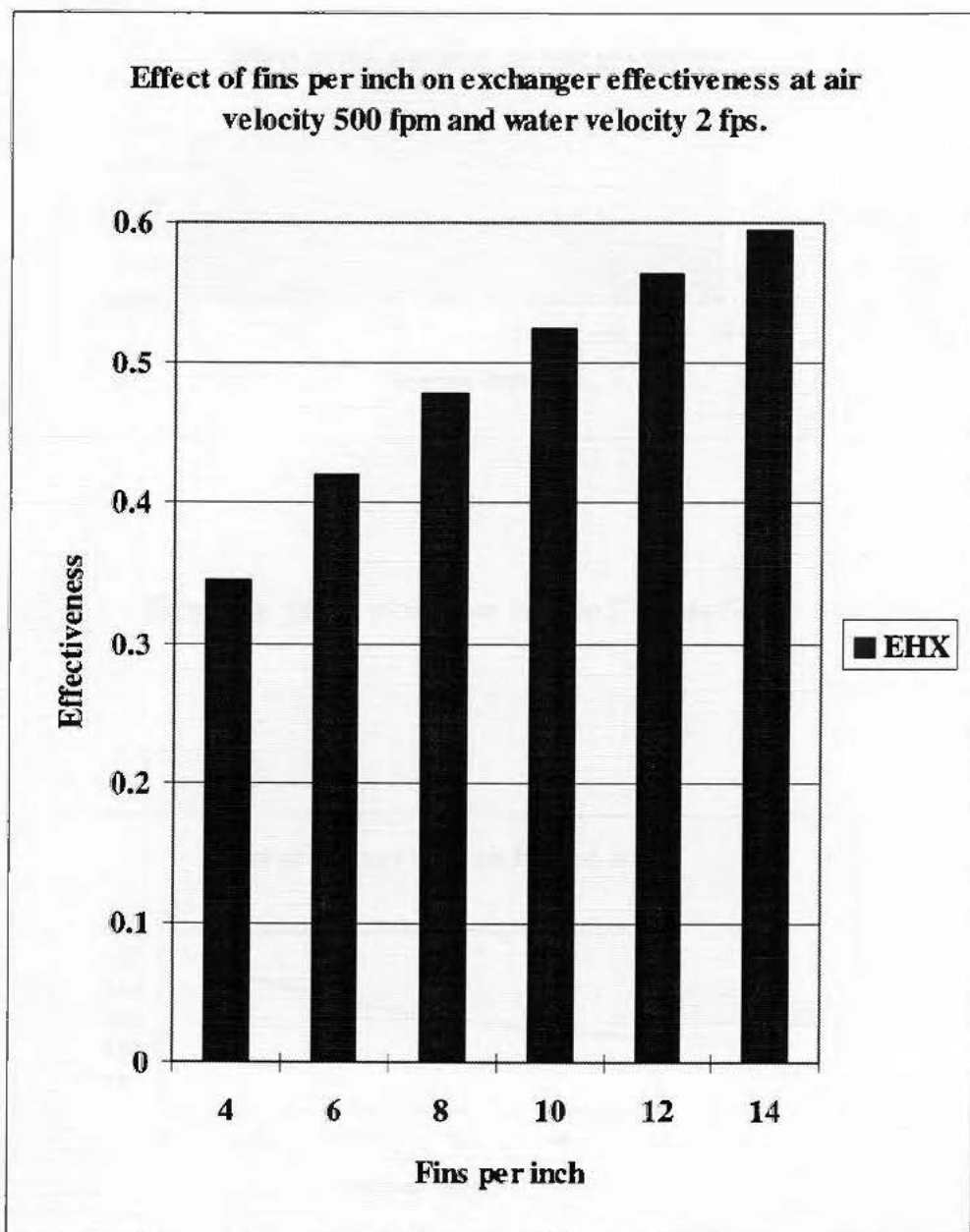


Figure 27 Effect of fins per inch on exchanger effectiveness

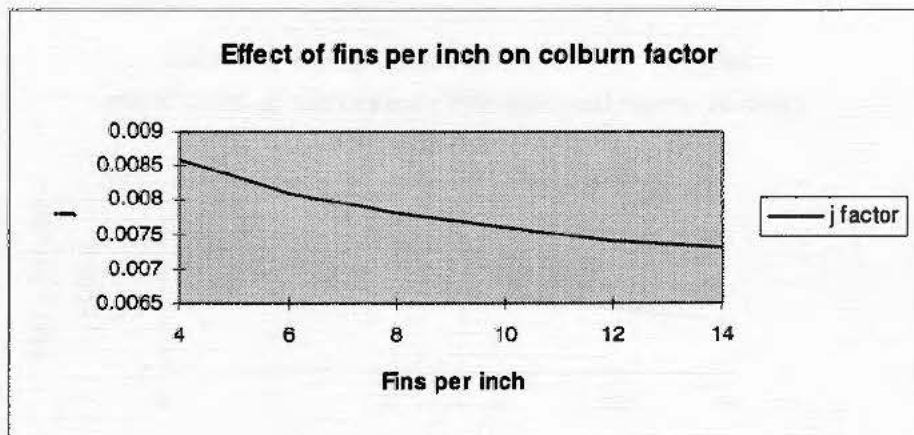


Figure 28 Effect of fins per inch on Colburn factor

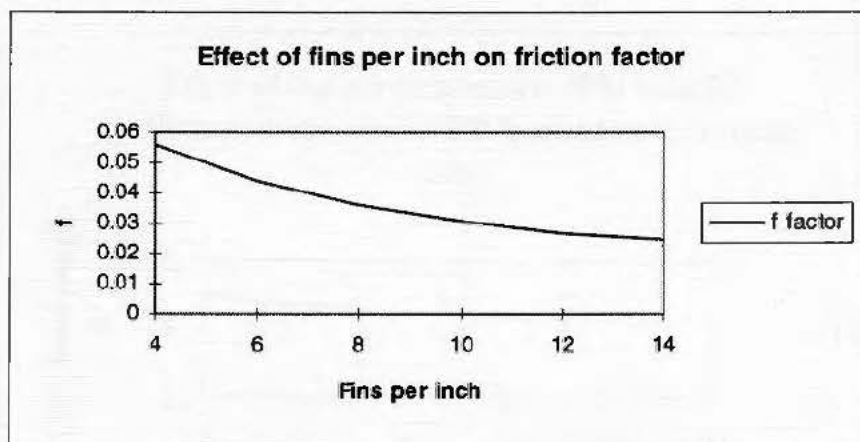


Figure 29 Effect of fins per inch on friction factor.

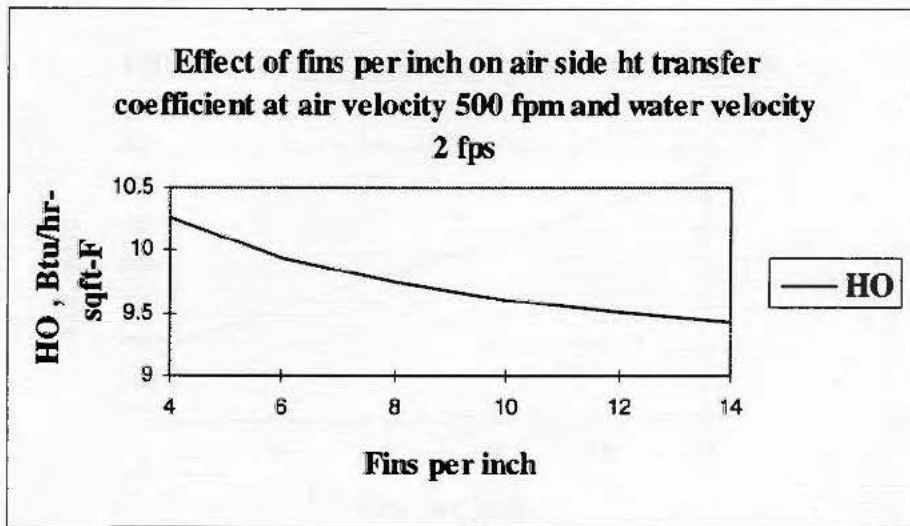


Figure 30 : Effect of fins per inch on airside heat transfer coefficient

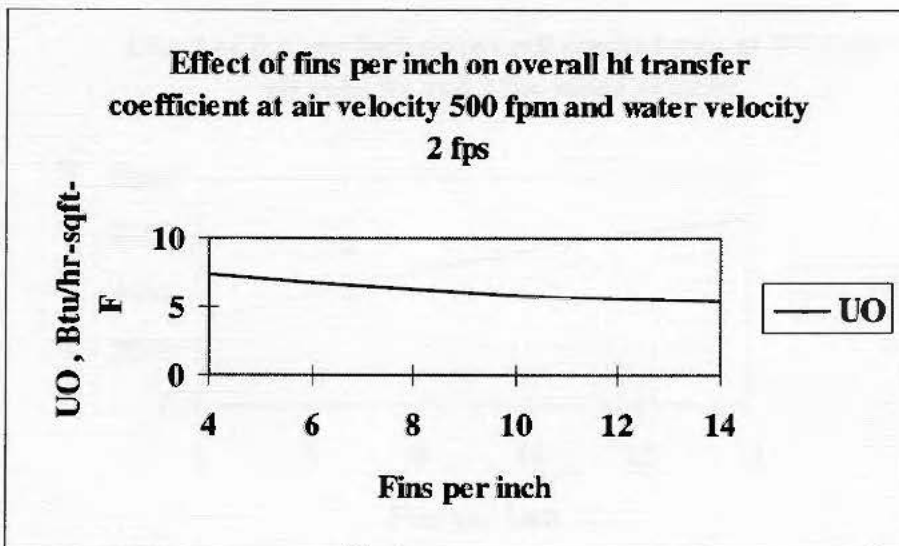


Figure 31 : Effect of fins per inch on overall heat transfer coefficient

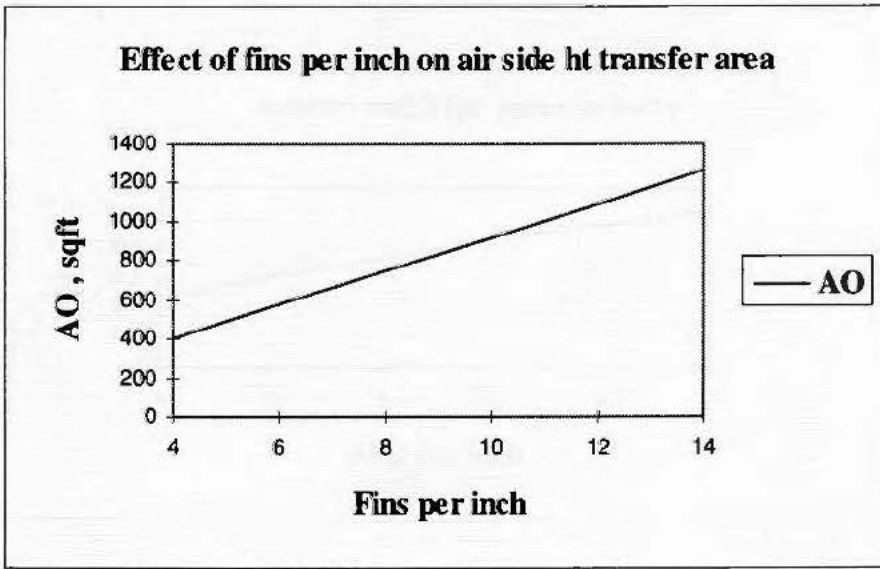


Figure 32 Effect of fins per inch on heat transfer area.

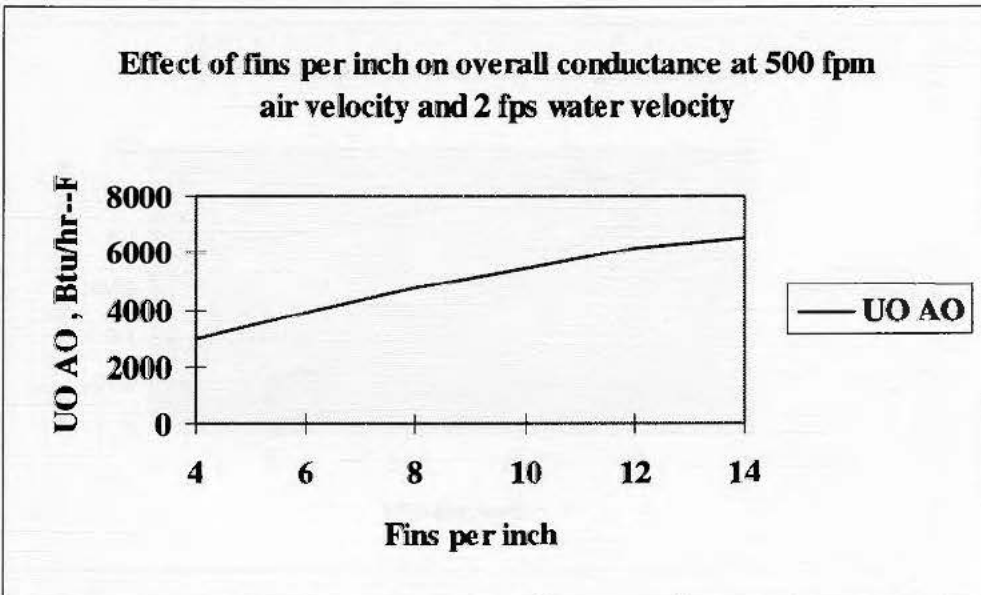


Figure 33 Effect of fins per inch on overall conductance

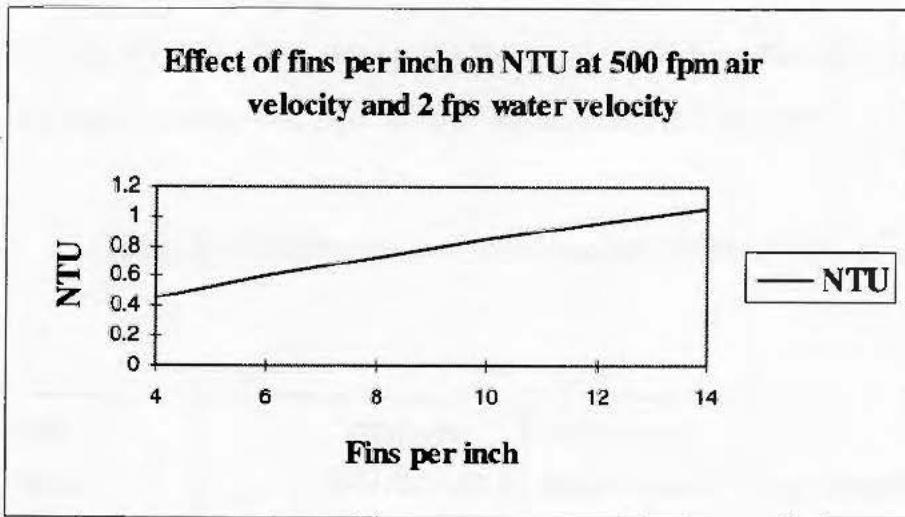


Figure 34 Effect of fins per inch on NTU

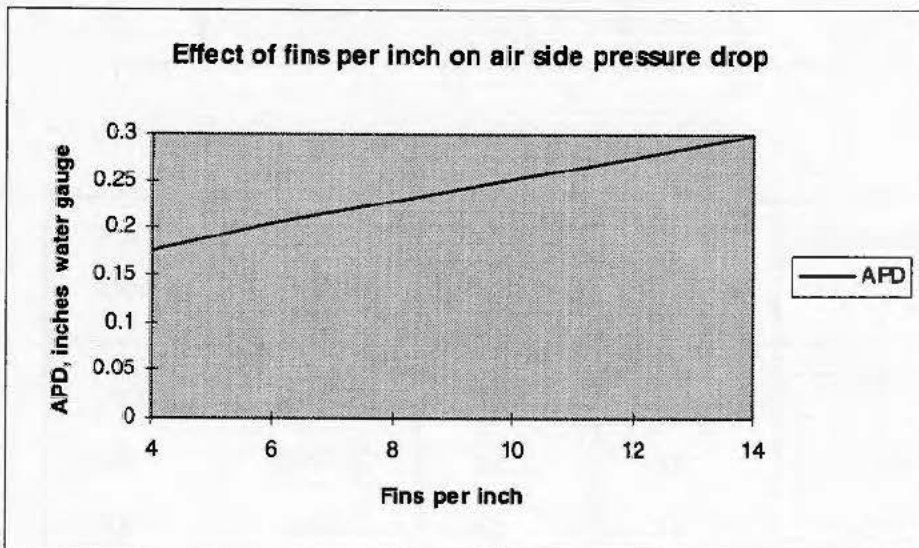


Figure 35 Effect of fins per inch on air side pressure drop

2) **Effect of air velocity :**

Program P4, was run at air velocity from 200 to 800 fpm. Fins per inch were fixed at 4 and water velocity was 2fps. Results are tabulated in Table 33.

Table 33 : Impact of air velocity on exchanger design.

VA fpm	j	f	HO(air) Btu /hr.sqft.F	HI(water) Btu /hr.sqft.F	UO Btu/hr.sqft.F	AO sqft
200	.017	.085	5.62	383.3	4.59	406
400	.0092	.062	8.84	↓	6.57	↓
600	.008	.051	11.58		8.00	
800	.0073	.045	14.06		9.149	

VA fpm	UOAO Btu/hr-F	NTU	EHX	APD inch.wg
200	1866.24	.72	.49	.04
400	2669.07	.51	.38	.12
600	3250.41	.41	.31	.23
800	3714.77	.35	.27	.37

Increase in air velocity decreased the Colburn factor and friction factor. Colburn factor, decreased from .017 to .0073. Friction factor decreased from .085 to .045. Air side heat transfer coefficient increased from 5.62 to 14.06 Btu/hr-sqft-F; in spite of decrease in the j factor. Overall heat transfer coefficient increased from 4.59 to 9.14 Btu/hr-sqft-F and overall conductance increased from 1866.24 to 3714.77 Btu/hr-F.

Exchanger NTU decreased from .72 to .3587 inspite of the increase in the overall conductance. This is because air flow rate is less than water flow rate for air velocity range, (200 to 800 fpm) considered for computer simulation. Effectiveness of exchanger decreased from 49.7 % to 27.7 %.

Air pressure drop increased from .041 to .374 inches water gauge.

The results are illustrated graphically in Figures 36 through 43. The combined impact of fins per inch and the air velocity on exchanger performance is illustrated in Figures 44 through 46.

Effect of water velocity :

Program was run at water velocity range of 1 to 6 fps and fins per inch, 4 to 14. Air velocity was constant at 500 fpm. Figures 47 and 48 illustrate the results. At low fins per inch water velocity did not have major effect on exchanger overall conductance, U_oA_o and effectiveness compared to high fins per inch. Figure 47 shows that at 2 FPI, increase in water velocity increased overall conductance from 1856.5 to 2084.3 Btu/hr-sqft-F, (increase of 12.3%) compared to the range of 5586.5 to 8195.3 Btu/hr-sqft-F, (increase of 47%). The possible explanation for this rise in values is that at low FPI, the change in resistance on water side due to variation in water velocity is not dominant in (U_oA_o) term because of large value of air side resistance. At high FPI, air side resistance decreases due to high heat transfer area; therefore water side heat transfer coefficient is more dominant. Figure 48 shows that at 4 FPI, the exchanger effectiveness increased from 30.5% to 38.4%, increase of only 7.9% compared to increase from 48.6% to 70%, increase of 21.4% at 14 FPI.

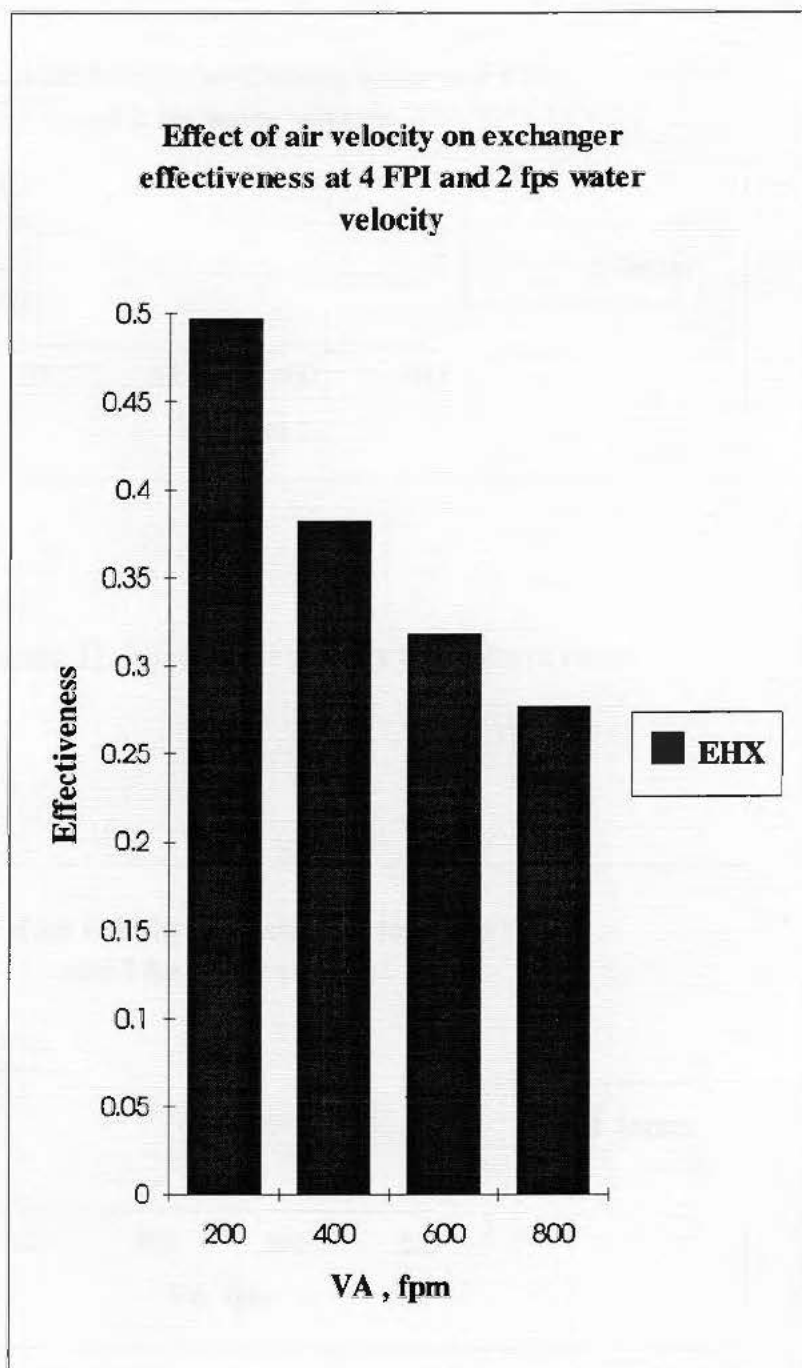


Figure 36 Effect of air velocity on exchanger effectiveness

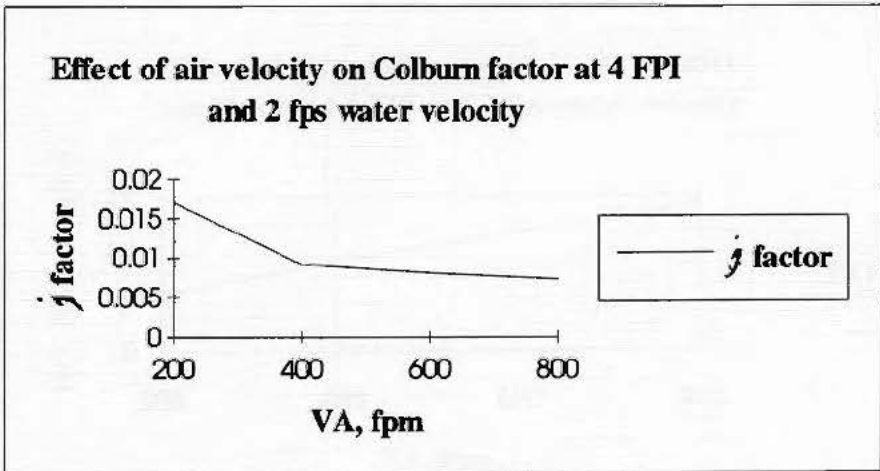


Figure 37 Effect of air velocity on Colburn factor.

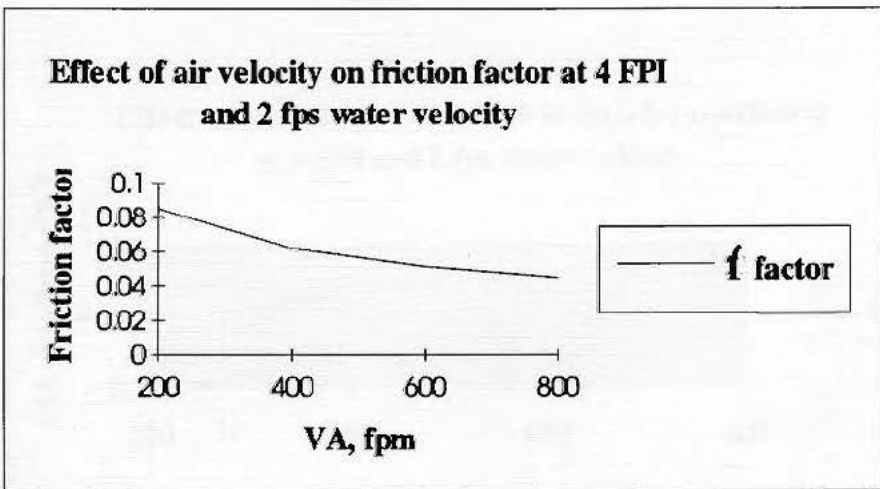


Figure 38 Effect of air velocity on friction factor.

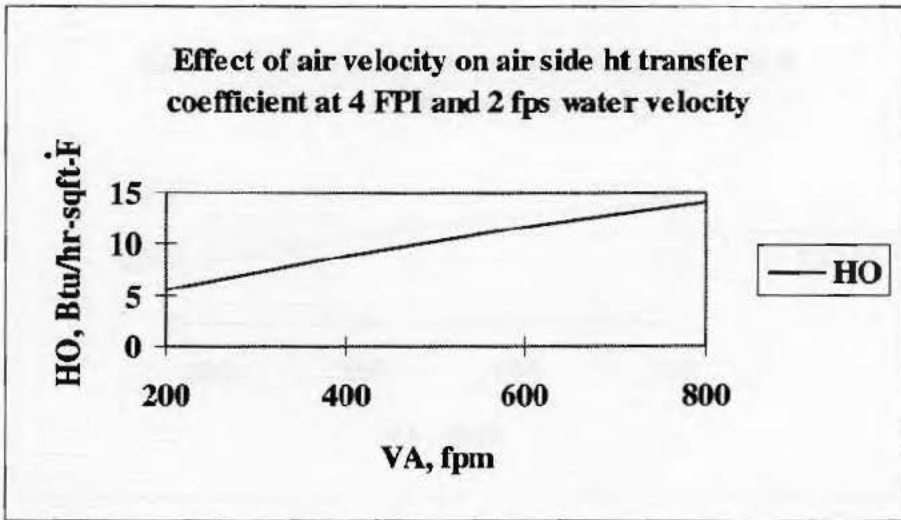


Figure 39 Effect of air velocity on air side heat transfer coefficient

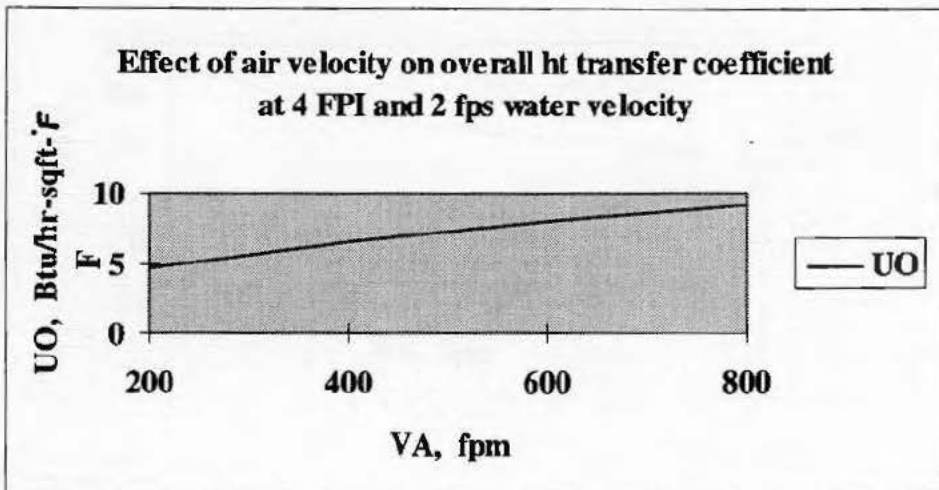


Figure 40 Effect of air velocity on overall heat transfer coefficient.

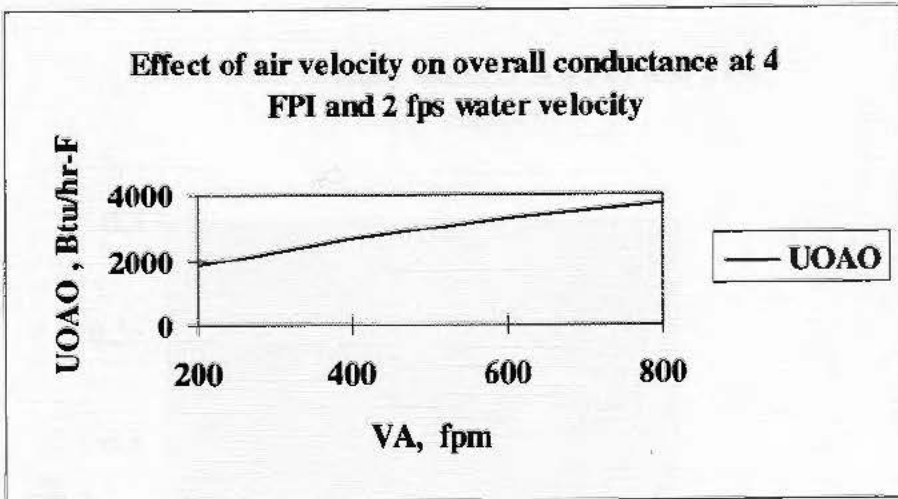


Figure 41 Effect of air velocity on overall conductance

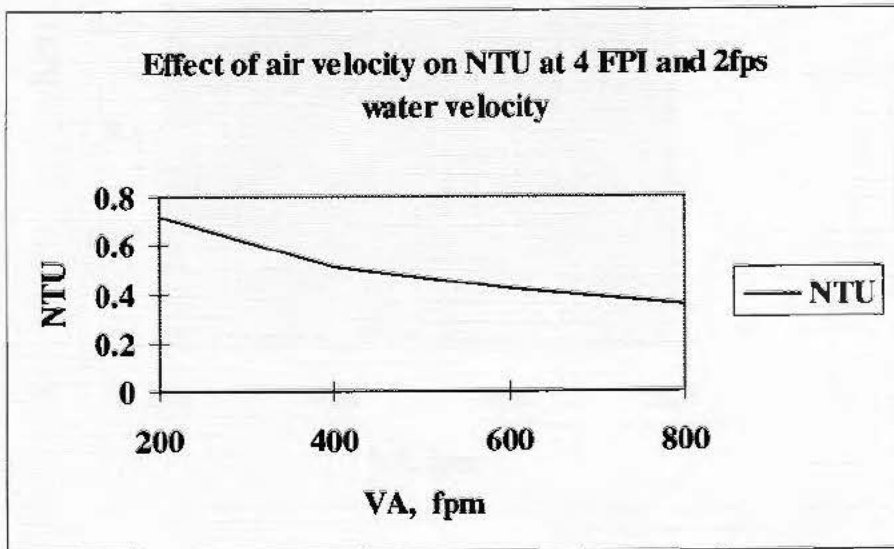


Figure 42 Effect of air velocity on NTU

Effect of air velocity on APD at 4 FPI and 2 fps water velocity

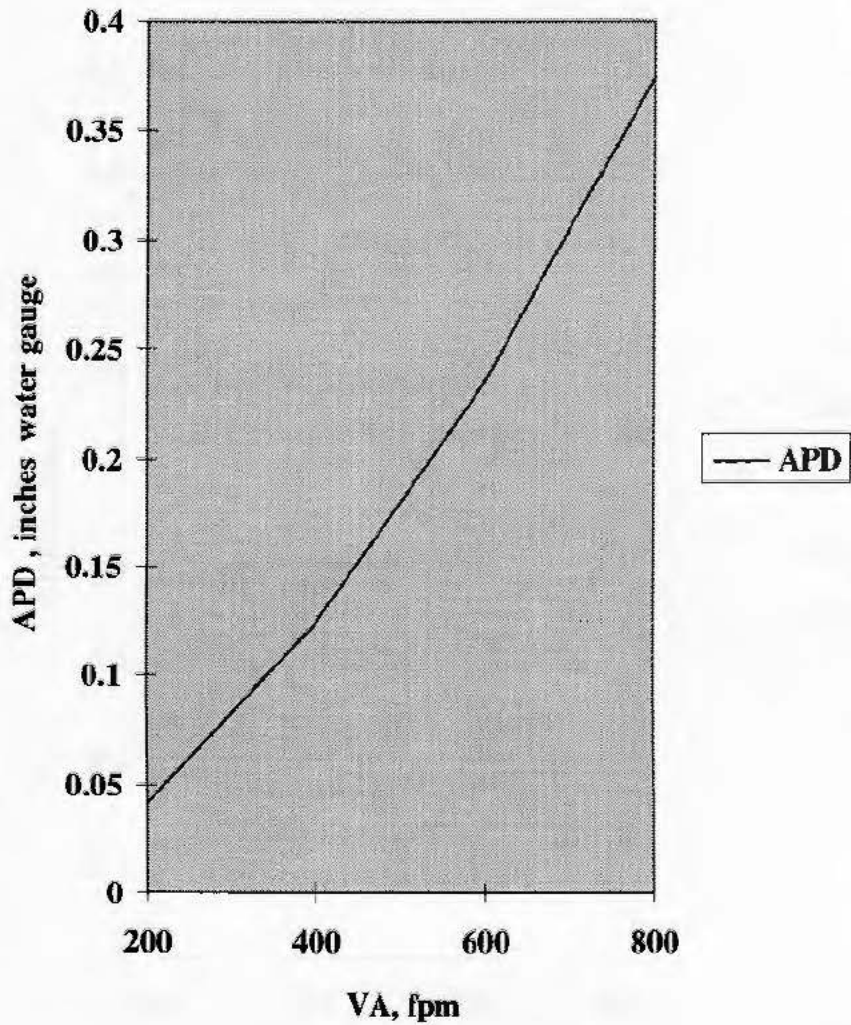


Figure 43: Effect of air velocity on air pressure drop

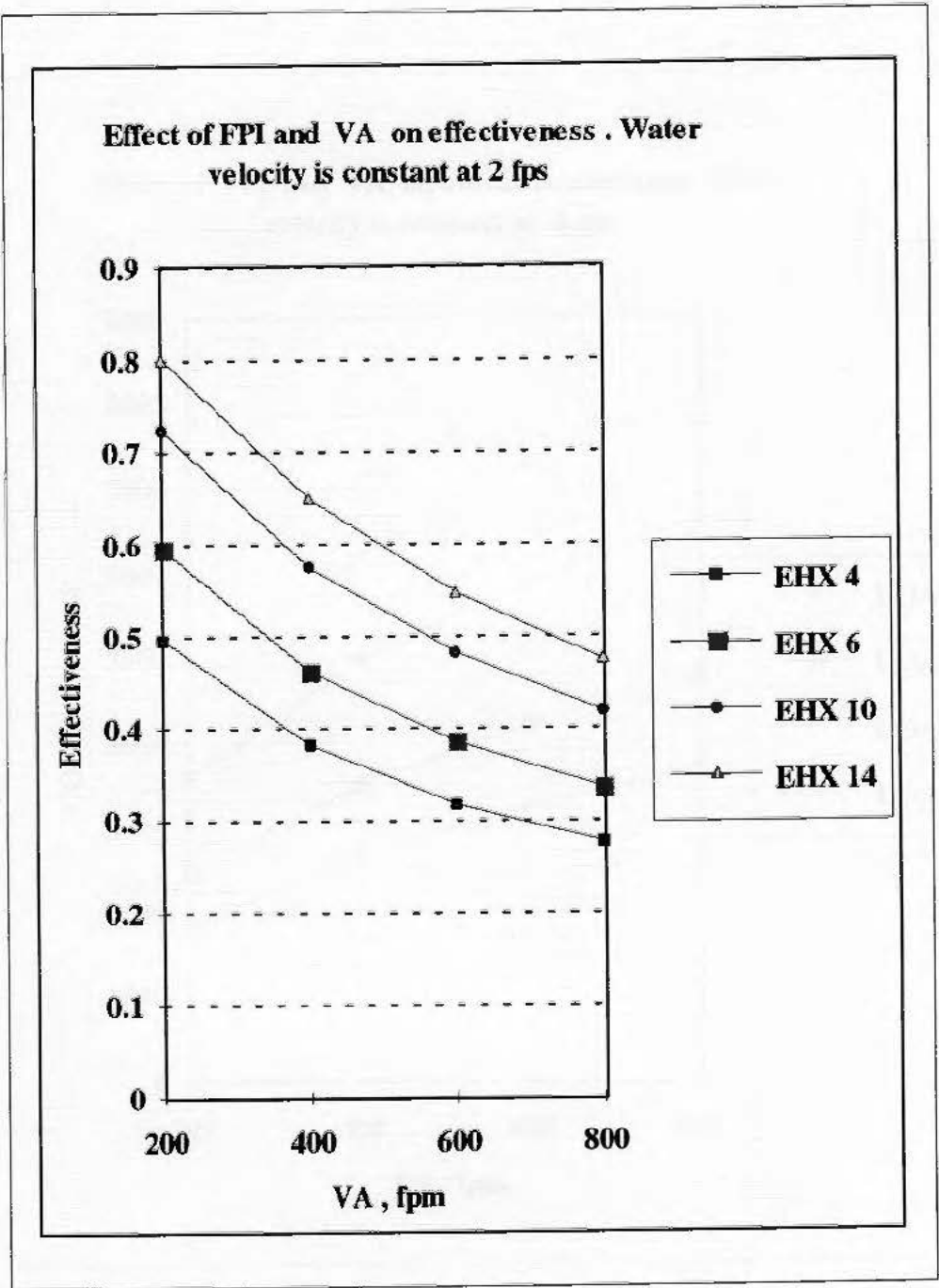


Figure 44 Effect of fins per inch and air velocity on effectiveness

Effect of FPI and VA on overall conductance. Water velocity is constant at 2 fps.

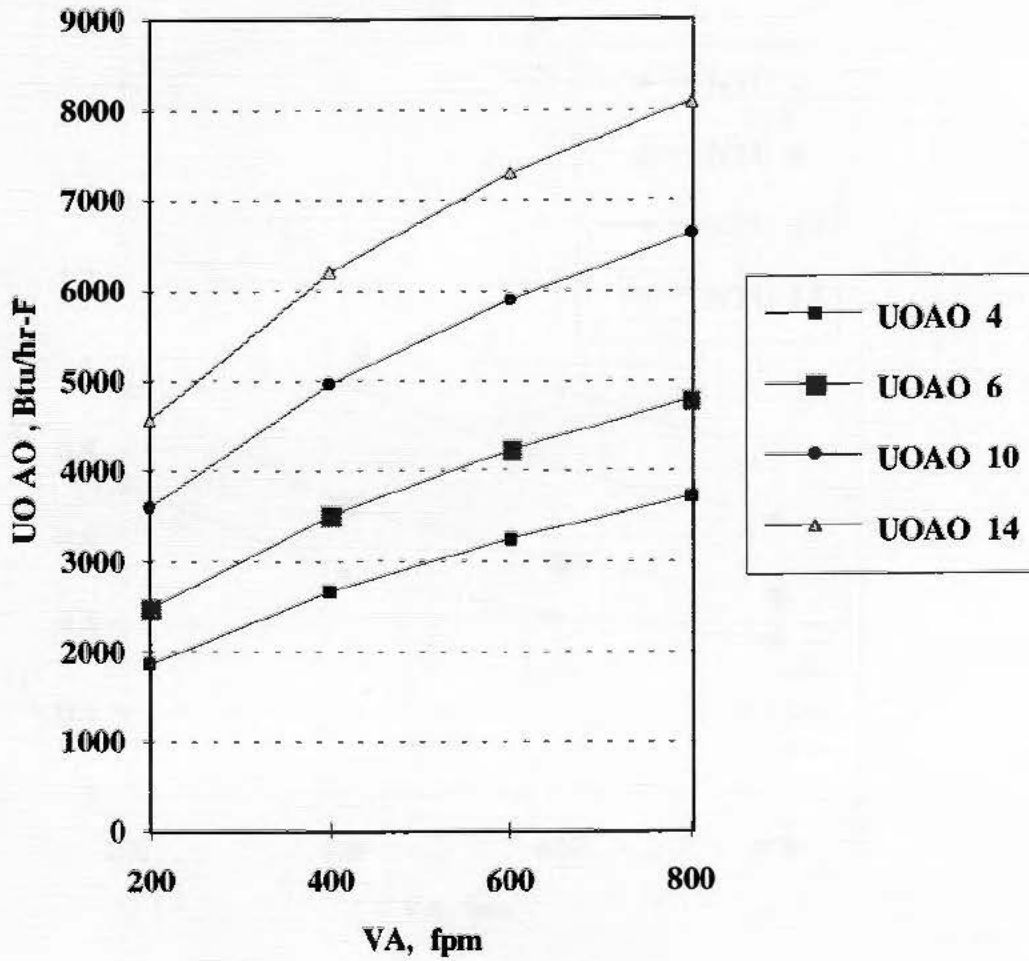


Figure 45 Effect of fins per inch and air velocity on overall conductance

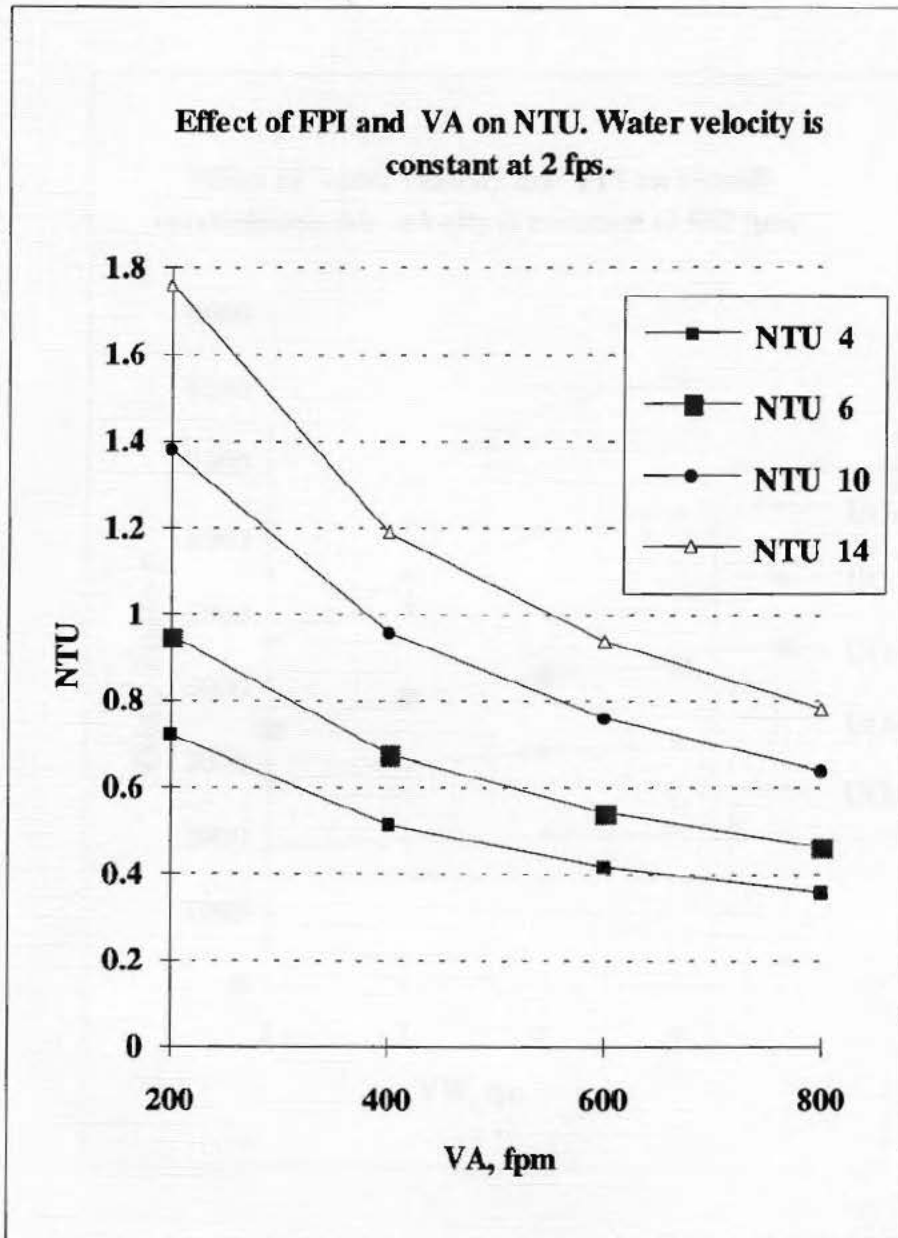


Figure 46 Effect of fins per inch and air velocity on NTU.

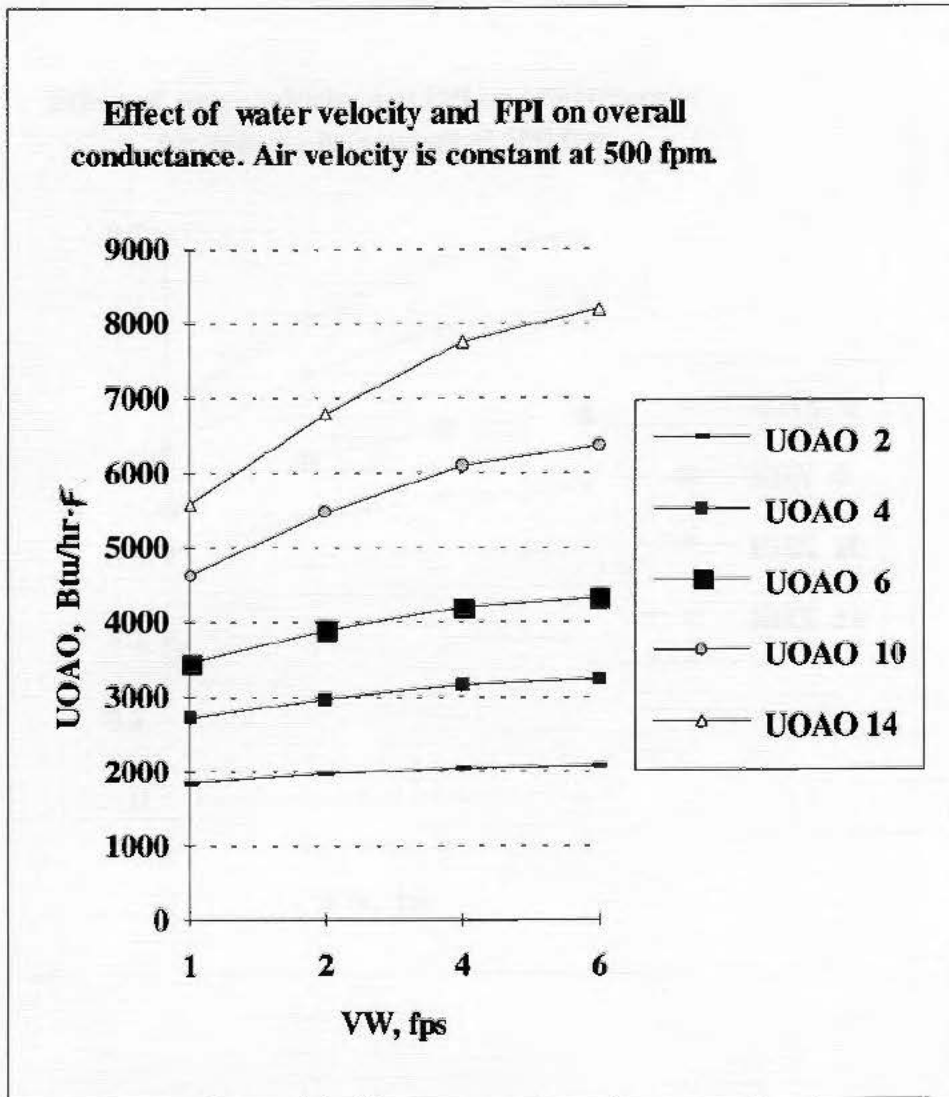


Figure 47 : Effect of water velocity on overall conductance at various fins per inch

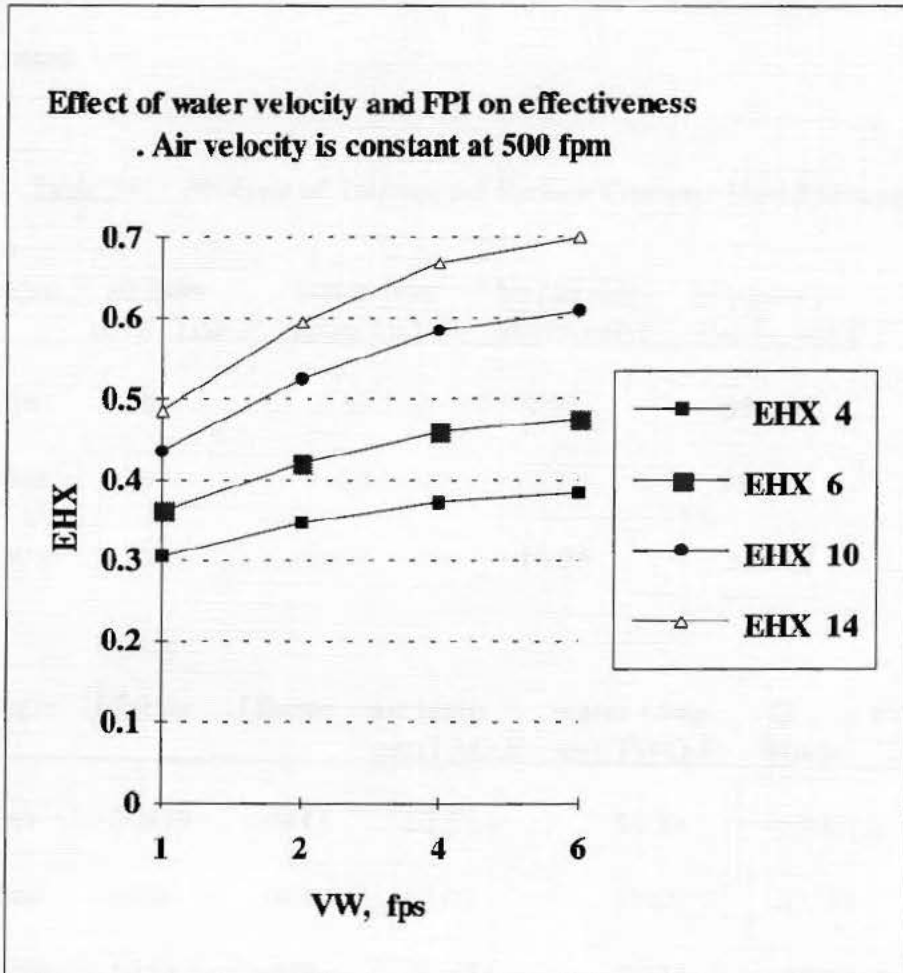


Figure 48 Effect of water velocity on effectiveness at various fins per inch

Compact Heat Exchanger with Interrupted Fins :

Results of the analysis to consider the impact of fin geometry, as outlined in previous chapter are presented in Table 34. The results are based on the same surface area for all three cases.

Table 34 : Analysis of Interrupted Surface Compact Heat Exchanger.

exchanger type	air inlet temp ,TAI ,F	water inlet temp,TWI ,F	ho (air side) Btu/hr.sqft.F	hi (water) Btu/hr.sqft.F	Uo(overall) Btu/hr.sqft.F
plate fins	70	50	9.94	384.46	6.81
wavy fins	70	50	12.12	385.01	7.78
offset strip fins	70	50	18.05	386.17	10.15

exchanger type	j factor	f factor	air temp out,TAO,F	water temp out,TWO,F	Q Btu/hr	fin efficiency
plate fins	.00819	.0443	61.5	53.34	55007.3	.80
wavy fins	.0098	.049	60.69	53.65	60189.5	.76
offset strip fins	.0153	.073	59.03	54.31	70991.1	.69

exchanger type	fin effectiveness	exchanger effectiveness , EHX	air pressure drop psi
plate fins	.82	42.4%	.206
wavy fins	.79	46.5%	.226
offset strip fins	.72	54.8%	.327

Lowest air side heat transfer coefficient of 9.94 Btu/hr.sqft-F was obtained for the plate fins, followed by the wavy, (12.12) and offset strip fins, (18.65). Higher heat transfer coefficients are produced for the interrupted surface heat exchanger because these surfaces do not allow the boundary layers to fully develop, thereby resulting in increased heat transfer coefficients [11]. The Colburn factor increased from .00819 (plate fins), to .0098 (wavy fins), and 0.0153 (offset strip fins). Overall heat transfer coefficient increased from 6.81 Btu/hr.sqft.F, (plate fins) to 10.15 (offset strip fins).

Water side heat transfer coefficient was nearly same for all the three heat exchanger types. The minor increase in value from 384.4 to 386.17 Btu/hr.sqft.F is due to increase in outlet water temperature. The exchanger effectiveness was found to be, 42.4% (plate fins), 46.5%, (wavy fins) and 54.80%, (offset strip fins). The results are also illustrated in Figures 49 through 52.

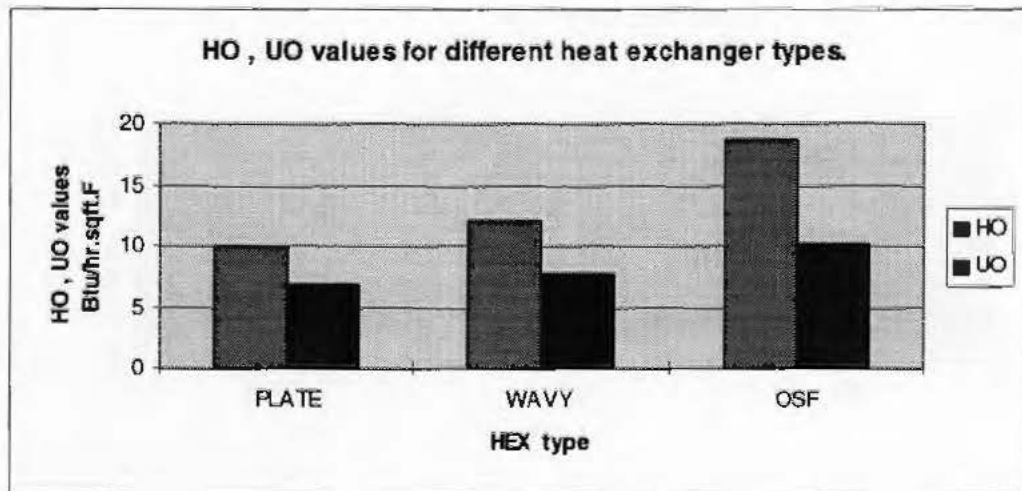


Figure 49: HO,UO for different HEX.

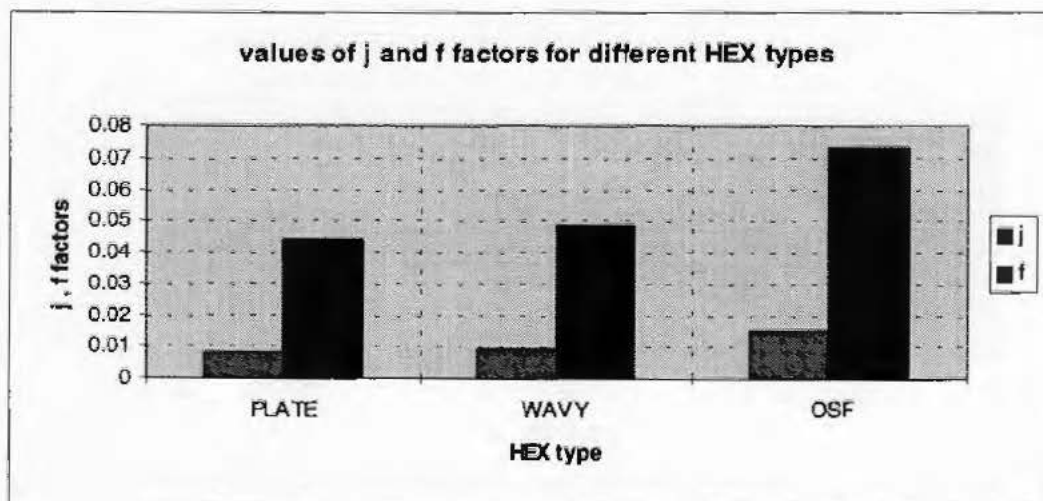


Figure 50 : j and f for the different HEX

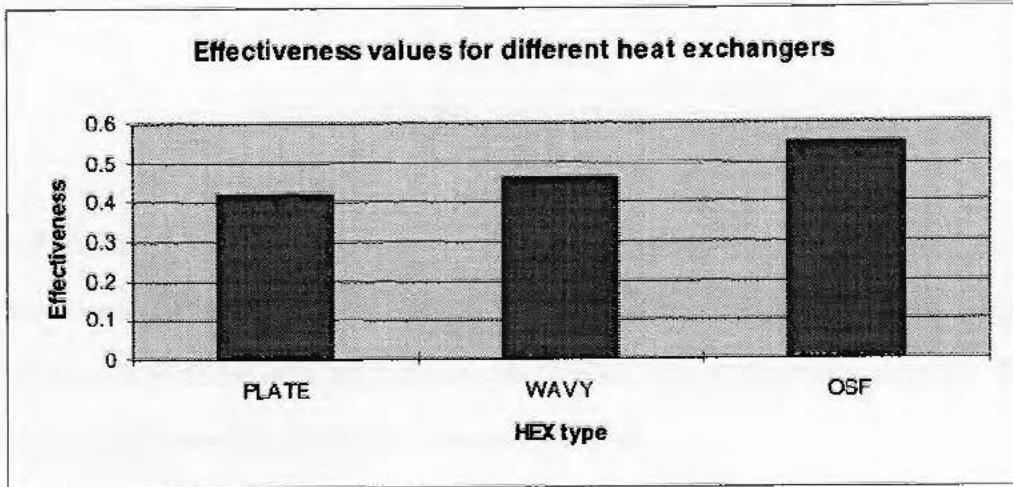


Figure 51 : Effectiveness for the different HEX

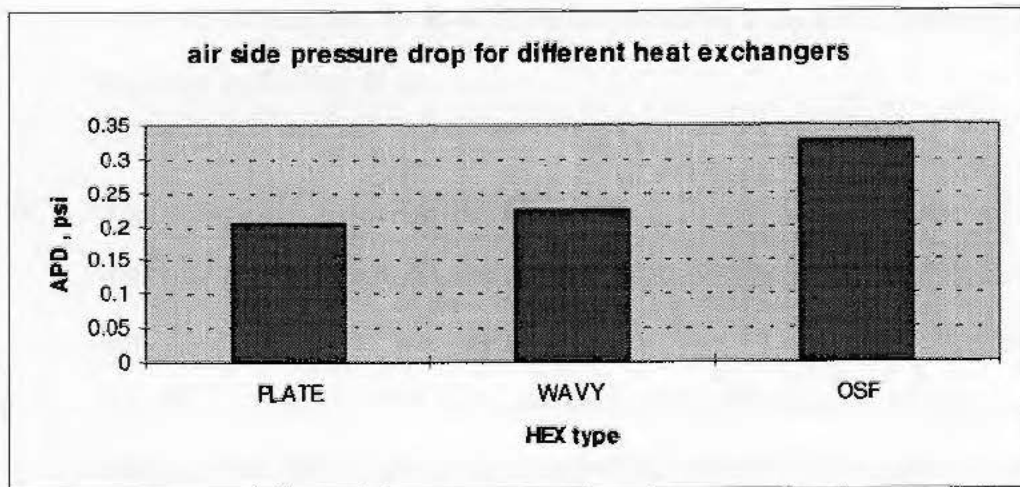


Figure 52 : Air side pressure drop for different HEX.

CHAPTER 4
CONCLUSIONS

• A thorough analysis of the impact of alternate refrigerants on the thermal design parameters of the evaporator is done. The performance of the evaporator using alternate refrigerant R-152a, is found to be the best among the refrigerants compared, for both the Plate-fin tube and the Shell and Tube evaporators.

- 1) The heat transfer surface area required for the plate fin tube heat evaporator using R-152a is about 4% less than that of R-22 and R-12. The reduction in surface area for R-134a is just about the same as that of R-152a. On the other hand, the required surface area for R-402a and R-404a are about 2.6% greater than that required by R-22 or R-12.

- 2) The air side pressure drop for refrigerants R-152a or R-134a is about 4.4% less than that for R-22 or R-12, while it is 2.2% more for R-402a and R-404a. The results for the drop-in evaluation in the plate-fin tube evaporator, showed that the effectiveness of R-152a evaporator is the highest at all the evaporator temperatures. The decrease in the evaporator temperature or the increase in the inlet refrigerant quality was found to increase the effectiveness.

- 3) The effectiveness or heat duty of a plate fin tube evaporator using R-134a or R-152a increases by 2.8% as compared to the case with R-22 or R-12 at evaporator temperature of 40 F.

- 4) The percentage improvement goes down to 1.8% when the evaporator temperature is lowered to 5 F.

- 5) The percentage improvement of heat transfer rate or effectiveness due to use of alternate refrigerants does not change appreciably, if the quality of refrigerants at the inlet of the evaporator varies from zero percent to 39 percent.
The impact of alternate refrigerants on design parameters of shell and tube evaporator showed the same trends as exhibited by the results of plate fin tube evaporator.
- 6) The surface area of a shell and tube exchanger required by the use of alternate refrigerants R-152a and R-134a decreases by 13.4 percent as compared to the case with refrigerant R-12 and the number of baffles decreased by 12.5 percent.
- 7) Refrigerants R-402a showed an opposite effect i.e, the required surface area is increased by 9.1 percent and the number of baffles by 6.3 percent.
- 8) The shell side pressure drop in case of R-152a and R-134a decreased by 10.3 percent, while it increased by the same amount for R-404a as compared to refrigerant R-12.
- 9) The alternate refrigerant refrigerant R-404a has no effect at all on the design parameters of shell and tube heat exchangers as compared to R-12 case.

- Increase in the number of fins increased the effectiveness and the air side pressure drop while increase in the air velocity decreased the effectiveness and increased the air side pressure drop. Water velocity did not have any appreciable effect on the exchanger effectiveness and overall conductance at lower fins per inch. Offset strip fins on the heat exchanger surface generated highest overall heat transfer coefficient and air-side pressure drop followed by the wavy and plate fins.

CHAPTER 5

RECOMMENDATIONS

Future research in this area may be directed towards the following topics :

- Impact of the Non-Azeotropic refrigerant mixtures on the thermal design parameters of the evaporator.
- Impact of alternate refrigerants on the mechanical design of heat exchangers. A particular case could be the analysis of their impact on stress distribution for U-type shell and tube heat exchanger.
- Investigation of heat and mass transfer process in compact heat exchanger, such as humidification and dehumidification coils.
- Second law analysis of compact heat exchanger with interrupted fin surfaces. This is proposed due to the immense use of interrupted surfaces in current heat exchanger industry.

REFERENCES

1. S. Kakac, A.E Bergles, F. Mayinger, Heat Exchanger Thermal Hydraulic Fundamentals and Design, Hemisphere Publishing Corporation., New York, 1990.
2. ASHRAE Handbook of Fundamentals, 1994, I-P edition, American Society of Heating, Refrigeration and Air Conditioning Engineers, Inc, Atlanta, GA.
3. R. Radermacher, D. Jung . “ Theoretical Analysis of Replacement Refrigerants for R-22 for Residential Uses”. “ ASHRAE Transactions”, Volume 99, part 1, 1993.
4. Halim Wijaya and Mark W. Spatz ,“Two-Phase Flow Heat Transfer and Pressure Drop Characteristics of R-22 and R-32/125 ”, “ASHRAE Transactions”, Volume 101, To be published in May 1995.
5. H.A Duarte-Garza and R.C. Miller, “Thermodynamic Properties of Pentafluoroethane (R-125) and 1,1- Dichloro-1-Fuoroethane (R-141b) , “ASHRAE Transactions”, part 1, 1993.
6. M.Y Poz and J.C Conklin ,” Heat Exchanger Analysis for Non Azeotropic Refrigerant Mixtures”, “ASHRAE Transactions”, Volume100, part 1, February 1994.
7. Nakhe Kattan and Daniel Favrat,“ R-502 and Two Near Azeotropic Alternatives, Part 2: Two Phase Flow Patterns ”,“ ASHRAE Transactions ”, Volume 101, Part 1, To be published in May 1995.
8. Samuel M. Sami and P.J. Tulej,“ Study of Heat and Mass Characteristics of Ternary Non Azeotropic Refrigerant Mixtures inside Air/Refrigerant-Enhanced Surface Tubing”, “ASHRAE Transactions ”, V 101, Pt 1, To be published in May 1995.
9. J. Darabi and M. Salehi ,“Review of the Available Correlations for Prediction of Flow Boiling Heat Transfer in Smooth and Augmented Tubes”,“ASHRAE Transactions” V 101, Pt 1, To be published in May 1995.

10. A.R. Weiting, "Empirical Correlations for Heat Transfer and Flow Friction Characteristics of Rectangular Offset-Strip Fin Heat Exchangers", "ASHRAE Transactions", 1974.
11. D.T Beecher and T.J Fagan, "Effects of Fin Pattern on the Air-Side Heat Transfer Coefficient in Plate Finned-Tube Heat Exchangers", "ASHRAE Transactions", 1987.
12. F.C. Mcquiston, "Correlation of Heat, Mass and Momentum Transport Coefficients for Plate Fin Tube Heat Transfer Surfaces", "ASHRAE Transactions", Volume 84, part 1, 1978.
13. Curve Fitting Software- 2D, Jandel Corporation, San Francisco, CA.
14. Donald G Rich, "The Effect of Number of Tube Rows on Heat Transfer Performance of Smooth Plate Fin Tube Heat Exchanger", "ASHRAE Transactions", Volume 81, Part 1, 1975.
15. W.M. Kays and A.L London. Compact Heat Exchangers, 2nd edition. Mc Graw-Hill Corporation, San Francisco, 1964.
16. Sadik Kakac, Boilers, Evaporators and Condensers, Hemisphere publishing corporation, New York 1990.
17. R.K Shah, A.D Kraus and D. Metzger, Compact Heat Exchangers, a festschrift for A.L London. Hemisphere Publishing Corporation, New York 1990.
18. A. Sahnoun and R.L Webb, Prediction of Heat Transfer and Friction Factor for Louver Fin Geometry, Intl Journal of Heat Transfer, March 1992.
19. Perry's Chemical Engineering Handbook, McGraw Hill Publications, 1993.

APPENDICES

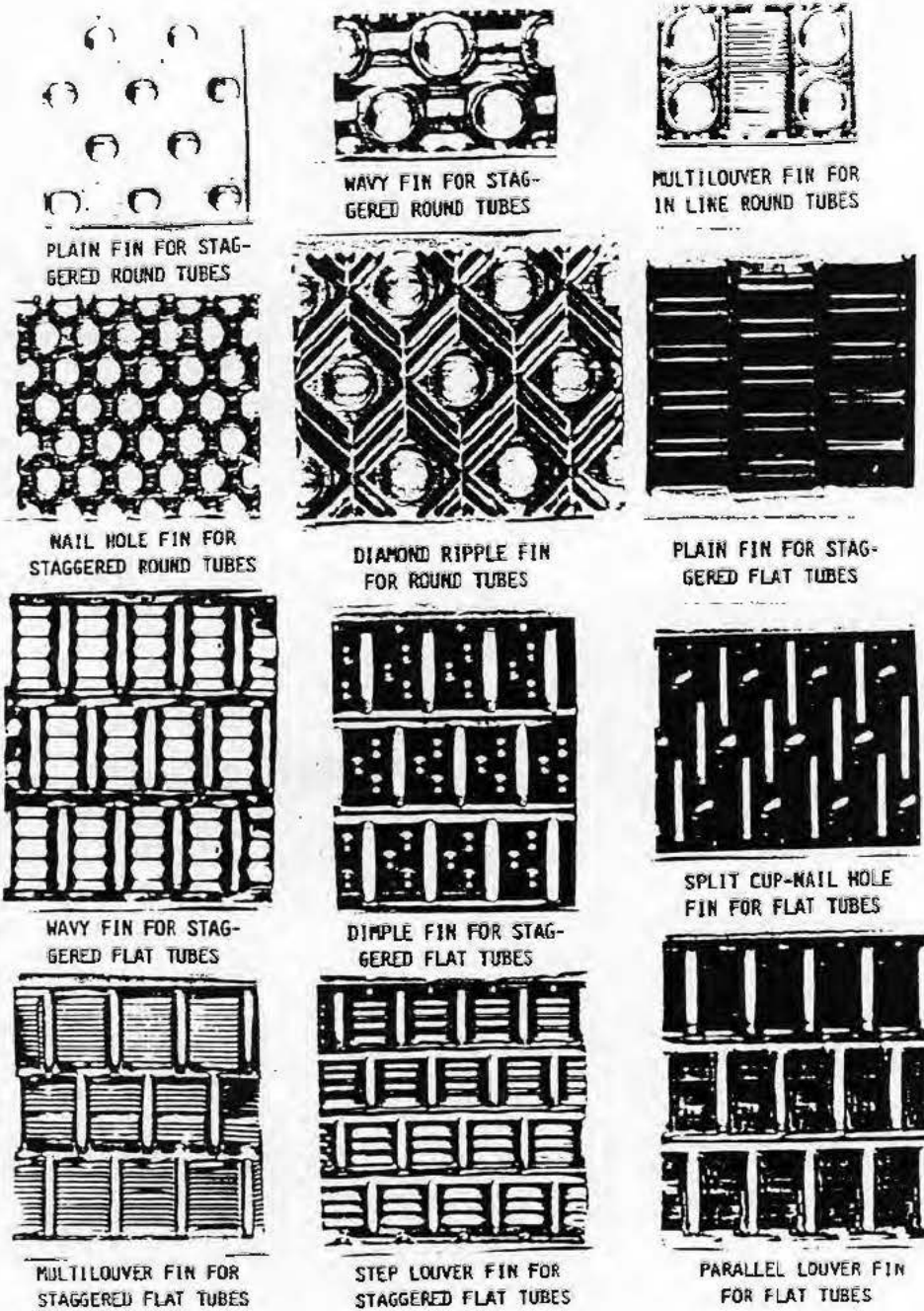


FIGURE 1.1: INTERRUPTED FIN SURFACES [1]

APPENDIX A 2

1. PLATE FIN TUBE EVAPORATOR DESIGN

```

31 REM DIT: tube inner diameter
40 DTO = .525
41 REM DTO: tube outer diameter
50 XA = 1.25
51 REM XA: transverse spacing
60 XB = 1.083
61 REM XB: longitudinal spacing
70 CTR = 277
80 ALK = 100
81 REM CTR, ALK: thermal conductivity
90 T = 400
91 REM T, fin thickness
95 S = 8
96 REM S: fins per inch

```

```

99 REM ***** INPUT DATA *****

```

```

100 INPUT "TAW="; TAW
101 REM TAW: cooling air temperature, F
110 INPUT "TAC="; TAC

```

Computer program (P1) : Plate fin tube evaporator design

```

120 DV = (TAW - TAC) / 18
121 REM TE: evaporator temperature, F
140 INPUT "QA="; QA
141 REM QA: air volume flow rate, SCFM
150 INPUT "VA="; VA
151 REM VA: air velocity, FPM
160 INPUT "VR="; VR
161 REM VR: refrigerant velocity, ft/s
170 INPUT "PA="; PA
171 REM PA: air pressure
190 DH = -2.509963E-03 + (.861731362E-01) * (S * (.807340938))
200 CC1 = 2.689112388 + (1.0838651E-02) * (S * S) * (LOG(S))
210 AR1 = (1) / (CC1)
211 REM AR1: unit free flow area to the frontal area
220 CC2 = 3211547 + (.326172) / (LOG(S))
230 AR2 = 1 / CC2
231 REM AR2: ratio of AFA
235 ALPHA = 14.65963 + 12.76445 * S
235.1 REM ALPHA: HEW area to the volume ratio
236 PRINT "DH="; DH, "AR1="; AR1, "AR2="; AR2, "ALPHA="; ALPHA
260 REM ***** PROPERTIES OF AIR *****
270 RA = 33.352
280 A1 = .1983649

```

1 REM PLATE FIN TUBE EVAPORATOR DESIGN

```
31 REM DTI: tube inner diameter
40 DTO = .525
41 REM DTO: tube outer diameter
50 XA = 1.25
51 REM XA: transverse spacing
60 XB = 1.083
61 REM XB: longitudinal spacing.
70 CUK = 227
80 ALK = 100
81 REM CUK, ALK thermal conductivity
90 T = .006
91 REM T, fin thickness
95 S = 8
96 REM S, fins per inch.

99 REM***** INPUT DATA*****
100 INPUT "TAI="; TAI
101 REM TAI: entering air temperature, F
110 INPUT "TAO="; TAO
111 REM TAO:leaving air temperature, F
120 INPUT "TE="; TE
121 REM TE: evaporator temperature, F
140 INPUT "QA="; QA
141 REM QA: air volume flow rate, SCFM
150 INPUT "VA="; VA
151 REM VA: air velocity, FPM.
160 INPUT "VR="; VR
161 REM VR: refrigerant velocity, fps.
170 INPUT "PA="; PA
171 REM PA: air pressure
190 DH = -2.569963E-02 + (.961731562#) * (S ^ (-.80734013#))
200 CC1 = 1.68911259# + (1.983865E-02) * (S ^ .5) * (LOG(S))
210 AR1 = (1) / (CC1)
211 REM AR1: min free flow area to the frontal area.
220 CC2 = .9218547 + (.336112) / (LOG(S))
230 AR2 = 1 / CC2
231 REM AR2: ratio of Af/A.
235 ALPHA = 14.65963 + 19.76648 * S
235.1 REM ALPHA: HEX area to the volume ratio.
236 PRINT "DH="; DH, "AR1="; AR1, "AR2="; AR2, "ALPHA="; ALPHA
260 REM****PROPERTIES OF AIR****
270 RA = 53.352
280 A1 = .1980649
```

```

290 A2 = 3.030648E-03
300 A3 = 7.75636E-04
310 A4 = 1.61686E-06
320 A5 = 7.07473E-07
330 AN1 = A1 + A3 * TAI + A5 * TAI * TAI
340 D1 = 1 + A2 * TAI + A4 * TAI * TAI
350 AVI = (AN1 / D1) ^ 2
351 REM AVI: air inlet viscosity.
360 AN2 = A1 + A3 * TAO + A5 * TAO * TAO
370 D2 = 1 + A2 * TAO + A4 * TAO * TAO
380 AVO = (AN2 / D2) ^ 2
381 REM AVO: air exit viscosity.
390 AV = (AVI + AVO) / 2
395 REM AV: bulk viscosity
400 A6 = .013071906#
410 A7 = 2.59434E-05
420 A8 = -5.0315E-09
430 A9 = 3.736332E-03
440 A10 = .041698788#
450 AKI = A6 + (A7 * TAI) + (A8 * TAI * TAI) + (A9 / TAI) + (A10) / (TAI * TAI)
460 AKO = A6 + (A7 * TAO) + (A8 * TAO * TAO) + (A9 / TAO) + (A10) / (TAO *
TAO)
470 AK = (AKI + AKO) / 2
471 REM AK :bulk thermal conductivity
480 ACP = .24
490 APR = (AV * ACP) / AK
500 ADI = (PA * 144) / ((RA) * (TAI + 460))
510 ADO = (PA * 144) / ((RA) * (TAO + 460))
520 ADM = (ADI + ADO) / 2
520.01 REM ADM: mean density of the air.
520.1 PRINT "AVI="; AVI, "AVO="; AVO, "AKI="; AKI, "AKO="; AKO, "ADM=";
ADM
521 REM***PROPERTIES OF SATD REFRIGERANT AT 40 F.
522 INPUT "DRL="; DRL
522.1 REM DRL: density of saturated liquid refrigerant.
523 INPUT "drv="; DRV
523.1 REM DRV : density of the saturated vapor refrigerant.
524 INPUT "HRL="; Hrl
524.1 REM HRL: enthalpy of the saturated liquid refrigerant.
525 INPUT "HRV="; HRV
525.1 REM HRV: enthalpy of the saturated refrigerant vapor.
528 INPUT "KRL="; KRL
529 INPUT "cpRl="; CPRL
529.1 INPUT "VSRL="; VSRL
529.3 INPUT "SIG="; SIG

```

```

529.4 X1 = 0
529.6 X = 1
529.7 HFG = (HRV - Hrl)
530 AM = (QA * 60 * ADI)
540 Q = AM * ACP * (TAI - TAO)
550 flr = Q / (HRV - Hrl)
560 AREAR = flr / (DRL * VR * 3600)
561 PRINT "AM="; AM, "Q="; Q, "FLR="; flr, "AREAR="; AREAR
570 TR1 = (4 * AREAR * 144) / (3.14159 * DTI * DTI)
580 Ntr = (FIX(TR1)) + 1
590 H = Ntr * XA / 12
600 AFR = QA / VA
610 L = AFR / H
611 PRINT "NTR="; Ntr, "H="; H, "L="; L
620 REM*****CALCULATION FOR HO
630 GFR = VA * 60 * ADI
640 GC = GFR / AR1
650 ARE = GC * (DTO / 12) / (AVI)
680 AR3 = 4 * XA * XB * AR1 / (3.14159 * DH * DTO)
681 REM AR3 is A/At ratio.
685 AJP = (ARE ^ (-.4)) * (AR3 ^ (-.15))
686 REM AJP,JP parameter
690 AJ = .0014 + .2618 * (AJP)
701 REM AJ: colburn factor (J factor for the air side flow)
710 HO = (AJ * GC * ACP) / (APR ^ .666)
710.1 REM HO : air side heat transfer coefficient.
711 PRINT "GFR="; GFR, "GC="; GC, "AJ="; AJ, "HO="; HO
730 GREF = flr / (AREAR)
730.1 PRINT "GREF="; GREF
740 HPL1 = (KRL ^ .79) * (CPRL ^ .45) * (DRL ^ .49)
745 HPL2 = (SIG ^ .5) * (VSRL ^ .29) * (HFG ^ .24) * (DRV ^ .24)
746 HPOOL = .00122 * (HPL1 / HPL2)
747 PRRL = (CPRL * VSRL) / KRL
748 RERL = (DTI / 12) * (GREF) / (VSRL)
750 HL = .023 * (KRL * 12 / DTI) * (RERL ^ .8) * (PRRL ^ .4)
760 X = 1
762 E = (1 + E1) ^ .35
762.1 REM E, enhancement factor.
763 S11 = .055 * (E ^ .1) * (RERL ^ .16)
764 S12 = 1 / (1 + S11)
764.1 REM S12, supression factor.
765 HTP1 = ((E * HL) ^ 2) + (S12 * HPOOL) ^ 2
770 HTP = HTP1 ^ .5
770.1 HI = HTP
790 Z1 = XA / 2

```

```

800 Z2 = (((Z1 ^ 2) + (XB ^ 2)) ^ .5) / 2
810 Z3 = Z1 / (DTO / 2)
820 Z4 = Z1 / Z2
830 Z5 = 1.27 * (Z3) * ((Z4 - .3) ^ .5)
840 Z6 = (Z5 - 1) * (1 + .35 * LOG(Z5))
850 Y1 = (((2 * HO) / (ALK * T / 12)) ^ .5)
860 AY1 = Y1 * (DTO / 24) * Z6
870 AY2 = EXP(AY1)
880 AY3 = EXP(-AY1)
890 AY4 = (AY2 - AY3) / (AY2 + AY3)
900 FE = AY4 / AY1
910 FEF = 1 - (AR2 * (1 - FE))
911 REM FEF: fin effectiveness.

930 Y5 = 1 / (HO * FEF)
940 Y6 = (3.14159 * 12 * DTI) / (XA * XB * ALPHA)
950 Y7 = 1 / (HI * Y6)
960 Y8 = (DTI / 12) * LOG(DTO / DTI)
970 Y9 = 2 * CUK * Y6
980 Y10 = Y8 / Y9
990 UO = 1 / (Y5 + Y7 + Y10)
1010 U4 = TAI - TE
1020 U5 = TAO - TE
1030 U6 = U4 - U5
1040 U7 = LOG(U4 / U5)
1050 lmtd = U6 / U7
1060 F = 1
1070 AO = Q / (UO * F * lmtd)
1080 vol = AO / (ALPHA)
1090 w = vol / AFR
1100 ROW1 = (w * 12) / XB
1200 ROW = (FIX(ROW1)) + 1
1210 PRINT "AO="; AO, "W="; w, "ROW="; ROW, "LMTD="; lmtd
1215 REM*** AIR SIDE PRESS DROP****
1216 S1 = 1 / S
1217 B1 = (XA - DTO) / S1
1218 B2 = (AR3) / (1 + B1)
1219 B3 = (XA - DTO) / (4 * (S1 - T))
1220 B4 = (XA) / (DTO * B2)
1221 B5 = ((ARE) ^ (-.25))
1222 B6 = ((1 / B2) ^ (.25))
1223 B7 = ((B3) ^ (-.4))
1224 B8 = ((B4 - 1) ^ (-.5))
1225 FP = B5 * B6 * B7 * B8
1226 F = .004904 + 1.382 * (FP * FP)

```

```

1226.1 REM F: friction factor.
1227 XI = .4048288 - ((.40470568#) * (AR1 ^ 2))
1228 CC9 = .998965464# - (1.00505 * AR1)
1229 XE = CC9 ^ 2
1230 AR4 = AO / (AFR * AR1)
1240 G = 32.2
1250 V = (GC ^ 2) / (2 * G * 3600 * 3600 * ADI)
1260 V1 = (XI + 1 - (AR1 ^ 2))
1270 V2 = (2) * ((ADI / ADO) - 1)
1280 V3 = F * AR4 * ADI / ADM
1290 V4 = (1 - (AR1 ^ 2) - XE) * (ADI / ADO)
1300 APD = V * (V1 + V2 + V3 - V4) * (12 / 62.4)
1301 PRINT "DRL="; DRL, "HRL="; Hrl, "HRV="; HRV, "VSRL="; VSRL, "KRL=";
KRL
1310 PRINT "FP="; FP, "F="; F, "APD="; APD, "flr="; flr
1330 PRINT "QA="; QA, "VA="; VA, "VR="; VR, "TAI="; TAI, "TAO="; TAO,
"TR="; TR
1340 PRINT "Q="; Q, "H="; H, "L="; L, "ROW="; ROW, "w="; w, "vol="; vol
1350 PRINT "HI="; HI, "HO="; HO, "UO="; UO, "AO = "; AO
1510 END

```

10 REM DROP IN EVALUATION

20 DIM TAD(30), HRQ(20), EHX(20), TACE(5), X(20)

21 REM TAD= outside air temperature

22 REM HRQ(1)= outside refrigerant enthalpy

23 REM EHX(1)= exchanger effectiveness

24 REM TAGE= bulk air temp

25 REM X(1)= exit refrigerant quality

30 DRI = .483

40 DTD = .325

50 KA = 1.25

60 KB = 1.683

70 CLK = 227

80 ALX = 100

100 INPUT "COIL HT(FT)=", H

110 INPUT "COIL LENGTH(FT)=", L

120 INPUT "COIL DEPTH W(FT)=", W

130 INPUT "TAGE=", TAJ

131 INPUT "TD=", TE

132 Computer program (P2) : Drop-in evaluation

150 INPUT "VA(FPM)=", VA

160 INPUT "RMASS(LBM PER 100)=", RMASS

170 INPUT "FIN PER INCH=", S

171 INPUT "TE=", T

172 INPUT "DRI=", DRI

172.1 INPUT "DRV=", DRV

172.2 INPUT "XRIN=", XRIN

173 INPUT "HRL=", HRL

174 INPUT "HRV=", HRV

174.1 HRIN = (XRIN * HRV) + (1 - XRIN) * HRL

175 INPUT "KRL=", KRL

176 INPUT "VSRL=", VSRL

177 INPUT "CPRL=", CPRL

178 INPUT "SIG=", SIG

179 HIG = HRV - HRL

180 SI = 1 / S

190 DH = $2.5699635E-02 + (.8617315624) * (S * (.507340138))$

200 CC1 = $1.689112598 + (1.963865E-02) * (S * .5) * (LOG(S))$

210 AR1 = 1 / (CC1)

220 CC2 = $.9218547 + (.336112) / (LOG(S))$

230 AR2 = 1 / (CC2)

240 ALPHA = $14.639 + 19.76549 * S$

10 REM" DROP IN EVALUATION

20 DIM TAO(20), HRO(20), EHX(20), TA(20), X(20)

21 REM TAO: outlet air temperature.

22 REM HRO(I): outlet refrigerant enthalpy

23 REM EHX(I): exchanger effectiveness

24 REM TA(I): bulk air temp

25 REM X(I) : exit refrigerant quality

30 DTI = .483

40 DTO = .525

50 XA = 1.25

60 XB = 1.083

70 CUK = 227

80 ALK = 100

100 INPUT " COIL HT(FT)="; H

110 INPUT " COIL LENGTH(FT)="; L

120 INPUT " COIL DEPTH W(FT)="; W

130 INPUT "TAI(F)="; TAI

131 INPUT "TE="; TE

132 REM TE: EVAPORATOR TEMPERATURE.

150 INPUT "VA(FPM)="; VA

160 INPUT "RMASS(LBM PER HR)="; RMASS

170 INPUT "FIN PER INCH ="; S

171 INPUT "T="; T

172 INPUT "DRL="; DRL

172.1 INPUT "DRV="; DRV

172.2 INPUT "XRIN="; XRIN

173 INPUT "HRL="; HRL

174 INPUT "HRV="; HRV

174.1 HRIN = (XRIN * HRV) + (1 - XRIN) * HRL

175 INPUT "KRL="; KRL

176 INPUT "VSRL="; VSRL

177 INPUT "CPRL="; CPRL

178 INPUT "SIG="; SIG

179 HFG = HRV - HRL

180 S1 = 1 / S

190 DH = -2.569963E-02 + (.961731562#) * (S ^ (-.80734013#))

200 CC1 = 1.68911259# + (1.983865E-02) * (S ^ .5) * (LOG(S))

210 AR1 = 1 / (CC1)

220 CC2 = .9218547 + (.336112) / (LOG(S))

230 AR2 = 1 / (CC2)

240 ALPHA = 14.659 + 19.76649 * S

```

250 PRINT "AR1="; AR1, "AR2="; AR2, "ALPHA="; ALPHA, "DH="; DH
260 REM*****PROPERTIES OF AIR*****
270 RA = 53.32
280 ACP = .24
281 PA = 14.7

285 REM ***** FIRST GUESS VALUES*****
290 HRO(1) = 0
300 TAO(1) = 0
305 X(1) = 1
310 FOR I = 1 TO 5

320 TA(I) = (TAI + TAO(I)) / 2
320.1 X(I) = X(I)

321 REM TA: average air temperature
340 A1 = .1980649
350 A2 = 3.030648E-03
360 A3 = 7.5636E-04
370 A4 = 1.61686E-06
380 A5 = 7.07473E-07
390 AN1 = A1 + A3 * TAI + A5 * TAI * TAI
400 D1 = 1 + A2 * TAI + A4 * TAI * TAI
410 AVI = (AN1 / D1) ^ 2
420 AN2 = A1 + A3 * TA(I) + A5 * TA(I) * TA(I)
430 D2 = 1 + A2 * TA(I) + A4 * TA(I) * TA(I)
440 AV = (AN2 / D2) ^ 2
450 A6 = .013071906#
460 A7 = 2.59434E-05
470 A8 = -5.0315E-09
480 A9 = 3.736332E-03
490 A10 = .041698788#
500 AK = A6 + (A7 * TA(I)) + (A8 * TA(I) * TA(I)) + (A9 / TA(I)) + (A10) / (TA(I) *
TA(I))
510 ADI = (PA * 144) / ((RA) * (TAI + 460))
520 APR = (AV * ACP) / AK
530 AFR = H * L
540 AM = (VA * AFR * 60 * ADI)
541 REM AM : air mass flow rate, lbm/hr.
550 PRINT "AM="; AM
780 TR = 12 * H / XA
790 AREAR = (3.1415 / 4) * (DTI ^ 2) * (1 / 144) * TR
810 GREF = RMASS / (AREAR)
820 VOL = H * L * W
830 AO = VOL * ALPHA

```

```

840 GFR = VA * 60 * ADI
850 GC = GFR / AR1
860 PRINT "GC="; GC
870 REM**** CALCULATION OF HO ***
880 ARE = GC * (DTO / 12) / (AVI)
910 AR3 = 4 * XA * XB * AR1 / (3.14159 * DH * DTO)
920 AJP = (ARE ^ (-.4)) * (AR3 ^ (-.15))
930 AJ = .0014 + .2618 * (AJP)
950 HO = (AJ * GC * ACP) / (APR ^ .666)
960 PRINT "HO="; HO
980 RER = GREF * (DTI / 12) / (VSRL)
990 PRR = VSRL * CPRL / KRL
1000 HL = .023 * (RER ^ .8) * (PRR ^ .4) * (KRL) * (12) / DTI
1001 HPOOL1 = (KRL ^ .79) * (CPRL ^ .45) * (DRL ^ .49)
1002 HPOOL2 = (SIG ^ .5) * (VSRL ^ .29) * (HFG ^ .24) * (DRV ^ .24)
1005 HPOOL = .00122 * (HPOOL1 / HPOOL2)
1006 E1 = ((DRL / DRV) - 1) * PRR * X(I)
1007 E = (1 + E1) ^ .35
1008 S11 = (E ^ .1) * (RER ^ .16) * .055
1009 S12 = 1 + S11
1009.1 S13 = 1 / (S12)
1009.11 REM S13: SUPPRESSION FACTOR.
1009.2 HTP = (((E * HL) ^ 2 + (S13 * HPOOL) ^ 2)) ^ .5
1009.3 HI = HTP

1020 Z1 = XA / 2
1030 Z2 = (((Z1 ^ 2) + (XB ^ 2)) ^ .5) / 2
1040 Z3 = Z1 / (DTO / 2)
1050 Z4 = Z1 / Z2
1060 Z5 = 1.27 * (Z3) * ((Z4 - .3) ^ .5)
1070 Z6 = (Z5 - 1) * (1 + .35 * LOG(Z5))
1080 Y1 = (((2 * HO) / (ALK * T / 12)) ^ .5)
1090 AY1 = Y1 * DTO / 24 * Z6
1100 AY2 = EXP(AY1)
1110 AY3 = EXP(-AY1)
1120 AY4 = (AY2 - AY3) / (AY2 + AY3)
1130 FE = AY4 / AY1
1140 FEF = 1 - (AR2 * (1 - FE))
1160 Y5 = 1 / (HO * FEF)
1170 Y6 = (3.14159 * DTI * 12) / (XA * XB * ALPHA)
1180 Y7 = 1 / (HI * Y6)
1190 Y8 = DTI / 12 * LOG(DTO / DTI)
1200 Y9 = 2 * CUK * Y6
1210 Y10 = Y8 / Y9
1220 UO = 1 / (Y5 + Y7 + Y10)

```

```

1240 UOAO = UO * AO
1250 REM***EHX ****
1260 CAIR = AM * ACP
1280 CM = CAIR
1290 CR = 0
1300 NTU = (UO * AO) / CM
1310 Z20 = EXP(-NTU)
1320 Z21 = 1 - Z20
1350 EHX(I) = Z21
1360 HRO(I + 1) = HRIN + ((EHX(I)) * (CM / RMASS) * (TAI - TE))
1370 TAO(I + 1) = TAI - ((EHX(I)) * (TAI - TE))
1370.1 X(I + 1) = (HRO(I + 1)) / HRV
1380 Q = CAIR * (TAI - TAO(I + 1))
1500 PRINT "TAO(I+1)="; TAO(I + 1)
1510 PRINT "HRO(I+1)="; HRO(I + 1)
1510.1 PRINT "X(I+1)="; X(I + 1)
1520 PRINT "Q="; Q
1530 NEXT I
1540 PRINT "I="; I
1550 PRINT "EHX(1)="; EHX(1)
1560 PRINT "EHX(2)="; EHX(2)
1570 PRINT "EHX(3)="; EHX(3)
1570.1 PRINT "X(1)="; X(1)
1580 PRINT "TAO(1)="; TAO(1)
1590 PRINT "TAO(2)="; TAO(2)
1600 PRINT "TAO(3)="; TAO(3)
1610 PRINT "HRO(1)="; HRO(1)
1620 PRINT "TAO(6)="; TAO(6)
1630 PRINT "HRO(6)="; HRO(6)
1640 PRINT "EHX(5)="; EHX(5)
1640.1 PRINT "X(2)="; X(2)
1640.2 PRINT "X(6)="; X(6)
1641 IF (EHX(5) - EHX(4)) > .01 GOTO 2100
1650 PRINT "UO="; UO
1655 PRINT "HO="; HO, "CR="; CR
1660 PRINT "UOAO="; UOAO, "HI="; HI, "AJ="; AJ, "CAIR="; CAIR
1671 REM APD : air pressure drop
1680 B1 = (XA - DTO) / S1
1690 B2 = (AR3) / (1 + B1)
1700 B3 = (XA - DTO) / (4 * (S1 - T))
1710 B4 = (XA) / (DTO * B2)
1720 B5 = ((ARE) ^ (-.25))
1730 B6 = ((1 / B2) ^ (.25))
1740 B7 = ((B3) ^ (-.4))
1750 B8 = ((B4 - 1) ^ (-.5))

```

```

1760 FP = B5 * B6 * B7 * B8
1770 F = .004904 + 1.382 * (FP * FP)
1780 XI = .4048288 - (.40470568#) * (AR1 ^ 2)
1790 CC8 = .998965464# - (1.00505 * AR1)
1800 XE = CC8 ^ 2
1810 AR4 = AO / (AFR * AR1)
1820 G = 32.2
1830 ADO = (PA * 144) / ((RA) * (TAO(I) + 460))
1840 ADM = (ADI + ADO) / 2
1841 REM ADO, ADM are the outlet and mean air densities.
1850 V = (GC ^ 2) / (2 * G * 3600 * 3600 * ADI)
1860 V1 = (XI + 1 - (AR1 ^ 2))
1870 V2 = (2) * ((ADI / ADO) - 1)
1880 V3 = F * AR4 * ADI / ADM
1890 V4 = (1 - (AR1 ^ 2) - XE) * (ADI / ADO)
1900 APD = V * (V1 + V2 + V3 - V4) * (12 / 62.4)
2040 LPRINT "****INPUT DATA****"
2050 LPRINT "S="; S
2060 LPRINT "VA="; VA
2080 LPRINT " RESULTS"
2090 LPRINT "TAO(6)="; TAO(6)
2090.1 GOTO 2110
2100 PRINT "SOLN DOES NOT CONVERGE"
2100.1 GOTO 2230
2110 LPRINT "hro(6)="; HRO(6)
2120 LPRINT "Q="; Q
2130 LPRINT "AO="; AO
2140 LPRINT "EHX(5)="; EHX(5)
2150 LPRINT "HO="; HO
2160 LPRINT "UO="; UO
2170 LPRINT "AO ="; AO
2180 LPRINT "UOAO="; UOAO
2190 LPRINT "HI="; HI
2220 LPRINT "APD="; APD
2230 END

```

10 REM SHELL AND TUBE EVAPORATOR DESIGN

```
20 FLW = 3260
30 REM FLW: water flow rate, lbs/hr
50 TWT = 45.2
70 TWD = 49.6
100 FW = 14.7
120 DW = 62.4
130 KW = 256
140 VSW = 1.54
150 CPW = 1
160 REM REFRIGERANT PROPERTIES
161 INPUT "DRI="; DRI
162 INPUT "DRV="; DRV
163 INPUT "HRI="; HRI
164 INPUT "HRV="; HRV
165 INPUT "VHRL="; VHRL
166 INPUT "KRI="; KRI
166.1 INPUT "CPRI="; CPRI
169.3 INPUT "TE="; TE
169.4 INPUT "SIG="; SIG
```

Computer program (P3) : Shell and tube evaporator design

```
300 X1 = 1
305 X2 = 1
310 REM ***TUBE LAYOUT***
320 DT0 = .75
330 DT1 = .596
335 REM S - TUBE PITCH, IN. PITCH RATIO
340 S = 1
345 PR = 57 (DT0)
350 (META = 30
360 REM S - tube pitch, in. tube pitch ratio
365 ST = 5 * S
370 SL = 8 * S
370.1 REM ST, SL, TRANSVERSE/STUDIAL SPACING
371 PRINT "ST="; ST; "SL="; SL
380 KCF = 25
390 A1 = 400 - 10
400 A2 = 390 - 10
410 A3 = 41 - 10
415 A4 = 1400 - 10
420 LMTD = 47.46
430 F = 1
440 Q = (FLW * 2.26 * (TWT) - TWD)
450 FLI = Q / (256 * 256)
```

10 REM SHELL AND TUBE EVAPORATOR DESIGN

20 FLW = 3260
51 REM FLW: water flow rate, lbm/min
60 TWI = 45.2
70 TWO = 44.6
100 PW = 14.7
120 DW = 62.4
130 KW = .336
140 VSW = 3.44
150 CPW = 1
160 REM REFRIGERANT PROPERTIES
161 INPUT "DRL="; DRL
162 INPUT "DRV="; DRV
163 INPUT "HRL="; Hrl
164 INPUT "HRV="; HRV
167 INPUT "VSRL="; VSRL
169 INPUT "KRL="; KRL
169.1 INPUT "cprl="; CPRL
169.3 INPUT "TE="; TE
169.4 INPUT "sig="; SIG
265 HFG = HRV - Hrl
300 X1 = 0
305 X2 = 1
310 REM***TUBE LAYOUT****
320 DTO = .75
330 DTI = .606
331 REM S : TUBE PITCH, PR : PITCH RATIO.
340 S = 1
345 PR = S / DTO
350 THETA = 30
351 REM theta is the tube layout angle.
360 ST = S * .5
370 SL = S * .866
370.1 REM ST,SL : TRANSVERSE, LONGITUDINAL SPACING.
371 PRINT "ST="; ST, "SL="; SL
380 KCU = 227
390 A1 = TWI - TE
400 A2 = TWO - TE
410 A3 = A1 - A2
415 A4 = LOG(A1 / A2)
420 LMTD = A3 / A4
430 F = 1
440 Q = (FLW * 60) * (CPW) * (TWI - TWO)
450 FLR = Q / (HRV - Hrl)

```

470 DS = 20
472 CTP = .8
473 CL = .87
474 NT1 = (.78539) * (CTP / CL) * (DS ^ 2) / ((PR ^ 2) * (DTO ^ 2))
474.1 NT = (FIX(NT1)) + 1
476 AREAR = (3.14159 / 4) * (DTI ^ 2) * (1 / 144) * (NT / 2)
478 GREF = FLR / AREAR
490 PB = .4 * DS
500 AC = DS * PB * (S - DTO) * (1 / 144) * (1 / S)
500.1 REM SHELL SIDE FLOW CROSS FLOW AREA.
501 PRINT "AC="; AC
510 GW = (FLW * 60) / AC
511 PRINT "GW="; GW
520 VELW = GW / DW
521 PRINT "VELW="; VELW
530 REW = (DTO * (1 / 12) * GW) / (VSW)
531 PRW = (CPW * VSW) / (KW)
532 PRINT "REW="; REW
540 IF (REW > 200000) THEN M = .3 ELSE
560 IF (300 < REW < 200000) THEN M = .365 ELSE
580 IF (REW < 300) THEN M = .64
581 PRINT "M="; M
582 IF (REW > 200000) THEN A = .166 ELSE
590 IF (300 < REW < 200000) THEN A = .273 ELSE
600 IF (REW < 300) THEN A = .742
610 PRINT "A="; A
630 HOIDEAL = (CPW) * (GW) * (A) * (REW ^ -M) * (PRW ^ -.666)
632 PRINT "HOIDEAL="; HOIDEAL
670 FC = 1.1
680 FB = .9
690 FL = .8 * (PB / DS) ^ .25
700 IF (REW < 100) THEN FR = .2 * REW ^ .333 ELSE
710 FR = 1
720 PRINT "FR="; FR
730 HORL = HOIDEAL * FL * FR * FC * FB
740 PRINT "HORL="; HORL
750 REM TUBE SIDE COEFFICIENT
800 HPOOL1 = (KRL ^ .79) * (CPRL ^ .45) * (DRL ^ .49)
810 HPOOL2 = (SIG ^ .5) * (VSRL ^ .29) * (HFG ^ .24) * (DRV ^ .24)
815 HPOOL = .00122 * HPOOL1 / HPOOL2
816 RER = GREF * DTI / (12 * VSRL)
817 PRR = CPRL * VSRL / KRL
818 HL = .023 * (KRL * 12 / DTI) * (RER ^ .8) * (PRR ^ .4)
820 E11 = (DRL / DRV) - 1
825 E12 = 1 * PRR * E11

```



```

826 E13 = (1 + E12) ^ .35
827 S11 = .055 * (E13 ^ .1) * (RER ^ .16)
828 S13 = 1 / (1 + S11)
829 HTP = ((E13 * HL) ^ 2 + (S13 * HPOOL) ^ 2) ^ .5
829.1 HI = HTP
829.2 B1 = 1 / HORL
829.3 B2 = 1 / HI
829.4 B3 = (DTO - DT1) * (1 / 12) * (1 / KCU) * (DTO / DT1)
830 B4 = B1 + (B2 * DTO / DT1) + B3
840 UO = 1 / B4
841 PRINT "UO="; UO
842 F = 1
850 B5 = F * UO * LMTD
860 AO = Q / B5
865 PRINT "AO="; AO
870 REM A : EFFECTIVE AREA AND A=AO*F1*F2*F3
880 REM F1,F2,F3 : CORRECTION FACTORS
910 F1 = 1.14
920 F2 = 1.04
930 F3 = 1!
940 A = AO * F1 * F2 * F3
950 L1 = A * (1 / 3.1415927#) * (12 / DTO) * (1 / NT)
951 PRINT "A="; A; "L1="; L1
2030 L = (FIX(L1)) + 1
2030.1 PRINT "L="; L
2030.5 PRINT "Q="; Q
2040 REM *****PRESSURE DROP SHELL SIDE*****
2080 DG = S - DTO
2090 REW1 = (DG / 12) * (GW) / (VSW)
2100 PRINT "REW1="; REW1
2110 IF (REW1 > 100) THEN FRW = 1 / (REW1 ^ .25) ELSE
2120 IF (REW1 < 100) THEN FRW = 10 / (REW1 ^ .725)
2130 PRINT "FRW="; FRW
2150 NR = (.7 * DS / ST)
2160 RL = .6 * (PB / DS) ^ .5
2170 RB = .8 * (DS / 12) ^ .08
2180 REM NB: **NUMBER OF BAFFLES**
2190 NB1 = ((L * 6) / (PB)) - 1
2191 NB = (FIX(NB1)) + 1
2200 PRINT "NB="; NB
2210 REM***PDBAF : PRESSURE DROP IN THE BAFFLE SECTION ***
2220 PDBAF = 4 * FRW * (GW ^ 2) * NR * (NB - 1) * RL * RB * (1 / 2) * (1 / 144) *
(1 / 4.173E+08) * (1 / DW)
2230 PRINT "PDBAF="; PDBAF

```

```

2240 REM ***PDBAF1 : PRESSURE DROP FOR INLET & OUTLET BAFFLE
SECTIONS***
2250 PDBAF1 = 4 * (2.66) * (FRW) * (GW ^ 2) * (NR) * (RB) * (1 / 2) * (1 / 144) * (1 /
4.173E+08) * (1 / DW)
2260 PRINT "PDBAF1="; PDBAF1
2280 REM***PDWIN : PRESSURE DROP FOR THE WINDOW SECTION***
2290 AW = .055 * (DS ^ 2) * (1 / 144)
2300 M1 = 3.5
2310 PDWIN = (GW ^ 2) * (1 / 2) * (1 / 144) * (1 / 4.173E+08) * (1 / DW) * (AC / AW)
* (M1) * ((DS / 12) ^ .625) * (NB) * (RL)
2320 PRINT "PDWIN="; PDWIN
2330 PDSHELL = PDBAF + PDBAF1 + PDWIN
2340 PRINT "PDSHELL="; PDSHELL
3190.1 LPRINT
3200 LPRINT "FLW(LBM PER MINUTE)="; FLW
3210 LPRINT "TWI( DEGREES F)="; TWI
3220 LPRINT "TWO(DEGREES F)="; TWO
3240 LPRINT "TR(DEG F)="; TR
3250 LPRINT "PRef(Psi)="; PREF
3271 LPRINT " DTO="; DTO
3271.1 LPRINT
3272 LPRINT "DTI="; DTI
3272.1 LPRINT
3273 LPRINT "DS="; DS
3274 LPRINT "PB="; PB
3280 LPRINT "***** OUTPUT *****"
3290 LPRINT "FLR (LBM PER HOUR)="; FLR
3300 LPRINT "Q (BTU / HR)="; Q
3310 LPRINT " NT (NO OF TUBES)="; NT
3320 LPRINT " HORL (SHELL SIDE)="; HORL
3330 LPRINT "HI REF SIDE ="; HI
3340 LPRINT " UO ="; UO
3350 LPRINT " A ="; A
3350.1 LPRINT
3360 LPRINT "L ="; L
3370 LPRINT "NB ="; NB
3380 LPRINT "PDSHELL="; PDSHELL
4290 END

```

10 REM PLATE FIN TUBE HEX. PARAMETRIC ANALYSIS

```

20 DIM TAC(20), TWO(20), DEX(20), TW(20), TAI(20)
30 DT1 = .453
40 DTD = .523
50 XA = 1.25
60 XB = 1.083
70 CLK = 237
80 ALX = 100
90 INPUT " COIL HEIGHT="; H
100 INPUT " COIL LENGTH(FT)="; L
110 INPUT " ROW="; ROW
120 INPUT " TAI(1)="; TAI
130 INPUT " TW(1)="; TW
140 INPUT " VA(FPM)="; VA
150 INPUT " VW(FPS)="; VW
160 INPUT " FIN PER INCH="; S
175 INPUT " T="; T
180 B1 = 1 / S
190 DH = 2.59263E-03 + (.561731982E-04 * (S + (.507340189E-01
200 CC1 = 1.589112589 + (.982866E-05 * (S + 3) * (LOG(S)

```

Computer program (P4) : Parametric analysis, plate fin tube HEX

```

210 AR1 = 1.25 / (2 * S)
220 AR2 = 1 / (4 * S)
230 ALPHA = 34.659 + 19.75649 * S
240 PRINT "AR1="; AR1, "AR2="; AR2, "ALPHA="; ALPHA, "DN="; DN
250 RA = 31.52
260 ACT = .24
270 PA = 14.7
280 TWIR(1) = 0
290 TAC(1) = 0
300 POR T = 1 / 30.5
310 TAD(1) = (TAI + TADIR) / 2
320 TW(1) = (TWI + TWIR) / 2
330 A1 = .192899
340 A2 = 7.28944E-02
350 A3 = 7.5875E-03
360 A4 = 1.61086E-05
370 A5 = 2.07433E-08
380 AN1 = A1 + A2 * TAI + A3 * TAI * TAI
390 D1 = 1 + A2 * TAI + A4 * TAI * TAI
400 AV1 = (AN1 / D1) * S
410 AN2 = A1 + A2 * TAD + A3 * TAD * TAD
420 D2 = 1 + A2 * TAD + A4 * TAD * TAD
430 AV = (AN2 / D2) * S

```

10 REM "PLATE FIN TUBE HEX, PARAMETRIC ANALYSIS"

```
20 DIM TAO(20), TWO(20), EHX(20), TW(20), TA(20)
30 DTI = .483
40 DTO = .525
50 XA = 1.25
60 XB = 1.083
70 CUK = 227
80 ALK = 100
100 INPUT " COIL HT(FT)="; H
110 INPUT " COIL LENGTH(FT)="; L
120 INPUT " ROW="; ROW
130 INPUT "TAI(F)="; TAI
140 INPUT "TWI(F)="; TWI
150 INPUT "VA(FPM)="; VA
160 INPUT "VW(FPS)="; VW
170 INPUT "FIN PER INCH="; S
175 INPUT "T="; T
180 S1 = 1 / S
190 DH = -2.569963E-02 + (.961731562#) * (S ^ (-.80734013#))
200 CC1 = 1.68911259# + (1.983865E-02) * (S ^ .5) * (LOG(S))
210 AR1 = 1 / (CC1)
220 CC2 = .9218547 + (.336112) / (LOG(S))
230 AR2 = 1 / (CC2)
240 ALPHA = 14.659 + 19.76649 * S
250 PRINT "AR1="; AR1, "AR2="; AR2, "ALPHA="; ALPHA, "DH="; DH
270 RA = 53.32
280 ACP = .24
281 PA = 14.7
290 TWO(1) = 0
300 TAO(1) = 0
310 FOR I = 1 TO 5
320 TA(I) = (TAI + TAO(I)) / 2
330 TW(I) = (TWI + TWO(I)) / 2
340 A1 = .1980649
350 A2 = 3.030648E-03
360 A3 = 7.5636E-04
370 A4 = 1.61686E-06
380 A5 = 7.07473E-07
390 AN1 = A1 + A3 * TAI + A5 * TAI * TAI
400 D1 = 1 + A2 * TAI + A4 * TAI * TAI
410 AVI = (AN1 / D1) ^ 2
420 AN2 = A1 + A3 * TA(I) + A5 * TA(I) * TA(I)
430 D2 = 1 + A2 * TA(I) + A4 * TA(I) * TA(I)
440 AV = (AN2 / D2) ^ 2
```

```

450 A6 = .013071906#
460 A7 = 2.59434E-05
470 A8 = -5.0315E-09
480 A9 = 3.736332E-03
490 A10 = .041698788#
500 AK = A6 + (A7 * TA(I)) + (A8 * TA(I) * TA(I)) + (A9 / TA(I)) + (A10) / (TA(I) *
TA(I))
510 ADI = (PA * 144) / ((RA) * (TAI + 460))
520 APR = (AV * ACP) / AK
530 AFR = H * L
540 AM = (VA * AFR * 60 * ADI)
550 PRINT "AM="; AM
570 WCP = 1
580 A11 = 62.31798536#
590 A12 = 7.133019E-03
600 A13 = -1.1418E-04
610 A14 = 1.15173E-07
620 WDI = A11 + (A12 * TWI) + ((A13) * (TWI ^ 2)) + ((A14) * (TWI ^ 3))
630 WD = A11 + (A12 * TW(I)) + (A13 * TW(I) * TW(I)) + (A14 * TW(I) * TW(I) *
TW(I))
640 A15 = .291975
650 A16 = 9.59507E-04
660 A17 = -2.821E-06
670 A18 = 2.58806E-09
680 WK = A15 + (A16 * TW(I)) + (A17 * TW(I) * TW(I)) + (A18 * TW(I) * TW(I) *
TW(I))
690 A19 = 9.949940748#
700 A20 = .045519659#
710 A21 = -6.2578E-06
720 A22 = 2.09856E-07
730 A23 = -.58617528#
740 WV = A19 + (A20 * TW(I)) + (A21 * (TW(I) ^ 2.5)) + (A22 * (TW(I) ^ 3)) + (A23 *
((LOG(TW(I))) ^ 2))
750 PRINT "WDI="; WDI, "WD="; WD, "WK="; WK, "WV="; WV
760 WPR = (WCP * WV) / WK
770 PRINT "WPR="; WPR
780 TR = 12 * H / XA
790 AREAW = 3.1415 / 4 * (DTI ^ 2) * (1 / 144) * TR
800 WMASS = WDI * (VW * 3600) * (AREAW)
810 W = ROW * (XB) / 12
820 VOL = H * L * W
830 AO = VOL * ALPHA
840 GFR = VA * 60 * ADI
850 GC = GFR / AR1
860 PRINT "GC="; GC

```

```

870 REM**** CALCULATION OF HO **
880 ARE = GC * (DTO / 12) / (AVI)
890 ARES = ARE * S / DTO
900 AREXB = ARE * XB / DTO
910 AR3 = 4 * XA * XB * AR1 / (3.14159 * DH * DTO)
920 AJP = (ARE ^ (-.4)) * (AR3 ^ (-.15))
930 AJ4 = .0014 + .2618 * (AJP)
940 AJ = AJ4
950 HO = (AJ * GC * ACP) / (APR ^ .666)
960 PRINT "HO="; HO
970 REM***CALCULATION OF HI **
980 WRE = WD * VW * 3600 * (DTI / 12) / (WV)
990 WPR = WV * WCP / WK
1000 HI = .023 * (WRE ^ .8) * (WPR ^ .3) * (WK) * (12) / DTI
1010 REM***CALCULATIONS FOR FIN EFF*****
1020 Z1 = XA / 2
1030 Z2 = (((Z1 ^ 2) + (XB ^ 2)) ^ .5) / 2
1040 Z3 = Z1 / (DTO / 2)
1050 Z4 = Z1 / Z2
1060 Z5 = 1.27 * (Z3) * ((Z4 - .3) ^ .5)
1070 Z6 = (Z5 - 1) * (1 + .35 * LOG(Z5))
1080 Y1 = (((2 * HO) / (ALK * T / 12)) ^ .5)
1090 AY1 = Y1 * DTO / 24 * Z6
1100 AY2 = EXP(AY1)
1110 AY3 = EXP(-AY1)
1120 AY4 = (AY2 - AY3) / (AY2 + AY3)
1130 FE = AY4 / AY1
1140 FEF = 1 - (AR2 * (1 - FE))

1160 Y5 = 1 / (HO * FEF)
1170 Y6 = (3.14159 * DTI * 12) / (XA * XB * ALPHA)
1180 Y7 = 1 / (HI * Y6)
1190 Y8 = DTI / 12 * LOG(DTO / DTI)
1200 Y9 = 2 * CUK * Y6
1210 Y10 = Y8 / Y9
1220 UO = 1 / (Y5 + Y7 + Y10)
1230 PRINT "UO="; UO
1240 UOAO = UO * AO
1260 CAIR = AM * ACP
1270 CWAT = WMASS * WCP
1271 IF CAIR < CWAT GOTO 1390
1280 CM = CWAT
1290 CR = CWAT / CAIR
1300 NTU = (UO * AO) / CM
1310 Z41 = (1 / CR) * (NTU ^ .22)

```

```

1320 Z51 = (-CR) * (NTU ^ .78)
1330 Z61 = (EXP(Z51)) - 1
1340 Z71 = EXP(Z41 * Z61)
1350 EHX(I) = 1 - EXP(Z71)
1360 TWO(I + 1) = TWI + ((EHX(I)) * (TAI - TWI))
1370 TAO(I + 1) = TAI - ((CWAT / CAIR) * (TWO - TWI))
1380 Q = CAIR * (TAI - TAO(I + 1))
1381 GOTO 1500
1390 CM = CAIR
1400 CR = CAIR / CWAT
1410 NTU = (UO * AO) / CM
1420 Z40 = (1 / CR) * (NTU ^ .22)
1430 Z50 = (-CR) * (NTU ^ .78)
1440 Z60 = (EXP(Z50)) - 1
1450 Z70 = EXP(Z40 * Z60)
1460 EHX(I) = 1 - Z70
1470 TAO(I + 1) = TAI - ((EHX(I)) * (TAI - TWI))
1480 TWO(I + 1) = TWI + ((CAIR / CWAT) * (TAI - TAO(I + 1)))
1490 Q = CAIR * (TAI - TAO(I + 1))
1500 PRINT "TAO(I+1)="; TAO(I + 1)
1510 PRINT "TWO(I+1)="; TWO(I + 1)
1520 PRINT "Q="; Q
1530 NEXT I
1540 PRINT "I="; I
1550 PRINT "EHX(1)="; EHX(1)
1560 PRINT "EHX(2)="; EHX(2)
1570 PRINT "EHX(3)="; EHX(3)
1580 PRINT "TAO(1)="; TAO(1)
1590 PRINT "TAO(2)="; TAO(2)
1600 PRINT "TAO(3)="; TAO(3)
1610 PRINT "TWO(1)="; TWO(1)
1620 PRINT "TAO(6)="; TAO(6)
1630 PRINT "TWO(6)="; TWO(6)
1640 PRINT "EHX(5)="; EHX(5)
1641 IF (EHX(5) - EHX(4)) > .01 GOTO 2100
1650 PRINT "UO="; UO, "Q="; Q
1660 PRINT "UOAO="; UOAO
1661 PRINT "HO="; HO, "J="; AJ, "AO="; AO, "HI="; HI, "AM="; AM, "WMASS=";
WMASS
1662 PRINT "FE="; FE, "FEF="; FEF
1670 REM **** APD *****
1680 B1 = (XA - DTO) / S1
1690 B2 = (AR3) / (1 + B1)
1700 B3 = (XA - DTO) / (4 * (S1 - T))
1710 B4 = (XA) / (DTO * B2)

```

```

1720 B5 = ((ARE) ^ (-.25))
1730 B6 = ((1 / B2) ^ (.25))
1740 B7 = ((B3) ^ (-.4))
1750 B8 = ((B4 - 1) ^ (-.5))
1760 FP = B5 * B6 * B7 * B8
1770 F = .004904 + 1.382 * (FP * FP)
1780 XI = .4048288 - (.40470568#) * (AR1 ^ 2)
1790 CC8 = .998965464# - (1.00505 * AR1)
1800 XE = CC8 ^ 2
1810 AR4 = AO / (AFR * AR1)
1820 G = 32.2
1830 ADO = (PA * 144) / ((RA) * (TAO(I) + 460))
1840 ADM = (ADI + ADO) / 2
1850 V = (GC ^ 2) / (2 * G * 3600 * 3600 * ADI)
1860 V1 = (XI + 1 - (AR1 ^ 2))
1870 V2 = (2) * ((ADI / ADO) - 1)
1880 V3 = F * AR4 * ADI / ADM
1890 V4 = (1 - (AR1 ^ 2) - XE) * (ADI / ADO)
1900 APD = V * (V1 + V2 + V3 - V4) * (12 / 62.4)
1910 PRINT "APD="; APD, "F="; F, "CR="; CR, "CWAT="; CWAT, "CAIR="; CAIR,
"NTU="; NTU

```

```

2040 LPRINT "****INPUT DATA****"
2050 LPRINT "S="; S
2060 LPRINT "VA="; VA
2070 LPRINT "VW="; VW
2080 LPRINT " RESULTS"
2090 LPRINT "TAO(6)="; TAO(6)
2090.1 GOTO 2110
2100 PRINT "SOLN DOES NOT CONVERGE"
2100.1 GOTO 2230
2110 LPRINT "TWO(6)="; TWO(6)
2120 LPRINT "Q="; Q
2130 LPRINT "AO="; AO
2140 LPRINT "EHX(5)="; EHX(5)
2150 LPRINT "HO="; HO
2160 LPRINT "UO="; UO
2170 LPRINT "AO ="; AO
2180 LPRINT "UOAO="; UOAO
2190 LPRINT "HI="; HI
2200 LPRINT "J="; J
2210 LPRINT "F="; F
2220 LPRINT "APD="; APD
2230 END

```


10 REM INTERRUPTED SURFACES ON HEX**

20 DIM TAO(20), TWO(20), EHXT(20), TWT(20), TAP(20)
 21 DIM EHXW(20), EHXO(20), EHXW(20), TWW(20), TAW(20)
 22 DIM EHX(20), EHX(20), EHX(20), TWO(20), TAO(20)

24 REM TAO: inlet air temperature: plain fin tube
 25 REM TAW: inlet air temp: wavy fin
 26 REM TAO: outlet air temperature: offset strip fin
 27 REM TWP: outlet water temperature: plain fin tube
 28 REM TWOW: outlet water temperature: wavy fin
 29 REM TWO: outlet water temperature: offset strip fin
 29.1 REM EHX: effectiveness: plain fin tube
 29.2 REM EHXW: effectiveness: Wavy fin
 29.3 REM EHXO: effectiveness: Offset strip fin
 29.4 REM TWT, TWW and TWO: bulk water temperatures
 29.5 REM TAP, TAW and TAO: bulk air temperatures

30 DTI = .491
 40 DTG = .375
 50 XA = 1.25

Computer program (P5): Interrupted surfaces on HEX

70 GOK = 20
 80 LALK = 100

10 REM INPUT DATA

100 INPUT "AG=", AG
 110 INPUT "H=", H
 120 INPUT "L=", L
 130 INPUT "TAI(°F)=", TAI
 140 INPUT "TWT(°F)", TWT
 150 INPUT "VA(FPM)=", VA
 160 INPUT "VW(FPM)=", VW
 170 INPUT "PIN PER INCH =", S
 171 INPUT "Tw=", Tw
 180 S1 = 1 / S
 190 DH = 2.569953E-02 + (.9617315628) * (S ^ 1.8973401349)
 200 CCT = 1.689112598 + (.953865E-02) * (S ^ .5) * (LOG(S))
 210 ARE1 = 1 / (CCT)
 220 CC2 = .9218547 + (.3581123) / (LOG(S))
 230 ARE = 1 / (CC2)
 240 ALPHA = 14.659 + 19.7649 * S
 270 RA = 53.32
 280 ACP = .24

10 REM**INTERRUPTED SURFACES ON HEXs**

20 DIM TAOP(20), TWOP(20), EHXP(20), TWP(20), TAP(20)
21 DIM taow(20), twow(20), EHXW(20), TWW(20), TAW(20)
23 DIM tao(20), twoo(20), EHXO(20), TWO(20), TAO(20)

24 REM TAOP: outlet air temperature: plain fin tube
25 REM TAOW: outlet air temp: wavy fin
26 REM TAOO: outlet air temperature: offset strip fin
27 REM TWOP: outlet water temperature: plain fin tube
28 REM TWOW: outlet water temperature: wavy fin
29 REM TWOO: outlet water temperature: offset strip fin
29.1 REM EHXP: effectiveness: plain fin tube
29.2 REM EHXW: effectiveness: Wavy fin
29.3 REM EHXO: effectiveness: Offset strip fin
29.4 REM TWP, TWW and TWO: bulk water temperatures
29.6 REM TAP, TAW and TAO: bulk air temperatures

30 DTI = .483
40 DTO = .525
50 XA = 1.25
60 XB = 1.083
70 CUK = 227
80 ALK = 100

82 REM INPUT DATA

100 INPUT "AO="; AO
110 INPUT "H="; H
120 INPUT "L="; L
130 INPUT "TAI(F)="; TAI
140 INPUT "TWI(F)="; TWI
150 INPUT "VA(FPM)="; VA
160 INPUT "VW(FPS)="; VW
170 INPUT "FIN PER INCH ="; S
171 INPUT "T="; T
180 S1 = 1 / S
190 DH = -2.569963E-02 + (.961731562#) * (S ^ (-.80734013#))
200 CC1 = 1.68911259# + (1.983865E-02) * (S ^ .5) * (LOG(S))
210 AR1 = 1 / (CC1)
220 CC2 = .9218547 + (.336112) / (LOG(S))
230 AR2 = 1 / (CC2)
240 ALPHA = 14.659 + 19.76649 * S
270 RA = 53.32
280 ACP = .24

281 PA = 14.7

282 REM PA: air side pressure.

283 REM Initial: outlet temperatures

290 TWOP(1) = 0

291 twow(1) = 0

292 twoo(1) = 0

300 TAOP(1) = 0

301 taow(1) = 0

303 taoo(1) = 0

310 FOR I = 1 TO 5

311 REM Bulk water, air temp

320 TAP(I) = (TAI + TAOP(I)) / 2

321 TAW(I) = (TAI + taow(I)) / 2

323 TAO(I) = (TAI + taoo(I)) / 2

330 TWP(I) = (TWI + TWOP(I)) / 2

331 TWW(I) = (TWI + twow(I)) / 2

333 TWO(I) = (TWI + twoo(I)) / 2

334 REM Properties of air

340 A1 = .1980649

350 A2 = 3.030648E-03

360 A3 = 7.5636E-04

370 A4 = 1.61686E-06

380 A5 = 7.07473E-07

390 AN1 = A1 + A3 * TAI + A5 * TAI * TAI

400 D1 = 1 + A2 * TAI + A4 * TAI * TAI

410 AVI = (AN1 / D1) ^ 2

420 AN2P = A1 + A3 * TAP(I) + A5 * TAP(I) * TAP(I)

421 AN2W = A1 + A3 * TAW(I) + A5 * TAW(I) * TAW(I)

423 AN2O = A1 + A3 * TAO(I) + A5 * TAO(I) * TAO(I)

430 D2P = 1 + A2 * TAP(I) + A4 * TAP(I) * TAP(I)

431 D2W = 1 + A2 * TAW(I) + A4 * TAW(I) * TAW(I)

433 D2O = 1 + A2 * TAO(I) + A4 * TAO(I) * TAO(I)

440 AVP = (AN2P / D2P) ^ 2

441 AVW = (AN2W / D2W) ^ 2

443 AVO = (AN2O / D2O) ^ 2

444 REM AVP, AVW, AVO : bulk air viscosities.

450 A6 = .013071906#

460 A7 = 2.59434E-05

470 A8 = -5.0315E-09
 480 A9 = 3.736332E-03
 490 A10 = .041698788#
 500 AKP = A6 + (A7 * TAP(I)) + (A8 * TAP(I) * TAP(I)) + (A9 / TAP(I)) + (A10) /
 (TAP(I) * TAP(I))
 501 AKW = A6 + (A7 * TAW(I)) + (A8 * TAW(I) * TAW(I)) + (A9 / TAW(I)) + (A10) /
 (TAW(I) * TAW(I))
 503 AKO = A6 + (A7 * TAO(I)) + (A8 * TAO(I) * TAO(I)) + (A9 / TAO(I)) + (A10) /
 (TAO(I) * TAO(I))
 504 REM AKP, AKW, AKO : bulk air thermal conductivities

 510 ADI = (PA * 144) / ((RA) * (TAI + 460))
 511 REM ADI : air density in
 520 APRP = (AVP * ACP) / AKP
 521 APRW = (AVW * ACP) / AKW
 522 APRO = (AVO * ACP) / AKO
 524 REM APRP, APRW , APRO: air prandtl numbers

 530 AFR = H * L
 531 REM AFR : FRONTAL area.
 540 AM = (VA * AFR * 60 * ADI)
 550 PRINT "AM="; AM
 551 REM AM air mass flow rate.

 560 REM***CALCULATION OF WATER PROPERTIES***
 570 WCP = 1
 580 A11 = 62.31798536#
 590 A12 = 7.133019E-03
 600 A13 = -1.1418E-04
 610 A14 = 1.15173E-07
 620 WDI = A11 + (A12 * TWI) + ((A13) * (TWI ^ 2)) + ((A14) * (TWI ^ 3))
 630 WDP = A11 + (A12 * TWP(I)) + (A13 * TWP(I) * TWP(I)) + (A14 * TWP(I) *
 TWP(I) * TWP(I))
 631 WDW = A11 + (A12 * TWW(I)) + (A13 * TWW(I) * TWW(I)) + (A14 * TWW(I) *
 TWW(I) * TWW(I))
 633 WDO = A11 + (A12 * TWO(I)) + (A13 * TWO(I) * TWO(I)) + (A14 * TWO(I) *
 TWO(I) * TWO(I))
 640 A15 = .291975
 650 A16 = 9.59507E-04
 660 A17 = -2.821E-06
 670 A18 = 2.58806E-09
 680 WKP = A15 + (A16 * TWP(I)) + (A17 * TWP(I) * TWP(I)) + (A18 * TWP(I) *
 TWP(I) * TWP(I))
 681 WKW = A15 + (A16 * TWW(I)) + (A17 * TWW(I) * TWW(I)) + (A18 * TWW(I) *
 TWW(I) * TWW(I))

```

683 WKO = A15 + (A16 * TWO(I)) + (A17 * TWO(I) * TWO(I)) + (A18 * TWO(I) *
TWO(I) * TWO(I))
690 A19 = 9.949940748#
700 A20 = .045519659#
710 A21 = -6.2578E-06
720 A22 = 2.09856E-07
730 A23 = -.58617528#
740 WVP = A19 + (A20 * TWP(I)) + (A21 * (TWP(I) ^ 2.5)) + (A22 * (TWP(I) ^ 3)) +
(A23 * ((LOG(TWP(I))) ^ 2))
741 WVW = A19 + (A20 * TWW(I)) + (A21 * (TWW(I) ^ 2.5)) + (A22 * (TWW(I) ^ 3))
+ (A23 * ((LOG(TWW(I))) ^ 2))
742 WVO = A19 + (A20 * TWO(I)) + (A21 * (TWO(I) ^ 2.5)) + (A22 * (TWO(I) ^ 3)) +
(A23 * ((LOG(TWO(I))) ^ 2))
750 PRINT "WDI="; WDI, "WDP="; WDP, "WKP="; WKP, "WVP="; WVP
760 WPRP = (WCP * WVP) / WKP
761 WPRW = (WCP * WVW) / WKW
762 WPRO = (WCP * WVO) / WKO
770 PRINT "WPRP="; WPRP
771 REM WPRP , WPRW, WPRO: water prandtl numbers
780 TR = 12 * H / XA
790 AREAW = (3.1415 / 4) * (DTI ^ 2) * (1 / 144) * TR
800 WMASS = WDI * (VW * 3600) * (AREAW)
840 GFR = VA * 60 * ADI
850 GC = GFR / AR1
860 PRINT "GC="; GC
880 ARE = GC * (DTO / 12) / (AVI)
885 AREWVY = GFR * (DTO / 12) / (AVI)
887 AREO = ARE
910 AR3 = 4 * XA * XB * AR1 / (3.14159 * DH * DTO)
920 AJP = (ARE ^ (-.4)) * (AR3 ^ (-.15))
930 AJ = .0014 + .2618 * (AJP)
941 AJPL = AJ
942 REM AJPL : j factor plain fin HEX.
950 HOP = (AJPL * GC * ACP) / (APRP ^ .666)
960 PRINT "HOP="; HOP
960.1 REM HOP : air side ht tr.coeff. for plain fin HEX.
962 A30 = .14 * ((AREWVY) ^ (-.328))
963 A31 = ((XA / XB) ^ (-.502))
964 A32 = ((1 / S) * (1 / DTO)) ^ .0312
965 AJW = (A30) * (A31) * (A32)
966 HOW = (AJW * GC * ACP) / (APRW ^ .666)
966.1 REM AJW : j factor wavy fins.
966.2 REM HOW is air side ht. tr. coeff. for wavy fins.
967 PRINT "AJW="; AJW, "HOW="; HOW
969.3 REM***CALCULATION OF J FACTOR,OSF

```

969.4 HOSF = .67
 969.41 REM HOSF , ht of OSF.
 969.5 WOSF = .108
 969.51 REM WOSF , passage width for OSF.
 969.6 XOSF = .0938
 969.61 REM XOSF,length of OSF.
 969.7 TOSF = T
 969.8 DhOSF = (2 * WOSF * HOSF) / (WOSF + HOSF)
 969.81 REM DhOSF, hydraulic diameter for OSF.
 969.9 AREO = (GC * DhOSF * 1 / 12) / (AVI)
 969.901 REM AREO : air side Rey.no for OSF.
 969.91 AJO = .242 * ((XOSF / DhOSF) ^ (-.322)) * ((TOSF / DhOSF) ^ .089) * (AREO ^ (-.368))
 969.92 HOO = (AJO * GC * ACP) / (APRO ^ .666)
 969.93 PRINT "AJO="; AJO, "HOO="; HOO
 970 REM***CALCULATION OF HI ****
 980 WREP = WDP * VW * 3600 * (DTI / 12) / (WVP)
 981 WREW = WDW * VW * 3600 * (DTI / 12) / (WVW)
 983 WREO = WDO * VW * 3600 * (DTI / 12) / (WVO)
 990 WPRP = WVP * WCP / WKP
 991 WPRW = WVW * WCP / WKW
 993 WPRO = WVO * WCP / WKO
 1000 HIP = .023 * (WREP ^ .8) * (WPRP ^ .3) * (WKP) * (12) / DTI
 1001 HIW = .023 * (WREW ^ .8) * (WPRW ^ .3) * (WKW) * (12) / DTI
 1003 HIO = .023 * (WREO ^ .8) * (WPRO ^ .3) * (WKO) * (12) / DTI
 1010 REM***CALCULATIONS FOR FIN EFF*****
 1020 Z1 = XA / 2
 1030 Z2 = (((Z1 ^ 2) + (XB ^ 2)) ^ .5) / 2
 1040 Z3 = Z1 / (DTO / 2)
 1050 Z4 = Z1 / Z2
 1060 Z5 = 1.27 * (Z3) * ((Z4 - .3) ^ .5)
 1070 Z6 = (Z5 - 1) * (1 + .35 * LOG(Z5))
 1080 Y1P = (((2 * HOP) / (ALK * T / 12)) ^ .5)
 1081 Y1W = (((2 * HOW) / (ALK * T / 12)) ^ .5)
 1083 Y1O = (((2 * HOO) / (ALK * T / 12)) ^ .5)
 1090 AY1P = Y1P * (DTO / 24) * Z6
 1091 AY1W = Y1W * (DTO / 24) * Z6
 1093 AY1O = Y1O * (DTO / 24) * Z6
 1100 AY2P = EXP(AY1P)
 1101 AY2W = EXP(AY1W)
 1103 AY2O = EXP(AY1O)
 1110 AY3P = EXP(-AY1P)
 1111 AY3W = EXP(-AY1W)
 1113 AY3O = EXP(-AY1O)
 1120 AY4P = (AY2P - AY3P) / (AY2P + AY3P)

1121 $AY4W = (AY2W - AY3W) / (AY2W + AY3W)$
1123 $AY4O = (AY2O - AY3O) / (AY2O + AY3O)$
1130 $fep = AY4P / AY1P$
1131 $few = AY4W / AY1W$
1133 $feo = AY4O / AY1O$
1140 $fefp = 1 - (AR2 * (1 - fep))$
1141 $fefw = 1 - (AR2 * (1 - few))$
1143 $fefo = 1 - (AR2 * (1 - feo))$
1144 REM fefp, fefw, fefo : fin effectiveness.
1160 $Y5P = 1 / (HOP * fefp)$
1161 $Y5W = 1 / (HOW * fefw)$
1163 $Y5O = 1 / (HOO * fefo)$
1170 $Y6 = (DTO / DTI) * (1 - AR2)$
1171 REM Y6 is Ai/ A ratio.
1180 $Y7P = 1 / (HIP * Y6)$
1181 $Y7W = 1 / (HIW * Y6)$
1183 $Y7O = 1 / (HIO * Y6)$
1190 $Y8 = DTI / 12 * LOG(DTO / DTI)$
1200 $Y9 = 2 * CUK * Y6$
1210 $Y10 = Y8 / Y9$
1211 REM Y10 : tube wall resistance.
1220 $UOP = 1 / (Y5P + Y7P + Y10)$
1221 $UOW = 1 / (Y5W + Y7W + Y10)$
1223 $UOO = 1 / (Y5O + Y7O + Y10)$
1230 PRINT "UOP="; UOP
1231 PRINT "UOW="; UOW
1233 PRINT "UOO="; UOO
1234 AOP = AO
1235 AOW = AO
1236 AOS = AO
1237 AOO = AO
1238 REM UOAOP, UOAOW, UOAOO :overall conductances.
1240 UOAOP = UOP * AOP
1242 UOAOW = UOW * AOW
1243 UOAOO = UOO * AOO
1250 REM***EHX COMPUTATION****
1260 CAIR = AM * ACP
1270 CWAT = WMASS * WCP
1271 IF CAIR < CWAT GOTO 1390
1280 CM = CWAT
1290 CR = CWAT / CAIR
1300 NTUP = (UOP * AOP) / CM
1301 NTUW = (UOW * AOW) / CM
1303 NTUO = (UOO * AOO) / CM
1310 Z20P = EXP((-NTUP) * (1 - CR))

1311 Z20W = EXP((-NTUW) * (1 - CR))
1313 Z20O = EXP((-NTUO) * (1 - CR))
1320 Z21P = 1 - Z20P
1321 Z21W = 1 - Z20W
1323 Z21O = 1 - Z20O
1330 Z30P = CR * Z20P
1331 Z30W = CR * Z20W
1332 Z30O = CR * Z20O
1340 Z31P = 1 - Z30P
1341 Z31W = 1 - Z30W
1343 Z31O = 1 - Z30O
1350 EHXP(I) = Z21P / Z31P
1351 EHXW(I) = Z21W / Z31W
1353 EHXO(I) = Z21O / Z31O
1360 TWOP(I + 1) = TWI + ((EHXP(I)) * (TAI - TWI))
1361 twow(I + 1) = TWI + ((EHXW(I)) * (TAI - TWI))
1363 twoo(I + 1) = TWI + ((EHXO(I)) * (TAI - TWI))
1370 TAOP(I + 1) = TAI - ((CWAT / CAIR) * (TWOP(I + 1) - TWI))
1370.1 taow(I + 1) = TAI - ((CWAT / CAIR) * (twow(I + 1) - TWI))
1370.3 tao0(I + 1) = TAI - ((CWAT / CAIR) * (twoo(I + 1) - TWI))
1380 QP = CAIR * (TAI - TAOP(I + 1))
1380.1 QW = CAIR * (TAI - taow(I + 1))
1380.3 QO = CAIR * (TAI - tao0(I + 1))
1381 GOTO 1500
1390 CM = CAIR
1400 CR = CAIR / CWAT
1410 NTUP = (UOP * AO) / CM
1411 NTUW = (UOW * AO) / CM
1413 NTUO = (UOO * AO) / CM
1420 Z50P = EXP((-NTUP) * (1 - CR))
1421 Z50W = EXP((-NTUW) * (1 - CR))
1423 Z50O = EXP((-NTUO) * (1 - CR))
1430 Z51P = 1 - Z50P
1431 Z51W = 1 - Z50W
1433 Z51O = 1 - Z50O
1440 Z60P = CR * Z50P
1441 Z60W = CR * Z50W
1443 Z60O = CR * Z50O
1450 Z61P = 1 - Z60P
1451 Z61W = 1 - Z60W
1451.2 Z61O = 1 - Z60O
1460 EHXP(I) = Z51P / Z61P
1461 EHXW(I) = Z51W / Z61W
1463 EHXO(I) = Z51O / Z61O
1470 TAOP(I + 1) = TAI - ((EHXP(I)) * (TAI - TWI))


```

1471 taow(I + 1) = TAI - ((EHXW(I)) * (TAI - TWI))
1473 taoo(I + 1) = TAI - ((EHXO(I)) * (TAI - TWI))
1480 TWOP(I + 1) = TWI + ((CAIR / CWAT) * (TAI - TAOP(I + 1)))
1481 twow(I + 1) = TWI + ((CAIR / CWAT) * (TAI - taow(I + 1)))
1483 twoo(I + 1) = TWI + ((CAIR / CWAT) * (TAI - taoo(I + 1)))
1490 QP = CAIR * (TAI - TAOP(I + 1))
1491 QW = CAIR * (TAI - taow(I + 1))
1493 QO = CAIR * (TAI - taoo(I + 1))
1500 PRINT "TAOP(I+1)="; TAOP(I + 1)
1510 PRINT "TWOP(I+1)="; TWOP(I + 1)
1520 PRINT "QP="; QP
1530 NEXT I
1540 PRINT "I="; I
1550 PRINT "EHXP(1)="; EHXP(1)
1560 PRINT "EHXP(2)="; EHXP(2)
1570 PRINT "EHXP(3)="; EHXP(3)
1580 PRINT "TAOP(1)="; TAOP(1)
1590 PRINT "TAOP(2)="; TAOP(2)
1600 PRINT "TAOP(3)="; TAOP(3)
1610 PRINT "TWOP(1)="; TWOP(1)
1620 PRINT "TAOP(6)="; TAOP(6)
1620.1 PRINT "taow(6)="; taow(6)
1620.2 PRINT "taoo(6)="; taoo(6)
1630 PRINT "TWOP(6)="; TWOP(6)
1630.1 PRINT "twow(6)="; twow(6)
1630.2 PRINT "twoo(6)="; twoo(6)
1630.3 PRINT "fep="; fep
1630.4 PRINT "few="; few
1630.5 PRINT "feo="; feo
1640 PRINT "EHXP(5)="; EHXP(5)
1640.1 PRINT "EHXW(5)="; EHXW(5)
1640.3 PRINT "EHXO(5)="; EHXO(5)
1640.4 PRINT "EHXP(4)="; EHXP(4)
1640.5 PRINT "EHXW(4)="; EHXW(4)
1640.7 PRINT "EHXO(4)="; EHXO(4)
1641 IF (EHXP(5) - EHXP(4)) > .01 GOTO 2100
1642 IF (EHXW(5) - EHXW(4)) > .01 GOTO 2100
1644 IF (EHXO(5) - EHXO(4)) > .01 GOTO 2100
1650 PRINT "UOP="; UOP, "UOW="; UOW, "UOO="; UOO
1655 PRINT "HOP="; HOP, "HOW="; HOW, "HOO="; HOO
1660 PRINT "UOAOP="; UOAOP, "HIP="; HIP, "AJPL="; AJPL, "CWAT="; CWAT,
"CAIR="; CAIR
1660.01 PRINT "AJW="; AJW, "AJO="; AJO
1660.1 PRINT "HIW="; HIW, "HIO="; HIO
1661 PRINT "QP="; QP, "QO="; QO, "QW="; QW

```

1670 REM calculations for air side pressure drop.

$$1680 B1 = (XA - DTO) / S1$$

$$1690 B2 = (AR3) / (1 + B1)$$

$$1700 B3 = (XA - DTO) / (4 * (S1 - T))$$

$$1710 B4 = (XA) / (DTO * B2)$$

$$1720 B5 = ((ARE) ^ (-.25))$$

$$1730 B6 = ((1 / B2) ^ (.25))$$

$$1740 B7 = ((B3) ^ (-.4))$$

$$1750 B8 = ((B4 - 1) ^ (-.5))$$

$$1760 FP = B5 * B6 * B7 * B8$$

1761 REM FP , FP parameter , plain fins.

$$1770 FPL = .004904 + 1.382 * (FP * FP)$$

1770.1 REM FPL , friction factor , plain fins.

$$1771 FW10 = .508 * (AREWVY ^ (-.521)) * ((XA / DTO) ^ 1.318)$$

$$1771.1 FW2 = ((XA - DTO) / (DTO)) ^ 1.08$$

$$1771.2 FW3 = (AREWVY ^ -.16)$$

$$1771.3 FW20 = ((.118) / (FW2 + .25)) * FW3$$

$$1771.4 FW = FW10 + FW20$$

1771.5 REM FW , friction factor , wavy fins.

$$1773 FO = 1.136 * ((XOSF / DhOSF) ^ -.781) * ((T / DhOSF) ^ .534) * ((AREO) ^ -.198)$$

1774 REM FO , friction factor , offset strip fins.

$$1780 XI = .4048288 - (.40470568\#) * (AR1 ^ 2)$$

$$1790 CC8 = .998965464\# - (1.00505 * AR1)$$

$$1800 XE = CC8 ^ 2$$

$$1810 AR4P = AOP / (AFR * AR1)$$

$$1811 AR4W = AOW / (AFR * AR1)$$

$$1813 AR4O = AOO / (AFR * AR1)$$

$$1820 G = 32.2$$

1821 REM G , gravitational constant.

$$1830 ADOP = (PA * 144) / ((RA) * (TAOP(I) + 460))$$

$$1831 ADOW = (PA * 144) / ((RA) * (taow(I) + 460))$$

$$1833 ADOO = (PA * 144) / ((RA) * (taoo(I) + 460))$$

1834 REM ADOP , air density out , plain fin

$$1840 ADMP = (ADI + ADOP) / 2$$

$$1841 ADMW = (ADI + ADOW) / 2$$

$$1843 ADMO = (ADI + ADOO) / 2$$

1844 REM ADMP, air mean density , plain fin

$$1850 V = (GC ^ 2) / (2 * G * 3600 * 3600 * ADI)$$

$$1860 V1 = (XI + 1 - (AR1 ^ 2))$$

$$1870 V2P = (2) * ((ADI / ADOP) - 1)$$

$$1871 V2W = (2) * ((ADI / ADOW) - 1)$$

$$1872 V2O = (2) * ((ADI / ADOO) - 1)$$

```

1880 V3P = FPL * AR4P * ADI / ADMP
1881 V3W = FW * AR4W * ADI / ADMW
1883 V3O = FO * AR4O * ADI / ADMO
1890 V4P = (1 - (AR1 ^ 2) - XE) * (ADI / ADOP)
1891 V4W = (1 - (AR1 ^ 2) - XE) * (ADI / ADOW)
1893 V4O = (1 - (AR1 ^ 2) - XE) * (ADI / ADOO)
1900 APDP = V * (V1 + V2P + V3P - V4P) * (12 / 62.4)
1901 APDW = V * (V1 + V2W + V3W - V4W) * (12 / 62.4)
1903 APDO = V * (V1 + V2O + V3O - V4O) * (12 / 62.4)
1904 REM APDP is air side pressure drop for plain fin tube HEX.
1910 PRINT "APDP="; APDP, "APDW="; APDW, "APDO="; APDO
1910.1 PRINT "FPL="; FPL, "FW="; FW, "FO="; FO
1950 GOTO 2200
2100 PRINT "SOLN DOES NOT CONVERGE"
2200 END

```

VITA

Parag Dadeech was born on April 7th, 1969 in Jaipur, Rajasthan, India. He had most of his early education in New Delhi. He passed the X grade from the Air Force School in New Delhi in May 1985. He graduated from senior school (XII grade) in May 1987 securing 98% marks in Physics and 95% marks aggregate in Sciences and Mathematics. He was among the merit list candidates in the "All India senior school certificate examination" held in 1987.

The following August he entered the "College of Technology", Osmania University, Hyderabad majoring in Chemical engineering. He graduated with B.Tech in Chemical engineering in " June 1991", in first division with distinction.

The next Fall, he joined the University of Tennessee at Chattanooga in the Masters program in Chemical engineering. He will be graduating in May 1995. He plans to work in the United States for a few years upon graduation. He also plans to pursue Phd. in Chemical engineering at a later stage.